The Development and Operating Characteristics of an Improved Plasma Torch for Supersonic Combustion Applications

by

Scott David Stouffer

Thesis submitted to the Faculty of the
Virginia Polytechnic Institute and State University
in partial fulfillment of the requirements for the degree of
Master of Science
in
Mechanical Engineering

APPROVED:

Dr. Walter F. O'Brien, Chairman

Dr. C. L. Dancey

Dr. J. R. Mahan

July, 1989

Blacksburg, Virginia

The Development and Operating Characteristics of an Improved Plasma Torch for Supersonic Combustion Applications

by

Scott David Stouffer

Dr. Walter F. O'Brien, Chairman

Mechanical Engineering

(ABSTRACT)

The design of the VPI plasma torch, which has been used as an ignitor and flameholder in supersonic combustion studies, has been modified in order to decrease the electrode wear and to increase stability. The plasma torch can be used as a source of hydrogen or nitrogen radicals which initiate and stabilize combustion. During previous testing of the unmodified torch, electrode erosion limited operation of the torch to about two hours.

The improved torch features a flow swirler in the gas inlet, which adds vortex stabilization to the arc. The vortex stabilization causes the anode attachment point of the arc to be anchored in the low pressure region, downstream of the constrictor. This lowers the heat flux to the anode, so that erosion is decreased. The torch body was redesigned with an emphasis on the alignment of the electrodes. Also, the electrode gap in the improved torch was made continuously adjustable, allowing fine adjustment of the electrode gap during operation of the torch.

The operational characteristics of the improved torch were monitored by a microcomputer-based data acquisition system. Stable operation of the improved torch with pure nitrogen was demonstrated, thus eliminating the requirement for argon to stabilize the arc. Operational characteristics of the improved torch running on argon, nitrogen, argon/hydrogen and argon/nitrogen mixtures as feedstocks, are reported. The

electrode wear was studied between tests by observation with a microscope, and by measuring the mass change of the electrodes. The electrode erosion of the improved torch was reduced significantly. Anode lifetimes of greater than 20 hours have been demonstrated with operation on mixtures of nitrogen and argon.

Acknowledgements

I would like to thank Dr. Walter F. O'Brien, for his patience and help as my advisor during this project. I would also like to thank Dr. Dancey and Dr. Mahan for their help as members of my committee. A special thanks goes out to for serving as a member of the examination committee.

I am grateful to NASA for the support I have received under the graduate student researchers program, and would like to thank of the Langley Research Center for providing me with the opportunity to work on this project, and for serving as technical monitor of this project.

I would like to thank and for their help on the current sensor. I would like to thank for allowing me to use the photography equipment in his lab. I am grateful to for a key suggestion on the design of my torch. A special thanks goes to of the NASA Lewis Research Center for his advice on how to form static gas seals.

I would like to thank fellow students and ex-students , and and , for all of their help and

suggestions while I was running experiments. A special thanks goes out to for the all of the help he has given me with the throughout this project. and of the Mechanical Engineering Instrumentation Shop are to be thanked for all of their help on wiring and the data acquisition systems. Also I would like to thank and the rest of the Mechanical engineering shop staff for in building the plasma torch.

I would like to thank my girlfriend for her constant encouragement. Finally, I would like to thank my parents, , and my sisters , for all of the love and moral support throughout my college career.

Table of Contents

List of Illustrations

List of Tables

Nomenclature

English

A	constant
c	constant
C	charge passed through the arc
e	charge of an electron
E	electric field strength
G	electrode gap
I	current
j	current density
k	Boltzmann constant
P	pressure
q	net heat flux
q_r	radiative heat flux
q_c	convective heat flux
q_e	electron heat flux
r	radius
T	temperature
T_e	electron temperature
T_r	temperature of surroundings
U_a	anode fall voltage

Greek

α	degree of ionization
ε_i	ionization potential
ε_o	permittivity constant
Θ	entropy production rate
ρ	electrical resistance per unit length
σ	electrical conductivity
ϕ_a	thermionic work function of anode
ϕ_c	thermionic work function of cathode

Chapter 1

Introduction

The need for economical access to space has led to the consideration of advanced airbreathing propulsion systems. For propulsion at low hypersonic speeds, conventional subsonic combustion ramjets may be used. However, as the vehicle speed increases, so does the total pressure loss that is encountered while diffusing the flow to subsonic combustion chamber velocities. The temperature also increases, so that the thermal loading of the structure and the frozen flow losses in the nozzle become significant. In addition, the chamber pressure rises dramatically as the Mach number increases, so a stronger, and therefore heavier, structure is required for the engine. For these reasons, at speeds around Mach 6 the supersonic combustion ramjet (SCRAMJET) becomes the optimum airbreathing engine [1].

In a SCRAMJET the fuel is burned in a supersonic stream of air. Due to the high combustion chamber velocity, ignition and flame-holding are difficult to achieve in a

supersonic flow. The finite rate of combustion reactions become significant when compared to the short residence times in a combustion chamber of reasonable length.

During ground testing of hydrogen-fueled scramjet engine models, at conditions corresponding to low flight Mach numbers, the static temperature was below the autoignition temperature and an ignition source was required [2,3]. Also, in a recent analytical study of the hydrogen-air reaction, Jachimowski [4] found that an ignition source may be required at vehicle speeds up to Mach 16, due to the slow rates of the reactions involved. Ground tests have also shown that, after ignition has occurred, a source of flame stabilization is required in order to compensate for the short residence times in the combustion chamber at high vehicle speeds [5].

Monosilane (SiH_4) is commonly used as an ignition source and pilot in supersonic combustion tests [39]. Silane is effective because it is a pyrophoric compound, that is, it reacts spontaneously on contact with air. To eliminate the hazards associated with the use of a pyrophoric compound, it would be desirable to have an ignition and piloting source which is inactive when it is not required and can be activated on demand. One alternative which incorporates this feature is a plasma torch used as a source of the required radicals for combustion ignition and piloting.

Research has been conducted at the Hypersonic Propulsion Branch of the NASA Langley Research Center on the flameholding and ignition properties of plasma torches, operated on mixtures of hydrogen and argon, in supersonic combustion. Northam et al. [6] used a commercially available, water-cooled plasma torch to study ignition and flameholding in hydrogen and hydrocarbon fuels at Mach 2 combustion chamber velocities. It was concluded that an adiabatic plasma torch at power levels of about 2 kW could be an effective ignition source and flameholder in supersonic combustion.

This work was extended to lower torch power levels by Wagner et al. [7], using a torch designed by Barbi et al. [8]. The torch was uncooled for propulsion applications,

and designed to run at low power inputs. Also, the flow though the nozzle throat was choked in order to prevent pressure pulses in the combustion chamber from upsetting torch operation. The torch functioned well as both an ignitor and flameholder. However, nozzle erosion was a severe problem. Choked operation of the torch was limited to about two hours on argon-hydrogen mixtures, due to the anode erosion. In addition, because of the electrode erosion, and therefore, the change in torch pressure with time, the torch performance was not always repeatable.

The objective of the work reported in this thesis was to improve the performance, repeatability, and lifetime of the plasma torch designed by Barbi et al. [8]. A goal of 20 hours of choked operation was set at the beginning of the research program. Another objective was to obtain stable operation of the torch on pure hydrogen, eliminating the necessity for argon mixtures to stabilize the arc. Also, since plasma torches operating on nitrogen feedstocks have been shown to be effective as ignitors and flameholders in supersonic combustion tests [24], it was of interest to explore the possibility of operating the torch on nitrogen and nitrogen-argon mixtures.

In an effort to achieve the performance goals, an improved plasma torch, based on the same electrode geometry as that used by Barbi [8], was designed and built. The new plasma torch body was built with emphasis on anode-cathode alignment. The cathode is held by a fine thread device which provides a continuously adjustable gap during arc operation. In order to achieve higher lifetimes and better arc stability, a flow swirler was added to the torch. This swirler provided vortex stabilization to the arc, and anchored the anode attachment point of the arc in the low pressure region of the arc.

This thesis presents the design details of the improved plasma torch. The improved torch was tested on pure argon, hydrogen, and nitrogen, and mixtures of hydrogen or nitrogen with argon. The torch parameters were monitored during long-term operation by a microcomputer-based data acquisition system which was built especially for this

research. The electrode wear was studied after each test by observation with a microscope, and by measuring the mass loss of the electrodes.

Chapter 2 of this thesis presents a brief review of the use of continuous plasma torches in combustion research. Chapter 3 gives an introduction to some of the considerations in the design of a plasma torch. Chapter 4 presents a summary of plasma torch designs which have previously been used in combustion research, including the design of the torch which was the starting point of the present investigation. A description of the improved torch is given in Chapter 5. The instrumentation and experimental apparatus which was used to monitor the torch during operation is described in Chapter 6. Chapter 7 presents a summary and discussion of the experimental results from tests performed on the torch. The final chapter presents the conclusions and recommendations for further design improvements to the torch. Appendix A gives a brief introduction to the physics of an electric arc.

Chapter 2

Plasma Torches In Combustion

The first application of plasma devices to combustion was to electrically augment the enthalpy of flames, in order to provide a higher flame temperature than that obtainable from combustion alone [9,10]. The objective was to uniformly distribute an electrical discharge through the flame. However, since electric arcs become constricted to small diameters at atmospheric pressure, this method was found to be inefficient. For this reason, interest in devices of this type has faded in favor of plasma torches. The plasma torch works by injecting a small quantity of specific radicals into the reacting region, instead of heating the entire reacting region.

Harrison and Weinberg [11] used a magnetically rotated, continuous plasma torch to stabilize the combustion of methane in air. In their study, the plasma jet was located at one end of a quartz flame tube, and the reactants were introduced separately, downstream from the plasma jet. The plasma torch was operated on feed gases of argon, nitrogen, oxygen and methane. With the torch operating on a mixture of nitrogen with

argon as an arc carrier, it was found that with the addition of 10 percent of the available chemical energy by way of the torch, it was possible to increase the flow rate of the reactants though the flame tube by 700 percent and sustain combustion. This was compared with the theoretical 50 percent increase in the reaction rate which would occur if the energy were added as thermal energy to the reactants in a perfectly stirred reactor. The conclusion was that the formation of radicals, rather than the addition of energy, was primarily responsible for the increased reaction rates.

Watersen [12] was the first to demonstrate the use of a plasma torch as an ignition source. The plasma torch used was a pulsed plasma torch which was based on a modified automobile engine spark plug. The application of pulsed plasma torches to combustion has been studied because of their possible application to the internal combustion engine in place of spark plugs. Most of the studies have been done on the possible improvements in the ignition and flame propagation in lean mixtures of fuel and air, in order to improve the fuel economy and reduce pollutants [13-16]. In addition to the extension of the lean flammability limit, Vince et al. [17] demonstrated the use of a pulsed torch to extend the rich flammability limit and reduce soot formation in rich ethylene/air flames. Since the object of the present investigation was to improve a continuous plasma torch, pulsed plasma torches will not be discussed further. The reader who is interested in further information on the use of pulsed plasma torches is referred to the review by Weinberg [18].

After the results of the study by Harrison and Weinberg [11], Weinberg and Hilliard [19] used a continuous plasma torch, operating on argon and nitrogen, to stabilize combustion in a model of a gas turbine flame tube. They found that it was possible to stabilize lean combustion of propane and air at high velocities, in the stream of nitrogen radicals from the torch. It was suggested that the reaction

$$N + O_2 \rightarrow NO + O \qquad (2.1)$$

was responsible for the enhanced flame stabilization.

The torch also demonstrated the ability to remove soot from flames injected with toluene to intentionally produce soot. The removal of soot was found to be greater with the torch operating on nitrogen than for operation on argon.

The removal of nitric oxide (NO), presumably by the reaction

$$N + NO \rightarrow N_2 + O \qquad (2.2)$$

was also shown by injecting the plasma into a fast flowing stream of synthetic engine exhaust gases contaminated with NO. Later, a practical demonstration of the torch was made in the exhaust of an automobile, and it was noted that "a considerable reduction in NO emission was achieved".

Behabahini et al. [20] also studied the reduction of NO by nitrogen atoms from a plasma torch. The details of the design used, which was developed by Chan et al. [21], are discussed in Chapter 4. The reaction rates of three elementary reactions of nitrogen atoms were considered. The first two reactions considered were reactions 2.1 and 2.2 listed above. These were compared to the three-body recombination of nitrogen by

$$N + N + M \rightarrow N_2 + M \qquad (2.3)$$

which has a reaction rate that decreases with increases in temperature. The rate of reaction 2.2 is almost independent of temperature, while the rate of reaction 2.1 increases with increases in temperature, so that nitrogen radicals reacting with oxygen at high temperatures tend to produce NO while nitrogen radicals reacting at lower temperatures with NO tend to reduce its concentration.

In the study by Behabahini et al. [20], both NO and pure O_2 were injected into the torch exhaust in separate experiments. Very little NO was formed when pure oxygen was injected into the torch exhaust. However, when NO was injected, the torch was efficient in removing it, even when the NO was injected several centimeters downstream of the torch. In fact, the reduction of NO was much greater than would be expected on the basis of the mean enthalpy of the plasma. On this basis, it was proposed that the nitrogen radicals were formed in small hot pockets of gas surrounded by relatively cool gas, so that the jet from the torch was thermally stratified. The nitrogen radicals would then diffuse out of the hot pockets of gas and react at low temperatures with NO, by reaction 2.2. The presence of the hot pockets of plasma was confirmed by their detection with ionization probes.

The plasma torch used in the study employed a magnet to rapidly rotate the arc through the gas. This was necessary in order to prevent excessive electrode erosion, but the rapid rotation of the arc through the gas tended to uniformly heat the gas. However, since it was determined that the thermal stratification of the plasma was responsible for the results observed, Behabahani et al. [22] used a vortex to rotate the arc through the gas. The reasoning was that by using the vortex arc rotation, the arc maintained contact with the same pockets of gas for longer periods of time, so that these pockets were heated more than the rest of the flow, increasing the thermal stratification.

With these changes, the removal rate of NO was improved somewhat. Shadowgraphs and ionization probes were used to study the plasma jet. It was found that increasing the power to the torch increased the distance downstream that the hot pockets of plasma survived, while increasing the flow rate increased both this distance and the frequency of occurrence of the hot pockets. The average velocity of the hot pockets was about ten times the mean gas flow velocity. The appearance of the hot

pockets was explained on the basis of a pressure gradient acting on a thermally stratified gas.

Warris and Weinberg [23] used continuous plasma torches to ignite and flamehold fast flowing, premixed propane and air in a 10-cm diameter duct. The flow velocity in the duct was between 5 and 30 m/s. The torch was operated on both argon and nitrogen. It was found that when the torch was operated on argon, neither ignition nor flameholding occurred. But, when the torch was operated on nitrogen, ignition and flameholding occurred in the flowing mixtures which were below the lean flammability limit for quiescent propane/air. No matter how lean the mixture was, it was seen that the luminous region of the plasma jet operating on nitrogen was extended past that of an inert environment when fuel was added, indicating that chemical activity was occurring.

Flameholding and ignition of supersonic streams of hydrogen and air with a plasma torch was studied by Kimura et al. [24]. Hydrogen fuel was injected into a cross flow of air at stagnation temperatures of 290 K, flowing at Mach numbers of 2.7 and 2.1, at different locations with respect to the plasma torch. The torch was operated on argon, nitrogen, and hydrogen, at powers of 2 to 5 kW. During operation of the torch on argon no combustion was observed. In contrast, ignition occurred, and a flame was stabilized when the torch was operated on both nitrogen and hydrogen. The progress of combustion was presented quantitatively as the area of the duct which reached a given temperature. On the basis of the total power to the torch required, for a given progress of combustion, operation of the torch on nitrogen was superior to that on hydrogen. Since the plasma torch which was used was water cooled, measurements of the inlet and outlet temperatures were made in order to calculate the amount of power actually going into the gas. When compared on the basis of the net input power to the gas itself, torch operation on hydrogen was better than that on nitrogen.

Northam et al. [6] used a plasma torch, operating on a mixture of argon and hydrogen, to ignite and flamehold supersonic (Mach 2) flows of air injected with different fuels. The existence of a flame was confirmed during open duct testing by observation with ultraviolet TV. The plasma torch was water cooled and had a thermal efficiency of about 50 %. The minimum total temperature of the air stream for ignition and flameholding with each fuel, was obtained with the torch at a nominal input power of 2 kW. The minimum total air temperature for the four fuels tested were; methane-1500 K, ethane-1110 K, ethylene-830 K, and hydrogen < 591 K, which may be compared to an autoignition temperature of 1550 K for hydrogen.

When the torch was mounted on the flat walls of the combustor, it was found to be an effective flameholder for all the fuels tested. When the torch was turned off, the flame would blow off. The location and amounts of the fuel injected was found to be an important factor in the success of the torch as an ignitor. Tests were also made with an expanding duct, simulating a SCRAMJET combustor. During some of these tests, enough fuel was burned to choke the combustor so that mixed subsonic-supersonic combustion occurred. However, combustion and the pressure rise associated with it, which could have the disastrous effect of unstarting the inlet, was prevented from propagating upstream of the plasma torch during its operation. Apparently, the flame was anchored downstream of the torch while it was turned on. When the torch was turned off, the upstream pressure was seen to rise.

Wagner et al. [7] used an uncooled, choked plasma torch to extend the results of this work to lower torch power levels. The design of this torch is discussed in detail in Chapter 4. The torch was located on one of the walls behind a rearward facing step. Fuel was injected simultaneously upstream and downstream of the torch. The step provided a recirculation region for fuel which was injected upstream of it. Most of the fuel was injected downstream of the plasma torch. The torch was operated on mixtures of argon

and hydrogen. Both open duct and confined duct tests were run with hydrogen used as the fuel.

Ignition occurred for torch powers as low as 630 W, which was the lowest torch power tested. The torch also ignited and stabilized the flame at airflow total temperatures as low as 290 K. With the injector configuration used, the flame was stabilized in the recirculation region located downstream of the step, after the torch was turned off. During the confined duct tests, the torch power was found to have no effect on the combustion efficiency. It was concluded that a low power plasma torch operating on argon and hydrogen mixtures could be an effective ignitor and flameholder in a scramjet combustor.

Chapter 3

Design Considerations In a Plasma Torch

A plasma torch is a device which produces a flow of plasma by passing an electric arc through a flowing gas. A plasma is an electrically conducting mixture of ions, electrons, and neutral particles. A short introduction to the physics of an electric arc is given in Appendix A.

A drawing of a typical plasma torch is shown in figure 1. The center electrode is the cathode and the outer electrode, which doubles as the nozzle of the torch, is the anode. The two electrodes are separated by an insulating material, and the anode always has a positive electrical potential with respect to the cathode. The design of the plasma torch looks deceptively simple, however, there are many factors to be considered in a plasma torch design.

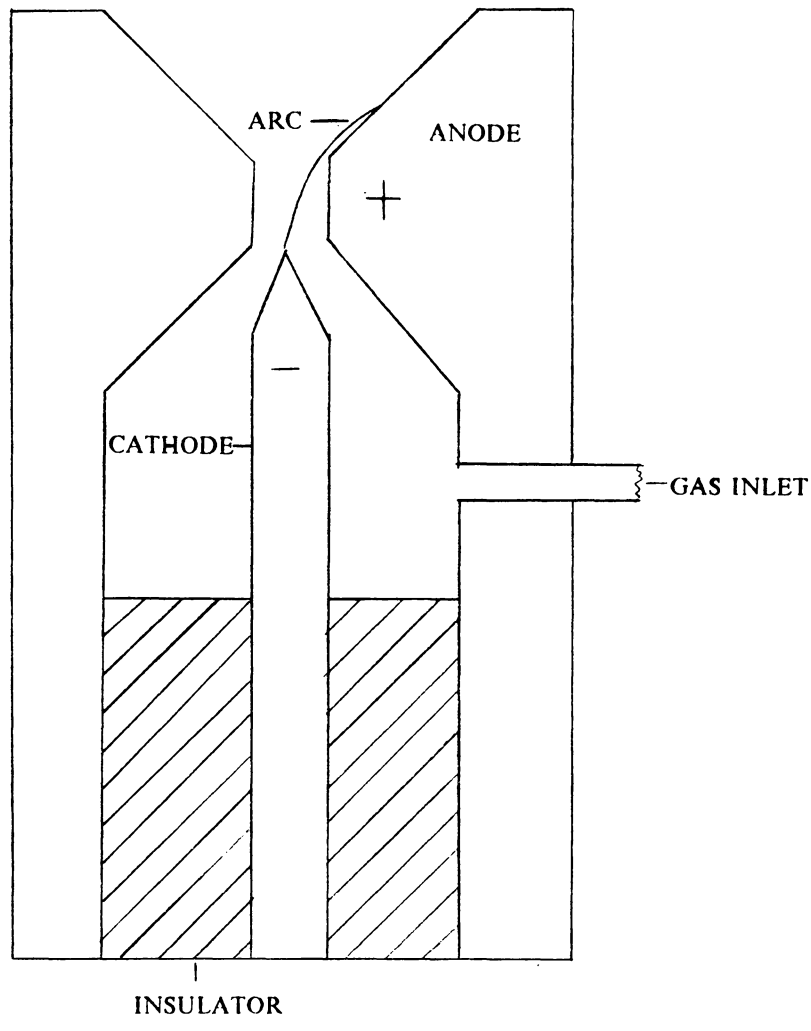

Figure 1. A Typical Plasma Torch

3.1 Heat transfer in a Plasma Torch

Inadequate cooling and the subsequent thermal erosion is the major mechanism of wear in plasma torch electrodes. This section covers the different modes of heat transfer and how these modes are affected by the pressure, current, gas flow and electrode alignment in a plasma torch.

The general equation for the heat flux to either the cathode or anode surface may be written as

$$q = q_r + q_c + q_e .$$

The total heat flux to a point on the surface, q, is due to the net radiative, convective, and electron heating terms, which are represented by q_r, q_c, and q_e, respectively. This total heat flux must be conducted to a cooler region of the electrode. The effect of each of these terms is different in the cathode and the anode so that each will be examined separately.

3.1.1 Anode Heat Transfer

Any high temperature spot on a metal electrode will radiate, providing a cooling mechanism. In addition, both electrodes are heated by radiation from the plasma. This radiation is known to increase with increasing current density [29], which will increase with increasing current and pressure. The heat transfer to either electrode due to radiation is expected to be small. In a study of an argon arc at a pressure slightly above atmospheric, Eberhart and Seban [34] found that only 2 to 8 percent of the heat transfer to a plane anode was due to radiation.

The convection heat transfer to the anode of a high pressure plasma torch may be either positive or negative, with the sign depending on the temperature difference between the anode and the adjacent layer of gas. Near the cathode the arc is very narrow, and a cool layer of gas is swept past the anode walls, providing passive regenerative cooling to the anode. Further downstream in the nozzle the plasma is closer to the walls, so that the walls are heated by convection.

Link and Incropera [35] studied the heat transfer in an insulated, variable area arc constrictor, which operated on argon at a back pressure of approximately 1 atm. Since the constrictor was insulated, none of the heat transfer was due to flow of electrons to the constrictor. They found that the local flux to the constrictor was proportional to $I^2 / r^{2.5}$ where I and r are the total current and the constrictor radius, respectively.

The convection heat transfer can be affected by the alignment of the electrodes. A constricted, high temperature, high velocity jet of plasma, known as the cathode jet, flows from the tip of a pointed cathode. If the electrode alignment is such that this high velocity stream is incident to the anode, rather than flowing past the anode surface, the convective heating of the anode surface will be severe.

The heat transfer at the anode due to the flow of electrons is the dominant term at the point of attachment, which is commonly known as the anode spot in a high pressure arc. This term, q_e , is given by Shih et al. [36] as

$$q_e = j[(5k\,T_e / 2e) + U_a + \phi_a].$$

In this equation the first term represents the thermal kinetic energy of the electrons at the edge of the anode fall region. The second term represents the energy these electrons gain in being accelerated through the anode fall voltage, while the last term represents the energy that the electrons give up when they "condense" on the surface of the anode

and is equal to the product of the current density and the thermionic work function of the anode material.

If the current range considered is small enough, the effect of current on the terms included in the brackets of the above equation can be considered as a secondary effect compared to the change in the current density j. Therefore, to a first approximation, the heat flux at the anode due to current flow is directly proportional to the current density at the anode spot. The total heat transfer at the anode due to the flow of electrons is equal to the integral of the above equation over the anode spot.

The way in which the current is distributed at the anode determines the current density there. The cross-sectional area of an arc is known to decrease as the pressure is increased. Therefore, an arcjet operating in a vacuum has a very diffuse current distribution at the anode, while the anode in a plasma torch at atmospheric pressure is subjected to intense heating at the anode spot due to the higher current density there.

The overall heat transfer to an anode was studied by Curren [37] in a water cooled arc jet simulator, which was operating on nitrogen. It was determined that the heat transfer to the anode was directly proportional to the current, and that it decreased with an increase in mass flow.

3.1.2 Cathode Heat Transfer

The current from a pointed cathode in an arc at high pressures is thought to emit electrons by both field and thermionic emission [38]. Field emission is the removal of an electron from the cathode due to a strong electric field. Thermionic emission is the thermal emission of electrons from the surface of the cathode due to the high temperature. The current density at the cathode, due to the two effects is given by

$$j = A T^2 \exp\left[\frac{-e}{kT} \left(\phi_c - \sqrt{\frac{Ee}{\pi\varepsilon_o}} \right) \right]$$

which is the Richardson-Schotky equation. As seen from this equation, the current density is a strong function of the temperature. For this reason, the region of electron emission from a cathode is confined to a small region at the tip where the temperature is high.

In contrast to the anode, where the surface is heated by the condensation of electrons, the thermionic emission of electrons from the cathode surface requires that energy, equal to the work function of the cathode material times the current density, be supplied from the rest of the cathode. Thus, the thermionic emission of electrons from the cathode surface provides cooling of the cathode.

In addition to the thermionic emission, the cathode is cooled by convection. Because the arc cross-section is very narrow at the cathode, the current density there is also high, and there is a body force on the plasma due to the interaction of the current with its own magnetic field. The current density decreases along the arc, so that the body force also decreases and a negative pressure gradient is developed along the axis. The net effect is that a "cathode jet" of hot plasma spreads from the cathode [29]. In order to satisfy mass conservation, cool gas is swept past the cathode surface, cooling it by convection. This provides passive regenerative cooling of the cathode.

The cathode can be heated by several mechanisms. One of these is radiation from the plasma, but, as for the anode, the radiation heat transfer will be small. The cathode is also heated by positive ions which are attracted to it in the same way that electrons are attracted to the anode. The ions that reach the cathode give up their kinetic energy and their ionization energy to it. The third way that the cathode is heated is by resistive

dissipation in the cathode fall region, which is equal to the current density times the cathode fall voltage.

The overall heat transfer to the cathode was also studied by Curren [37]. The power lost to the cathode was found to be only 1 to 5 percent of the total arc power. The total heat transfer to the cathode did not change much with an increase in current. In fact, the percentage of the arc power which was dissipated at the cathode decreased with an increase in current.

3.2 Arc Mode

In a plasma torch with a constrictor section in the anode, there are two possible modes of arc operation. Both are shown in figure 2. The high voltage mode, shown in figure 2 (a), corresponds to the case where the arc passes all of the way through the constrictor and attaches to the diverging section of the anode. The low voltage mode, shown in figure 2 (b), corresponds to arc attachment upstream of the constrictor in the converging section of the anode. Since the arc length is shorter in the low voltage mode of operation, the resistance, which is proportional to the length of the arc, is lower than that in an arc in high voltage mode.

Of the two arc modes, the low voltage mode is known to be the most damaging to the anode. This is because the pressure at the point of arc attachment in the low mode is higher than that of an arc in high mode. The higher pressure leads to a higher current density and thus to a higher heat flux due to the flow of electrons at the anode attachment point.

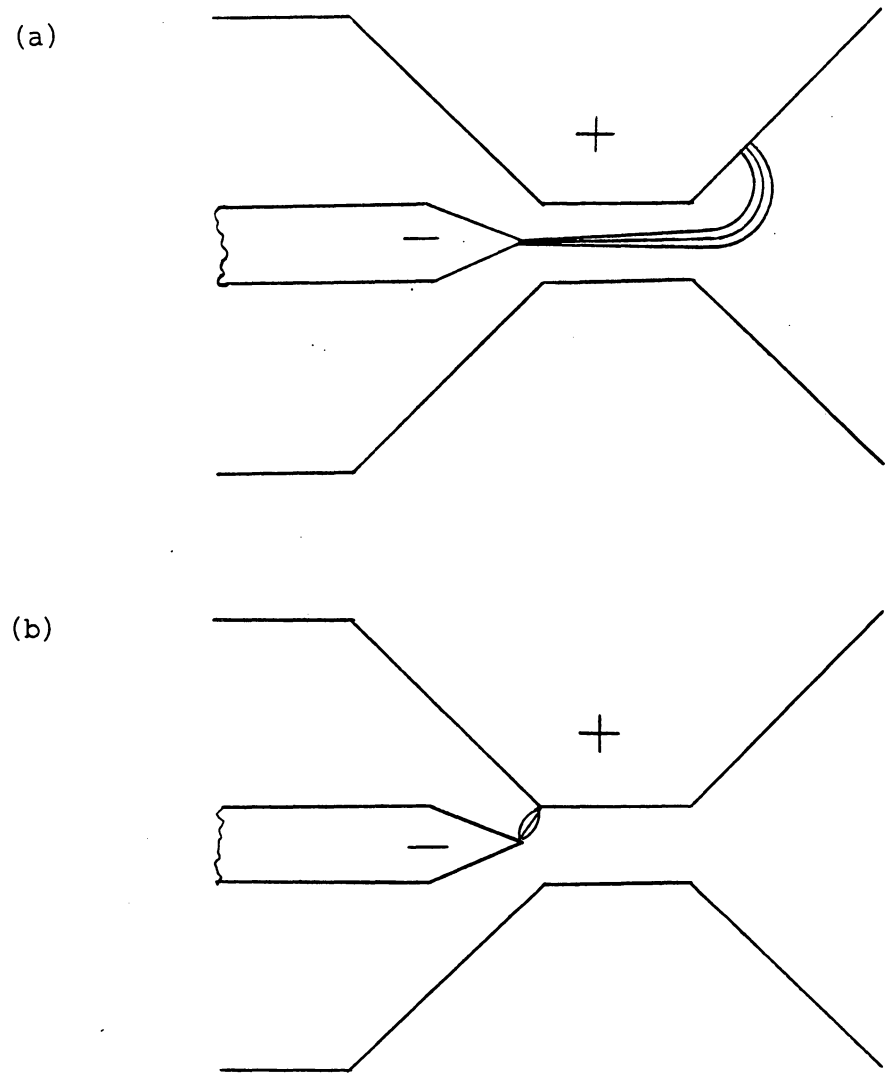

Figure 2. The Two Modes of An Arc: (a) High Voltage Mode (b) Low Voltage Mode

3.3 *The Effect of the Gas Properties On The Arc*

The structure of an arc is dependent on the thermal conductivity and the specific heat of the gases used. For this reason, there are important differences between arcs in monatomic and diatomic gases. There are several reasons for this. First, the vibrational and rotational degrees of freedom present in the diatomic gases lead to higher specific heats. Since the thermal conductivity of a gas is proportional to its specific heat, it will also be greater in a diatomic gas. Therefore, a diatomic gas is more efficient at extracting energy from the arc than a monatomic gas. Also, the dissociation process of the diatomic gas requires energy. Therefore, more energy is required to maintain an arc in a diatomic gas than in a monatomic gas.

In addition to the fact that diatomic gases have larger thermal conductivities and specific heats than monatomic gases, the structure of the arc is affected by the way in which these properties vary as a function of temperature. The specific heat increases in a diatomic gas as the temperature is raised until most of the gas is dissociated. After the gas is dissociated, it no longer has vibrational and rotational degrees of freedom and the specific heat starts to decrease as the temperature increases. The thermal conductivity, because of its dependance on the specific heat, shows the same kind of temperature variation. The result of the large change in the thermal conductivity is that the radial temperature profile of an arc in a diatomic gas will have a very narrow region where the temperature is high enough to ionize the gas [33].

Since the electrical conductivity is dependant on the temperature, the current carrying section of the arc will be narrow. In contrast, the specific heat and thermal conductivity of a monatomic gas such as argon vary little with temperature, so the temperature profile is flatter and the current carrying cross-section is greater. Noeske et

al. [33] note that the current carrying cross-section of the arc is nine times greater in an arc, with the same current, in a monatomic gas than that in a diatomic gas. In order to pass the same current through a smaller cross-section, arcs in diatomic gases have to have higher electrical conductivities, and therefore higher temperatures, at the center of the arc than arcs in monatomic gases. Also, despite the higher temperature and electrical conductivity at the center of the arc, the field strength will be higher in an arc in a diatomic gas than that in a monatomic gas.

3.4 Arc Stability

3.4.1 Arc Stability vs Arc Diameter

The cross-sectional area of an arc column has important implications with respect to its stability. In an arc with a wide cross-section, any waviness introduced to the column by external disturbances will have very little effect on the arc since it will be confined to the outer edges of the arc and there is still a large straight current carrying channel remaining. In contrast, if there is a small disturbance to a narrow arc its current carrying core will have a path which becomes wavy and thus it becomes longer. For this reason, the resistance and electric field can become greater. A problem with a narrow arc is that if fluctuations of the arc, due to turbulence, become great enough a narrow arc can be broken due to the disturbance before a wide arc will [33].

Because of its smaller area and larger required voltage, an arcs is less stable at high pressures than at low pressures. For the same reason, an arc in a diatomic gas is less stable than that in a monatomic gas. One way of making the arc wider, and thus more

stable, is to simply increase the current, however, due to the added heat transfer, the thermal erosion of the anode will be severe if the current is increased. A way of increasing the diameter of an arc in a diatomic gas is to mix a monatomic gas with the diatomic gas as was done in the the study by Barbi [8]. In his work Barbi used argon to provide a high temperature "bath" in which the intended dissociation of hydrogen was accomplished.

3.4.2 Wall Stabilization

Arc columns can be stabilized by constraining their radial movements. One way of achieving this is to use wall stabilization. In this method the arc is passed through a narrow cylindrical constrictor. Because of the radial diffusion of the charge carriers, away from the center of the arc, the arc will be constrained to the center of the constrictor. In the ideal case of wall stabilization, the arc diameter would be the same as the constrictor diameter and the arc would then be completely protected from radial movement. This ideal case is not practical because the melting point of all known solid materials is much lower than the plasma temperatures, thus a real arc will not completely fill any constrictor. But, an arc with a given diameter will be more stable in a smaller constrictor than in a large one since there is less room for the arc to move.

3.4.3 Vortex Stabilization

In a low power plasma torch operating at high pressures the arc diameter will be small. This means that the constrictor diameter will also have to be small for wall stabilization of the arc. Smaller constrictors require tighter tolerance in machining the torch components in order to prevent misalignment of the electrodes. The tolerances

required in building these small components may be difficult or impossible to meet when hard materials such as tungsten are used.

One way of increasing the stability of a wall stabilized arc is to use vortex stabilization. In a vortex stabilized arc, a tangential component is added to the gas velocity upstream of the constrictor section of the plasma torch. As the radius of the nozzle decreases the angular velocity of the gas must increase in order to conserve angular momentum. The increased angular velocity at the constrictor gives several benefits. First, because of the centrifugal forces on the gas, the heavier, and thus cooler, gas will be forced to flow along the constrictor walls while the hot gas will remain in the center of the constrictor. Since the arc will tend to follow the path of least resistance it will remain in the region of the hot gas in the center of a constrictor. Because the arc is constrained to the center of the constrictor, the anode attachment point is in the low pressure region of the nozzle, leading to the desired high voltage mode operation of the torch. As previously noted, the lower pressure will lead to a more diffuse attachment and thus lower the heat flux there. Another benefit of the swirling flow is that the cooler gas flowing by the anode walls will tend to cool them [40].

The swirl also has a major effect on the variation of pressure with radius in the nozzle. The isentropic, swirling flow through a nozzle was studied analytically by Mager [41]. It was found that for this ideal case the density, and therefore the pressure, of the gas becomes equal to zero for an area at the center of the nozzle. The size of this region of zero density was shown to increase with increasing swirl strength. Due to the presence of viscous effects, the region of zero density will never be realized in a real flow, but, the density and the pressure would be expected to be lower at the center axis of the nozzle than it would be at the walls. This was shown experimentally by Batson and Sfrozini [42] for flows with small swirl strengths. Having a region of lower pressure at the center of the nozzle allows the arc to assume a larger diameter and therefore be more stable.

Because of the decrease of the density with the radius, the mass flow for a given chamber pressure will decrease. It was found that even small amounts of swirl could cause large reductions in mass flow [42].

Chapter 4

Previous Plasma Torch Designs

This section presents a review of the designs of continuous plasma torches, which have been used in combustion research studies. Figure 3 shows the device which was used by Northam et al. [6]. The torch is a commercially available plasma torch (Plasmadyne model SG-1B), which was originally designed for flamespraying. The torch has an input power range up to 80 kW, but was only operated in the range of 2-5 kW. The torch has the conventional coaxial arrangement of a pointed cathode surrounded by an extensive straight anode surface. The electrodes were water-cooled in order to reduce the erosion. Because the torch had a large constrictor diameter, the flow was not choked at the flow rates (470 ml/s) which were used. The feedstock gas for this torch was an equal mixture, by volume, of hydrogen and argon. The argon was required to stabilize the arc.

Kimura et al. [24] used a water-cooled torch which was similar in appearance to the one just considered. The torch was operated at power levels of 2 to 5.5 kW. The gases

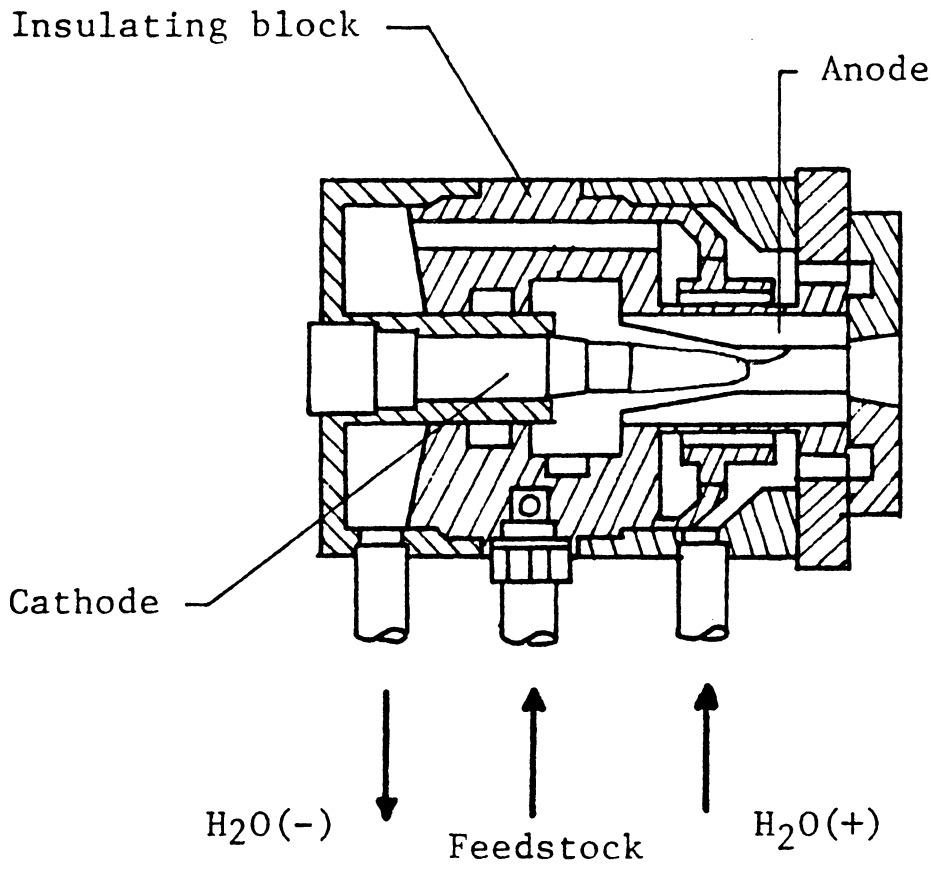

Figure 3. Plasmadyne Torch From Ref [6]

used in the torch were pure argon, nitrogen and hydrogen. The arc was stabilized when operating on pure hydrogen and nitrogen by a high-frequency voltage source coupled to the DC current source. This torch was not choked at the flow rates used (200-830 ml/s). This led to interruption of stable arc operation by pressure pulses outside of the torch.

In a study by Harrison and Weinberg [11], a water-cooled torch with a magnetically rotated arc was used. The torch was operated on feedstocks of nitrogen, argon, and mixtures of argon with hydrocarbons, water, or nitrogen. A field coil was used as the magnet. Arc rotation rates of up to 120,000 rpm were used, with the intent of uniformly heating the gas.

Chan et al. [21] developed a low-power, tunable plasma torch, which is shown in figure 4. The design used a threaded cathode support to provide adjustment of the anode-cathode gap. The converging-diverging anode was made of copper, and required water cooling at many of the operating points. The cathode was a flat ended, 2 percent thoriated tungsten rod. The arc was struck between the flat edge of the cathode and the converging wall of the anode, upstream of the constrictor. This torch was intentionally operated in the low voltage mode so that the voltage required to run the arc would be low. In order to decrease the added heat flux, and thus the electrode erosion, associated with low mode operation, the arc was forced to rotate in synchronization, around both the anode and cathode surfaces, by the interaction of the axial magnetic field, provided by a permanent magnet, and the radial component of the arc current. The arc rotation frequency reported was between 0.5 and 5 kHz.

The torch was designed to utilize various feedstocks, including pure diatomic gases, without the requirement of monatomic gases to stabilize the arc. The arc length is equal to the shortest distance between the cathode and the anode. That the arc length tended to stay at the shortest distance between the two electrodes follows from the Steenbeck minimum principle [29] which states that arcs tend to take on a configuration which

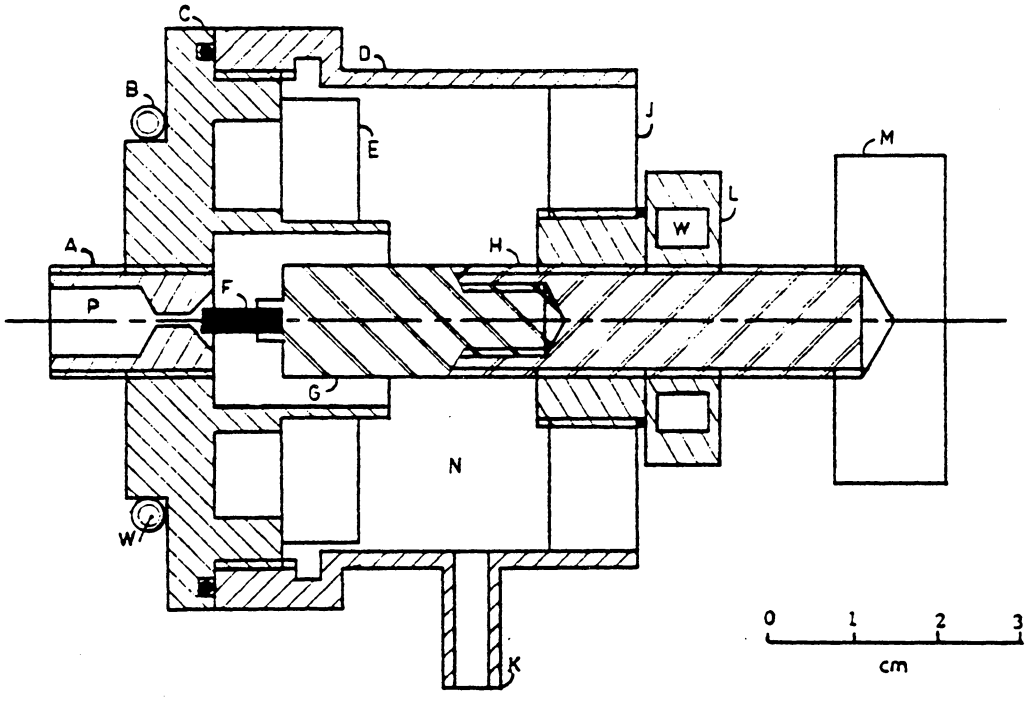

Figure 4. Plasma Torch from Ref [21] : A, anode; B, cooling pipe; C, magnet support; D, outer casing; E, bonded ferrite magnet; F, thoriated (2%) tungsten cathode; G, cathode support; H, arc tuning component; J, insulating plate; K, feedstock inlet; L, water-cooled tuning component; M, tuning knob; N, upstream pressure region; P,downstream pressure region; W, water cooling

minimizes the entropy production. In order to operate the plasma torch at low voltages even on diatomic feedstocks, the shortest distance between electrodes was varied between 0.2 and 0.5 mm depending on the feedstock and the intended application of the torch. The critical electrode dimensions which were used also varied with the intended application of the torch. Experimental data for operation of the torch on nitrogen is reported. For the one point reported which had choked flow, at a back pressure of 1 atm the power was 712 W, the flow rate was 480 ml/s, and the constrictor and cathode diameters were 2 mm and 3 mm, respectively.

This torch was then modified by Behbabani et al. [22], to further enhance the thermal stratification of the plasma jet produced by the torch. Using the same electrode configuration, the magnet, which was used to force the arc through the gas was replaced by a small tangential inlet, which imparted a swirling motion to the gas. The drag force on the arc forced it to rotate around the electrodes in this design. A drawing of this design is shown in figure 5. Since the arc is pushed around the electrodes by the gas, the arc is in contact with the same pockets of gas for longer periods of time. This has the effect of heating a small fraction of the gas to a high temperature rather than to uniformly heat all of the gas. Therefore, the flow of plasma upstream of the constrictor is thermally stratified. The thermally stratified plasma is then dispersed into tiny pockets of hot plasma surrounded by cooler gas by the pressure gradient in the nozzle.

Barbi et al. [8], designed a low-power, uncooled, choked plasma torch for use in supersonic combustion. A drawing of this torch is shown in figure 6. The torch body is machined out of stainless steel. A stainless steel gland fitting was threaded into the back of the torch body. Inside of the fitting were two ceramic insulating pieces to position the cathode and electrically insulate it from the torch body, and a crushable lava sealant, which holds the cathode in position and seals against gas leaks along it. Gas leakage is prevented in the front of the torch by compressing a silver-plated, inconel O-ring

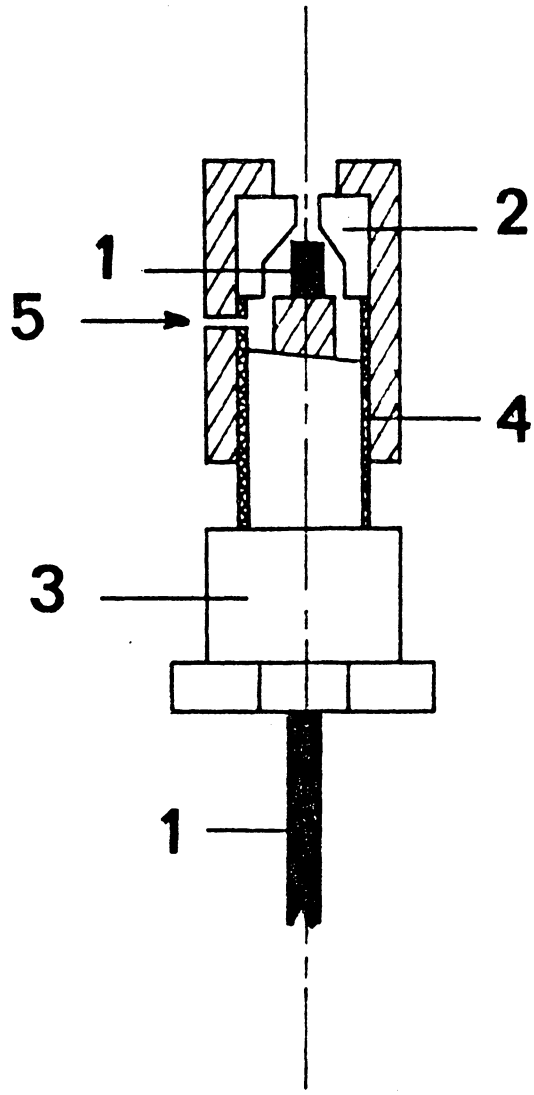

Figure 5. Aerodynamically Rotated Arc from Ref [22]: 1 Cathode; 2 Anode; 3 Spark plug body; 4 Fine thread for gap adjustment; 5 Tangential gas inlet.

between the anode and the torch body. The feedstock gas inlet is tangential in order to impart swirl to the gas, with the intent of forcing the arc to rotate around the anode surface. However, the swirl strength was insufficient to dislodge the arc attachment point when the arc was operated in the high voltage mode.

The anode and cathode geometry are shown in figure 7. The cathode is a 3.175 mm diameter rod of 2 percent thoriated tungsten, which is machined to a cone with a 20 deg half-angle. Thoriated tungsten was chosen as the cathode material because of its low thermionic work function. The anode is a converging-diverging nozzle with a 45 deg half-angle on both the converging and diverging sections. The anode material used was also 2 percent thoriated tungsten, which was chosen over pure tungsten because of its improved machinability. Between the converging and diverging sections is a 0.813-mm diameter, 1.02-mm long constrictor. The gap length, as defined by G in figure 7, was typically 0.178 mm.

The arc originates at the pointed cathode and is forced through the constrictor section by the motion of the gas to a point in the diverging section. The actual point where the arc attaches in the anode is a complex function of arc parameters, so that the arc length is not strictly fixed by the geometry of the electrodes as it was in the torch which was shown in figure 4. This torch design was the starting point for the modified torch design presented in the next chapter .

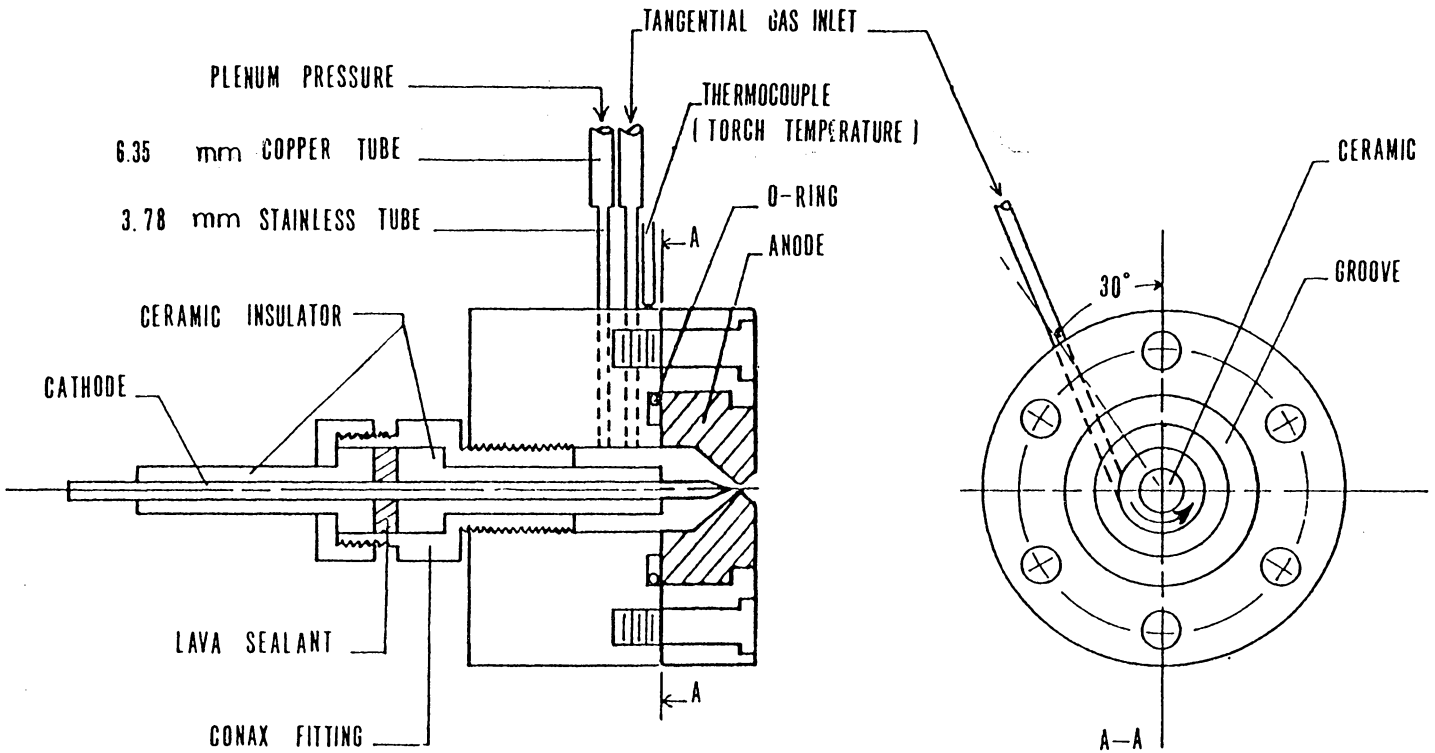

Figure 6. Uncooled, Choked Plasma Torch from Ref [8]

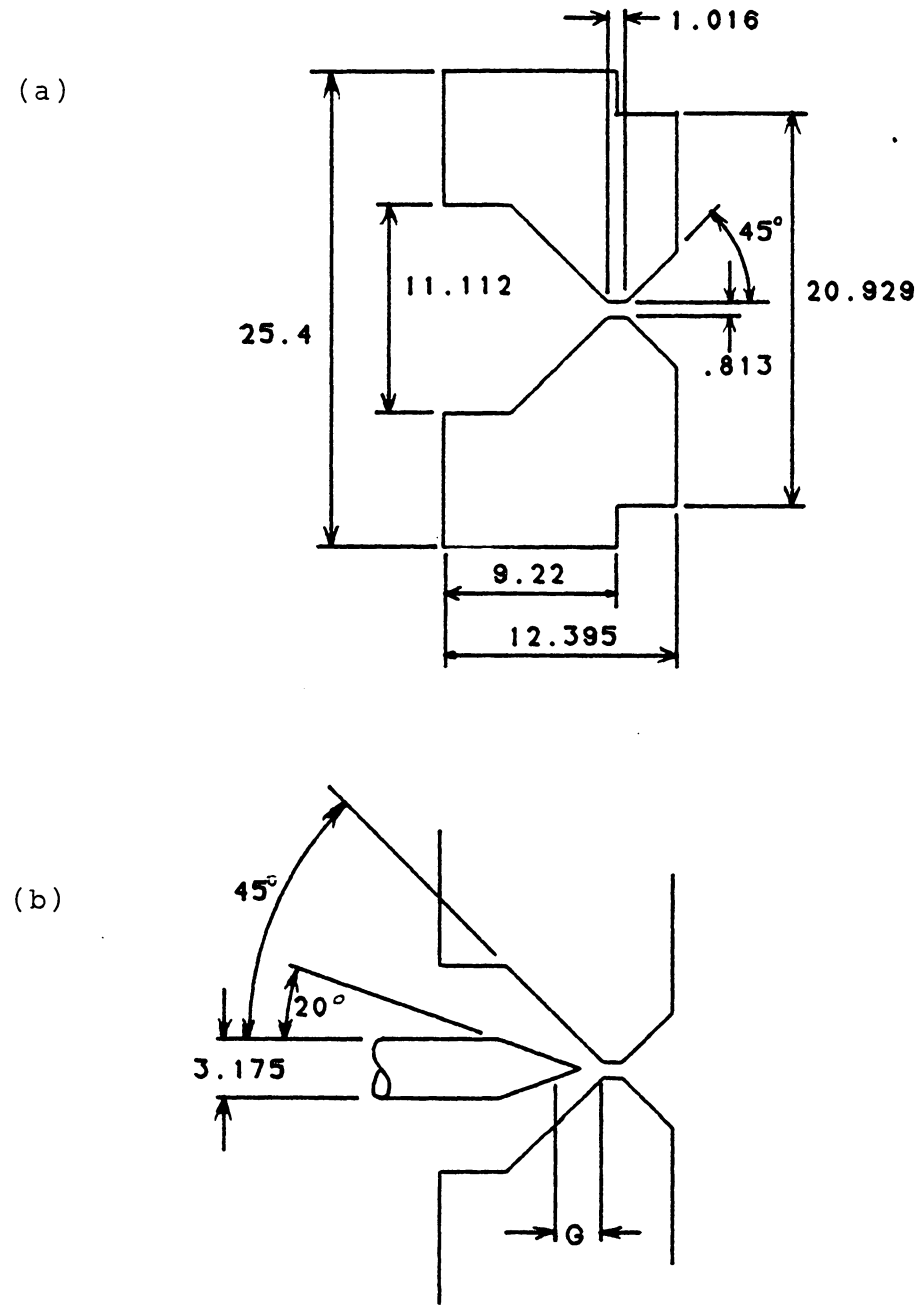

Figure 7. Electrode Geometry of the Torch from Ref [8]: (a) Anode. (b) Anode and Cathode.

Chapter 5

The Improved Plasma Torch Design

5.1 Overall Description

A cross-section of the final design of the torch is shown in figure 8. In the discussion of the torch in the following sections, frequent references are made to the components in this drawing by enclosing the letter denoting the part in figure 8 in parenthesis. Each of the components of the plasma torch can be considered as a member of one of three groups, depending on whether it is electrically positive, negative, or insulating. The anode (A) and the parts which are in electrical contact with it (B-G) form the electrically positive section of the torch, while the negative section of the torch is formed from the cathode (I) and the parts in electrical contact with it (H-Q). The positive and negative sections of the torch are electrically separated by the insulators (R-V).

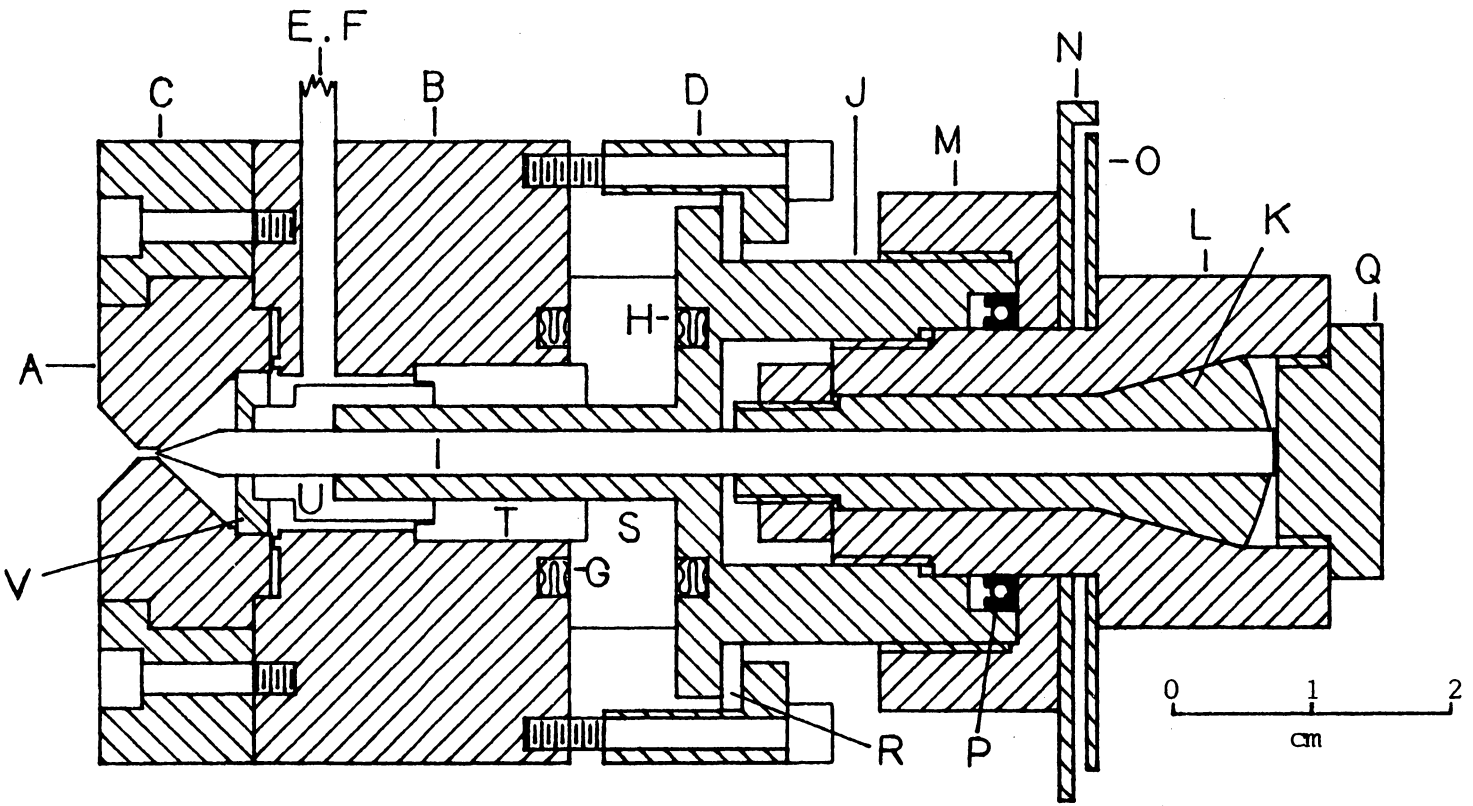

Figure 8. Adjustable Gap Plasma Torch A, anode; B, body; C, anode holder; D, pressure ring; E, gas inlet; F, pressure tap; G,H, E-ring seals; I, cathode; J, cathode alignment piece; K, collet; L, cathode adjustment knob; M, gland cap; N, mounting bracket; O, angle indicator; P, dynamic seal; Q, end cap; R,S, insulators; T, alignment piece; U, insulator; V, flow swirler

5.1.1 Positive Section of the Torch

The anode (A) is held against the torch body (B) by the anode holder (C), both of which are made of stainless steel. Six hardened-steel, Allen-head cap screws (size 3-48) are used to fasten the anode holder to the torch body. Two passages are drilled radially into the torch body to serve as the gas inlet and the chamber pressure tap. Two stainless steel tubes (E and F) fit into the passages and are held in place by silver solder. The tubes may be seen in the photograph of the torch in figure 9. Also shown in this picture is the k-type thermocouple which is soldered to the side of the torch body.

The remaining part of the positive section of the torch is the stainless steel pressure ring (D). This ring is used to hold the positive and negative sections of the torch together. Six hardened-steel Allen-head cap screws (size 3-48) supply the force necessary to hold the two sections of the torch together.

The positive section of the torch is allowed to float with respect to ground. The electrical connection to this part of the torch is made through the feedstock gas inlet tube (E).

5.1.2 Negative Section of the Torch

The negative section of the torch consists of the cathode and the pieces which guide it and make it possible to adjust its position. The construction of this section of the torch is centered on the cathode alignment piece (J), which is physically connected to the positive section of the torch. The Cathode (I) is held by a collet (K) which is fitted to the cathode adjustment knob (L). The adjustment knob has a fine thread (40 threads per inch) on the outside of it which mates with that on the inside of the cathode alignment piece (J), allowing axial adjustment of the cathode.

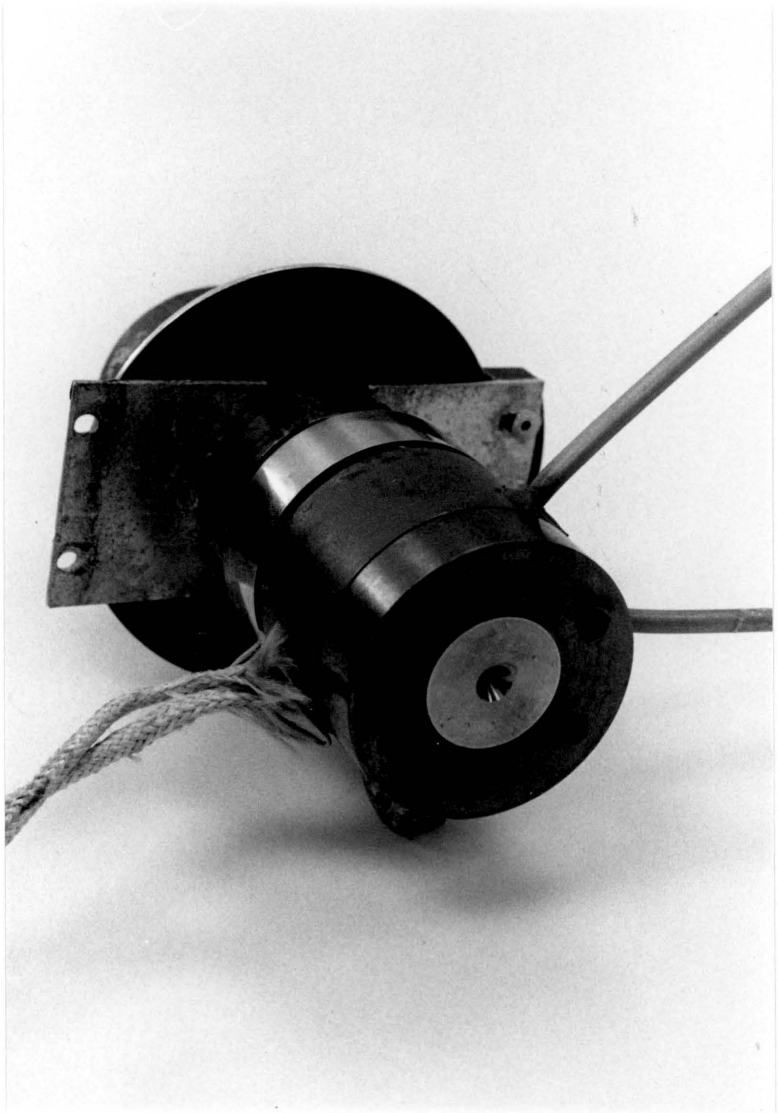

Figure 9. Photograph of the Improved Plasma Torch.

The angular position of the adjustment knob is determined by reading the angle indicator (O) which is mounted to it. Knowing the change in the angle and the pitch of the thread allows the the change in the axial position of the cathode to be calculated. The angular indicator may be seen in figure 10 which shows the rear view of the torch. Also shown is a phenolic knob which is used to insulate the cathode adjustment knob so that it may be safely adjusted during operation. The insulating knob is attached to the adjustment knob by six screws which are countersunk into it. For safety, the screws are covered by electrical tape.

The mounting bracket (N) is connected to the the gland cap (M) by four small flat screws. The gland cap is then screwed on to the outside of the cathode alignment piece (J). The mounting bracket is also attached to a piece of phenolic which is mounted to the test stand. The bracket and the angle indicator (O) are both made of aluminum while the adjustment knob (L), gland cap (M), and cathode alignment piece (J) are all made of stainless steel.

The negative section of the torch is allowed to float with respect ground. The electrical connection to this section of the torch is made through the mounting bracket (N).

5.1.3 Insulators

There are five insulators used in the construction of the torch. These are shown as components R-V in figure 8. The insulator U and the flow swirler V are the two closest insulators to the arc and are exposed to higher temperatures than the other insulators. Grade HP boron nitride (Sohio Materials) was chosen for these parts because of its high melting temperature. In an atmosphere of hydrogen it may be used at temperatures up

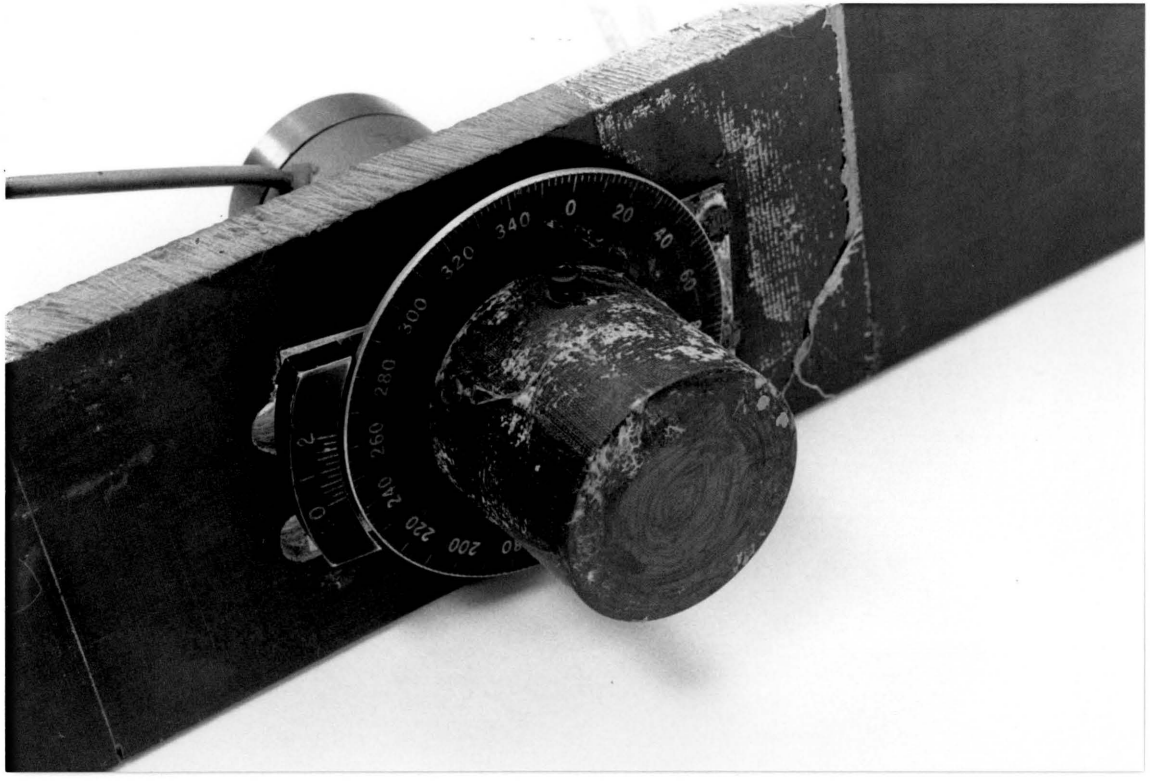

Figure 10. Back View of the Plasma Torch

to 3000 C. In addition, the boron nitride is soft enough that the grooves in the flow swirler (to be discussed later) can be easily machined.

The component (T) serves as an alignment piece and the component (S) is used to form a gas seal. A harder material than boron nitride was required for these pieces in order to keep the electrodes aligned. For this reason, Macor machinable glass ceramic (Corning) was used. Although macor has a lower melting point than boron nitride, melting was not a problem in this region of the torch. The insulators discussed above all fit together so that loose graphite from the gaskets (to be discussed later) cannot become wedged between the positive and negative portions of the torch, causing short circuits.

The insulator (R) is used to insulate the positive and negative sections of the torch from each other while transmitting the force which holds the two sections of the torch together and compresses the two E-ring seals, (G and H). The temperatures in this region of the torch are low enough that glass phenolic could be used for this part. The phenolic was used because it is less brittle than the ceramic materials.

5.2 Electrodes

Both of the electrodes were machined from 2 percent thoriated tungsten, which is the same material which was used in the old torch design. Since the objective of the redesign of the torch was to improve the torch performance without changing the internal electrode geometry of the existing torch, the internal electrode geometry was kept the same as that shown in figure 7. However, the external geometry of the anode was changed to ensure better alignment with the cathode.

Proper electrode alignment is important for several reasons. At the gaps used the cathode is very close to the anode, so that small errors in the alignment can lead to large changes in the electrode geometry in the region of the cathode tip. One effect of misalignment is to cause asymmetry in the electric and magnetic fields in the vicinity of the cathode tip. Also, misalignment can have major effects on the fluid mechanics in the region of the tip. The combination of the fluid mechanical and the electrical and magnetic fields can affect where the arc attaches to the anode. It is desirable to have arc attachment in the low pressure region of the anode.

The electrodes are in perfect alignment when the center lines of each are coincident. Figure 11 shows the two ways in which the electrodes may be out of alignment. The first way, shown in figure 11 (a), is that the centerlines of the two electrodes are parallel but are radially displaced from each other. The second type of misalignment is from having the centerlines nonparallel as shown in figure 11 (b). Both kinds of misalignment have been encountered in the old torch design. In addition, the method of gap adjustment used in the old torch tended to aggravate the misalignment, especially the angular offset.

The alignment of the electrodes in the new torch is ensured by aligning both of them with the centerline of the plasma torch body. In the old torch design the anode was seated against a metal O-ring, which had to be crushed in order to form a seal. The metal O-ring had several disadvantages. First, a large force was required to form the seal. In addition, there was no way to ensure that the O-ring was evenly crushed. The only alignment of the anode with the torch body was that provided by the anode holder and the screws used to hold it to the body. In the new torch, the O-ring was replaced by a graphoil gasket. Also, the new torch anode has a shoulder cut into it which mates with a groove cut into the torch body which is concentric with the centerline of the the torch body, so that the anode and the torch body are in radial alignment. The bottom surface of the anode and the ridge on the torch body which it rests against are both flat, and the

graphoil between them is easily crushed, so that the angular alignment of the torch body is ensured.

The gland fitting used in the old torch has been replaced with the cathode alignment piece (J) and the pieces associated with it. The cathode is aligned with the centerline of the cathode alignment piece which, in turn, is kept in alignment with the torch body by the alignment piece (T). The possibility of angular offset of the cathode is reduced by the long, tight fitting section of the cathode alignment piece, which guides the cathode.

5.3 Gas Seals

The prevention of gas leaks from the torch is essential to insure proper operation of the torch. Gas leaks cause a drop in the chamber pressure of the torch, which can lead to the undesirable low mode operation of the torch. Also, proper sealing of the torch is important to ensure accurate metering of the flow which actually passes through the torch. In addition, for safety, when hydrogen is used as a torch feedstock, it is important that all it pass through the anode, to prevent accumulation of hydrogen.

The gas inlet and pressure tap tubes are permanently sealed by the silver solder which holds them in place. The seal between the anode and the torch body is made by using 0.254-mm thick, grade GTA, graphoil tape (Union Carbide) to form a gasket. The gasket is pressed between the anode and the small ridge on the torch body. Graphoil is 99.5 percent graphite and may be used at temperatures up to 3000 C. It is also an excellent conductor of electricity. In fact, special care had to be taken while assembling the torch to prevent short circuits caused by loose graphite particles.

Leakage from the back of the torch body is prevented by two E-ring seals which are shown as G and H in figure 8. The E-rings are made of Inconel X-750 and are silver

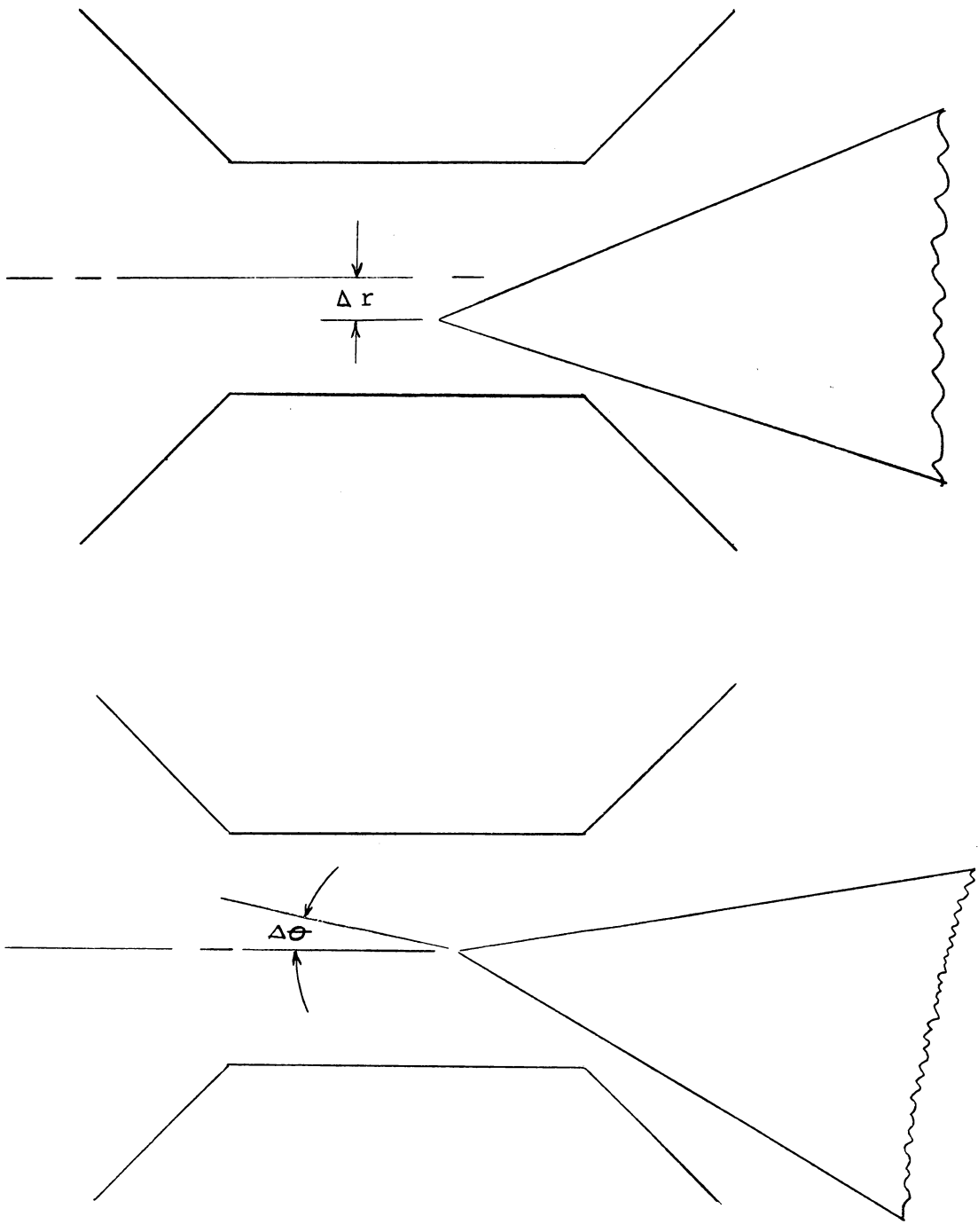

Figure 11. Electrode Misalignment: (a) Radial Offset (b) Angular Offset

plated. There are two contact lines along each face of the seals where the silver plating is smeared into the surface irregularities of the mating parts, thus forming a seal. The E-rings were chosen over other metal seals (such as O-rings) because the force necessary to form the seal against the macor insulator plate (S) is lower. During some of the later tests, graphoil gaskets were used between the E-rings and the macor plate to aid in sealing.

The remaining path of escaping gas from the torch is between the cathode (I) and the cathode support assembly (J). Two seals are used here. The first seal is formed between the end cap (Q) and the cathode adjustment (L) by using teflon thread sealant tape on the threads of the end cap. The remaining seal (P) is formed between the cathode adjustment and the cathode support. Unlike all of the other seals this is a dynamic seal which has to accommodate the sliding and rotation of the cathode adjustment. The seal used was an Enerseal Mark I spring energized seal from the Advance Products company. The seal consists of an inner stainless steel spring, surrounded by a 10 percent Ekonal-filled teflon jacket, which forms the sealing surface. The seal is placed into a gland in the cathode support piece and the end of the gland is formed by the gland cap (M) which screws onto the cathode support piece. This seal may be used at temperatures up to 315 C.

5.4 Flow Swirler

The establishment of a vortex in the nozzle of the plasma torch is desirable for several reasons. As noted in the previous chapter, the vortex can be used to provide stabilization of the anode attachment point in the low pressure region of the nozzle (high voltage mode). Also, the vortex increases the convection from the constrictor walls.

Another possible benefit is rotation of the anode attachment point of the arc, so that the heat flux to the anode and thus the erosion there is reduced. The original torch used a tangential fluid entrance to the chamber with the intent of causing the arc to rotate. However, the diameter of the tangential inlet used was much larger than the throat diameter, so that little rotation was imparted to the flow field. For this reason the tangential inlet was replaced by a straight inlet to the chamber followed by a flow swirler placed in the anode.

The flow swirler was required to be small, sturdy and able to withstand extended exposure to high temperatures. For these reasons a stationary swirler is used to introduce a tangential component of velocity to the flow. The swirl strength is proportional to the angular momentum of the flow divided by the radius of the nozzle [42]. The angular momentum of a given fluid is proportional to the product of radius and the tangential component of the velocity. It is desirable to have as much swirl as possible at the anode attachment point. While the angular momentum in an inviscid flow will remain constant throughout the nozzle, angular momentum will be dissipated in a viscous flow. The dissipation of angular momentum in the nozzle is expected to be negligible until the constrictor is reached, where the high velocity gradients occur.

The flow swirler is shown in figures 12 and 13. The swirler is simply a stationary plate of boron nitride with four flow passages cut into the outside circumference of it. The flow passages are 1.52 mm deep and 0.508 mm wide which are inclined at an angle of 45 deg with the cathode axis. The flow exits the swirler at the chamber radius, since this is the maximum radius available. The swirler sits in the anode against a shoulder, so that a small part of the outside surface of each flow passage is blocked. The back of the flow swirler is sealed by a graphoil gasket which is pressed between the swirler and the insulator (U). All of the gas flow through the torch passes through the flow passages. The net area of each flow passage at the entrance to the nozzle is about 0.5

mm^2 which may be compared with a constrictor area of 0.495 mm^2 so that the net area of flow passages is about four times the area of the constrictor. The smaller area of the flow passages means that the angular velocity, and thus the angular momentum of the gas exiting the swirler will be larger than that from the tangential inlet of the original design. The flow area of the swirler was chosen to be greater than the constrictor area so that the pressure drop across the swirler is negligible. Also, the larger swirler flow area allows the torch to be operated without choking the flow at the swirler if the nozzle erodes to a larger diameter.

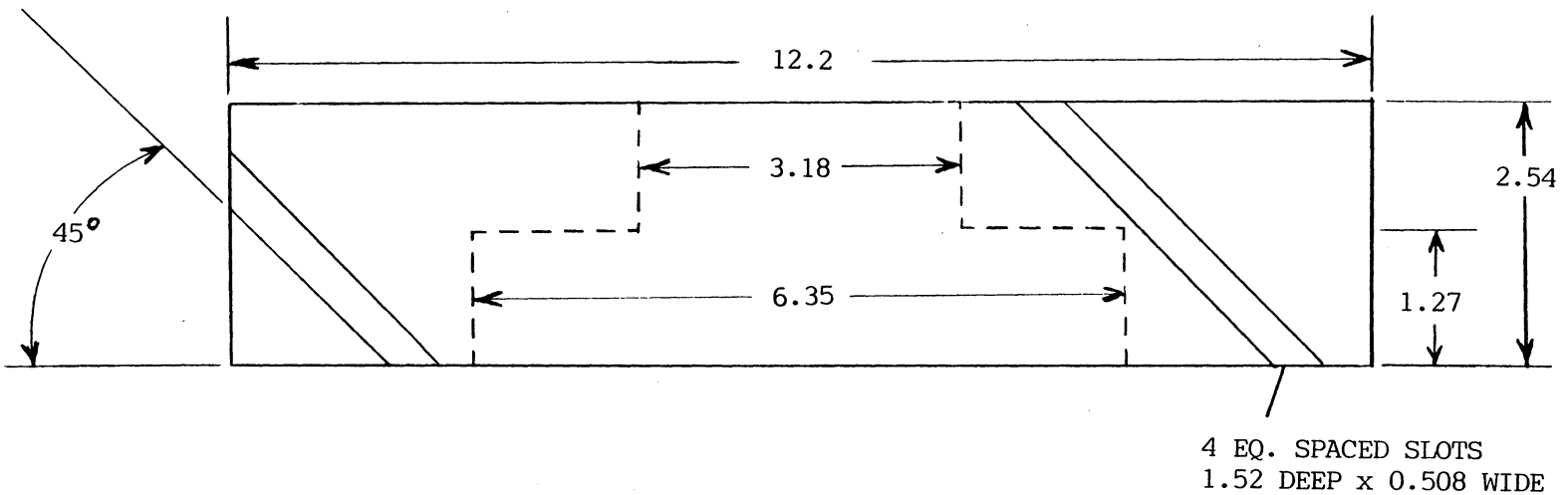

ALL DIMENSIONS IN mm

Figure 12. Cross Section of Flow Swirler.

Figure 13. Photograph of the flow swirler.

Chapter 6

Test Apparatus and Instrumentation

6.1 Experimental Setup

The facility which was used for this research is located within the Virginia Tech High Speed Turbomachinery Research Laboratory. A schematic diagram of the lab and equipment is shown in figure 14. Because hydrogen gas was used as a torch feedstock, special measures were taken for safety. The high pressure gas cylinders, gas supply lines, and test cell were located outside of the main lab building to ensure that there was no possibility of hydrogen gas accumulation within the building. The torch current and gas flow were controlled from inside of the main lab building. A video camera mounted inside of the test cell permitted continuous observation of the plasma torch from inside the main building.

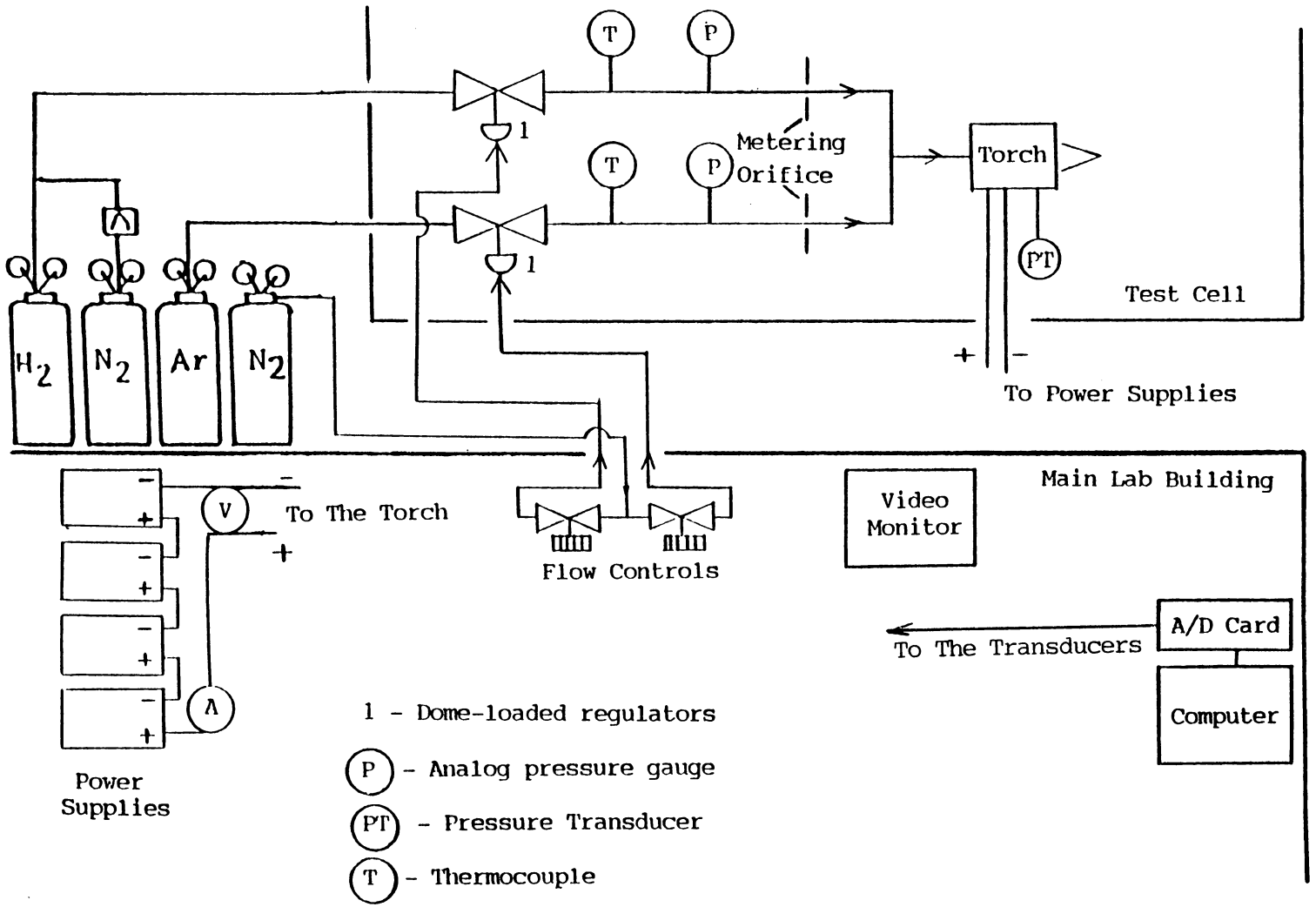

Figure 14. Schematic of the Laboratory.

The test cell was a modified metal utility building. In order to prevent hydrogen accumulation, vents were cut into the bottom of the test cell and a fan and exhaust hood were mounted over the torch exhaust. All pressure transducers and flow metering apparatus are located inside of the test cell. The torch was mounted on a support stand constructed of wood and phenolic. A picture of the torch mounted on the stand is shown in figure 15. When the electrode gap of the torch is adjusted during operation, it is necessary to look at the back of the torch, up, toward the exhaust hood. Two pieces of plywood, mounted on top of the torch stand, were used to shield the eyes of the person adjusting the gap from the radiation which is reflected from the exhaust hood.

6.2 Power Supply

The electric power was supplied by four Miller Electric constant current, D.C., welding power supplies (model SR-150-32), connected in series. The power supplies were each continuously adjustable through a range of 5 to 170 A. The set of four power supplies had to be used in order to supply the voltage necessary to operate the arc on high fractions of diatomic gases. Current adjustments were made by turning the control knob on each power supply. All four control knobs had to be set at about the same current setting for best performance. The supplies were each rated at an output open-circuit voltage of 80 V for an input open-circuit voltage of 230 V. However, the available input line voltage to the power supply was only 208 V, so that the open-circuit voltage available from the power supplies was actually only 68-70 V per machine. In the early experiments, only two power supplies were used and the arc was started by the use of a high frequency arc starter. With the addition of the other two power supplies the high frequency starter was disabled and the arc was started by the open-circuit voltage

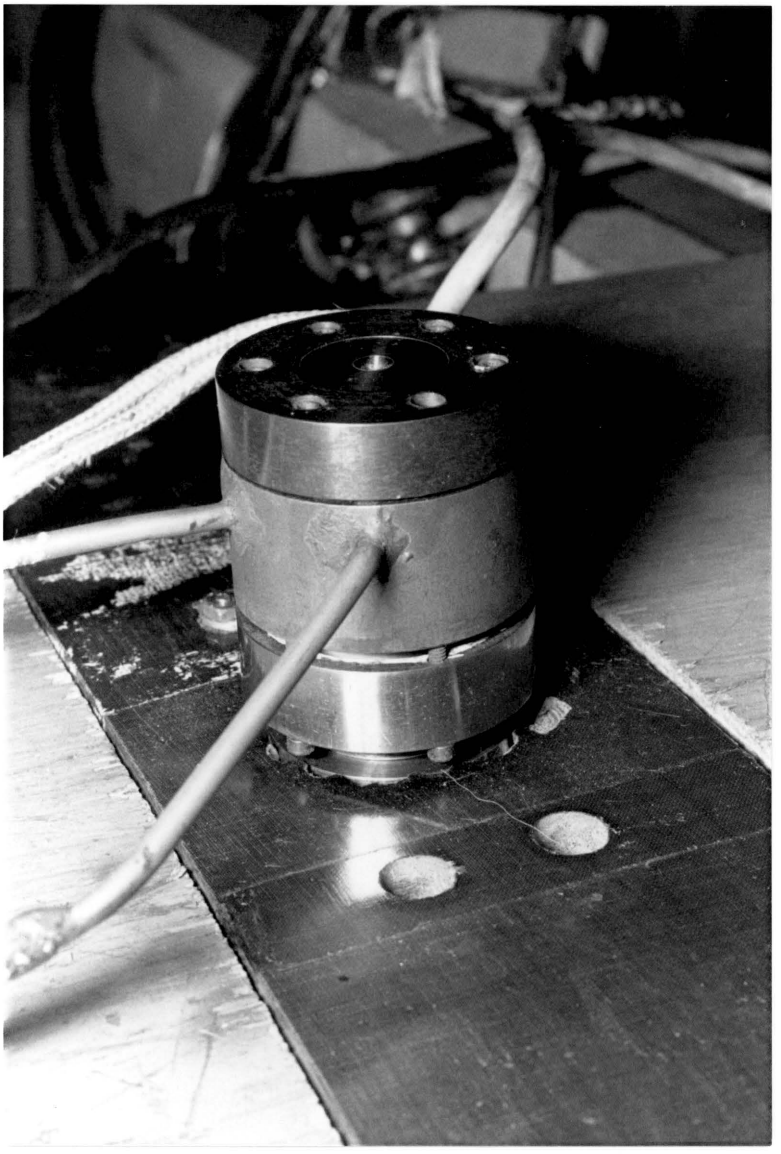

Figure 15. Plasma Torch and Test Stand.

available from the power supplies, which was about 280 V, and a small gap between the electrodes.

In order to reduce the amount of electromagnetic interference (EMI) radiated from the power supplies to the data acquisition system, the power supplies were located on the opposite side of the lab from the computer. Welding cable was used to connect the power supplies to the torch. Neither of the leads to the power supply were connected to ground.

6.3 Electrical Measurements

6.3.1 Current Measurement

Measurements of average current and voltage were recorded by a microcomputer-based data acquisition system, which is discussed later in this chapter. In initial tests, with argon as the feedstock, the current was measured by the voltage drop across a 1 mΩ shunt resistor, located in the positive lead to the torch. However, high EMI and a cross coupling between the voltage and current signals, occurred when diatomic gases were used in the torch. With the torch operating on hydrogen, the output voltage from the current shunt was several orders of magnitude less than the background noise. A larger shunt resistance could have been tried, but this would have resulted in a decrease in the voltage available to the torch. In addition, a larger resistance would not have solved the problem of cross coupling between the current and voltage signals.

In order to eliminate the problems associated with the shunt resistor, a current transducer operating on the Hall effect was used. The transducer used was an LEM

module LT 100-S, manufactured by Liasons Electroniques Mechaniques. The module uses a feedback system in which the magnetic flux, produced by the current in a primary coil (the current to be measured), is balanced by the flux produced by the current in a secondary coil. The magnetic flux balance between the primary and secondary coils is detected by a Hall effect sensor. The sensor is equipped with electronic circuitry which controls the secondary current, so that there is zero net magnetic flux. Therefore, the current in the secondary circuit is a related to that in the primary circuit by

$$N_p I_p = N_s I_s,$$

in which I is the current and N is the number of turns.

The ratio of primary to secondary turns, which is equal to the ratio of secondary to primary currents, was 8 to 1000. A power supply, with both positive and negative 12 V outputs with respect to ground, was used to supply the current in the secondary circuit, which was measured by the voltage drop across a 25 Ω, 40 W shunt resistor. The large power capacity resistor was used to eliminate any change of the resistance due to heating of the resistor. This arrangement gave a sensitivity which was 200 times higher that of using a shunt resistor in one of the torch leads. But, more importantly, the LEM module provided complete electrical isolation between the primary and secondary currents, eliminating any cross coupling between the current and voltage signals to the computer. The LEM module has a measuring range of 0 to 200 A, and a response time of less than 1 μs.

The adjustment of arc current was difficult because all four power supplies had to be adjusted to essentially the same current setting. In addition, the power supplies were capable of supplying much more current to the torch than desired. For these reasons, it was important to have an indication of the current while it was being adjusted. Therefore, a 1 mΩ shunt resistor was placed in the torch power leads at the power supply

and the voltage drop was measured by a digital voltmeter (Fluke 8050A), so that the average value of the current was known while it was being adjusted. During arc operation, the shunt resistor was used as a check against the average current reading from the LEM module. The two separate readings of current were found to be in good agreement. Also, the shunt provided a redundant measure of current in case of computer failure.

6.3.2 Voltage Measurement

The maximum steady voltage across the torch was the 280 V open-circuit voltage, which was floating with respect to ground. Therefore, a 50 to 1 voltage divider was used to keep the voltage signal to the A/D card within the input range to the card, and to protect the card from the common mode voltage.

Also, an analog voltmeter was used at the power supplies to monitor the condition of the power supplies at start-up and to provide an early indication of possible short circuits in the plasma torch. In addition, the analog voltmeter was used to verify that the computer was recording the correct voltage during arc operation.

6.4 Torch Pressure and Temperature

The pressure in the torch chamber was measured upstream of the swirler from the pressure tap shown in figure 8. The transducer (OMEGA PX 500) had a signal output of 0 to 5 V corresponding to pressures of 0 to 200 psig (0 to 1.38 MPa). The transducer was electrically isolated from the torch voltage by using a short piece of rubber tubing in the line between it and the torch. The output voltage from the transducer was

measured and the average was recorded by the data acquisition system once each second. Since the transducer was isolated from the torch voltage and the output from the transducer was on the order of 1-2 V, no analog filter was needed to further average the signal. The pressure transducer was calibrated with a dead weight tester. Also, during arc operation, the reading from the transducer was checked against an analog gauge in the test cell in order to verify that EMI did not cause any errors in the average signal from the transducer.

The torch temperature was measured on the outside of the torch body as shown in figure 9 by a chromel alumel (k type) thermocouple. The output from the thermocouple was displayed at the flow control panel on an analog indicator (API instruments) and recorded by hand.

6.5 Data Acquisition System

One of the goals of the test program was to continuously monitor the torch parameters, current, chamber pressure, and voltage, continuously, for periods lasting up to 20 hours. A microcomputer-based data acquisition system was used to accomplish this. The system was based on an IBM personal computer equipped with a 30 MByte memory card, a multifunction card (MF-100), and a data acquisition card (Data translation DT-2805).

The DT-2805 card was used to provide analog to digital conversion. It features software a 12-bit A/D converter, and software programmable gains of 1, 10, 100 or 500. The maximum useful input range to the card is -10 to + 10 V. The A/D speed of the card is 13,500 samples per second at lowest gain and 6000 samples per second at highest gain.

A DT-707T terminal strip was attached to the DT-2805 card in order to provide screw terminal connections for the transducer outputs.

Data acquisition was controlled by a program written in compiled BASIC. The program uses PCTHERM software from Data Translation. A copy of the program is listed in Appendix B. After being triggered by the presence of a current in the torch (arc ignition), the program acquires the torch pressure, voltage, and current, displays them to the computer monitor, and records them in a file on the memory card. Because the tests were expected to last for hours, data were recorded only once each second for each of the channels.

Due to EMI from the arc, the signals from the transducers had large fluctuations associated with them, so that filtering was needed. Since the speed of data acquisition was greater than the time interval at which data was recorded, it was possible to sample each channel many times each second and compute an average value from the samples for each channel, thus filtering some of the noise from the signal. In addition to digital averaging, low-pass R-C filters, which can be seen in figure 16, were used on the voltage and current signals.

To determine the average value for the signal the PCTHERM routine "Measure Volts" is used, this program sets the amplifier to the best gain for the input signal, takes 16 readings of the voltage, and returns the average. The data acquisition program uses a loop which is repeated 65 times per second, in which this routine is called once for each of the three input channels. The average is then computed and recorded for each of the 3 data channels.

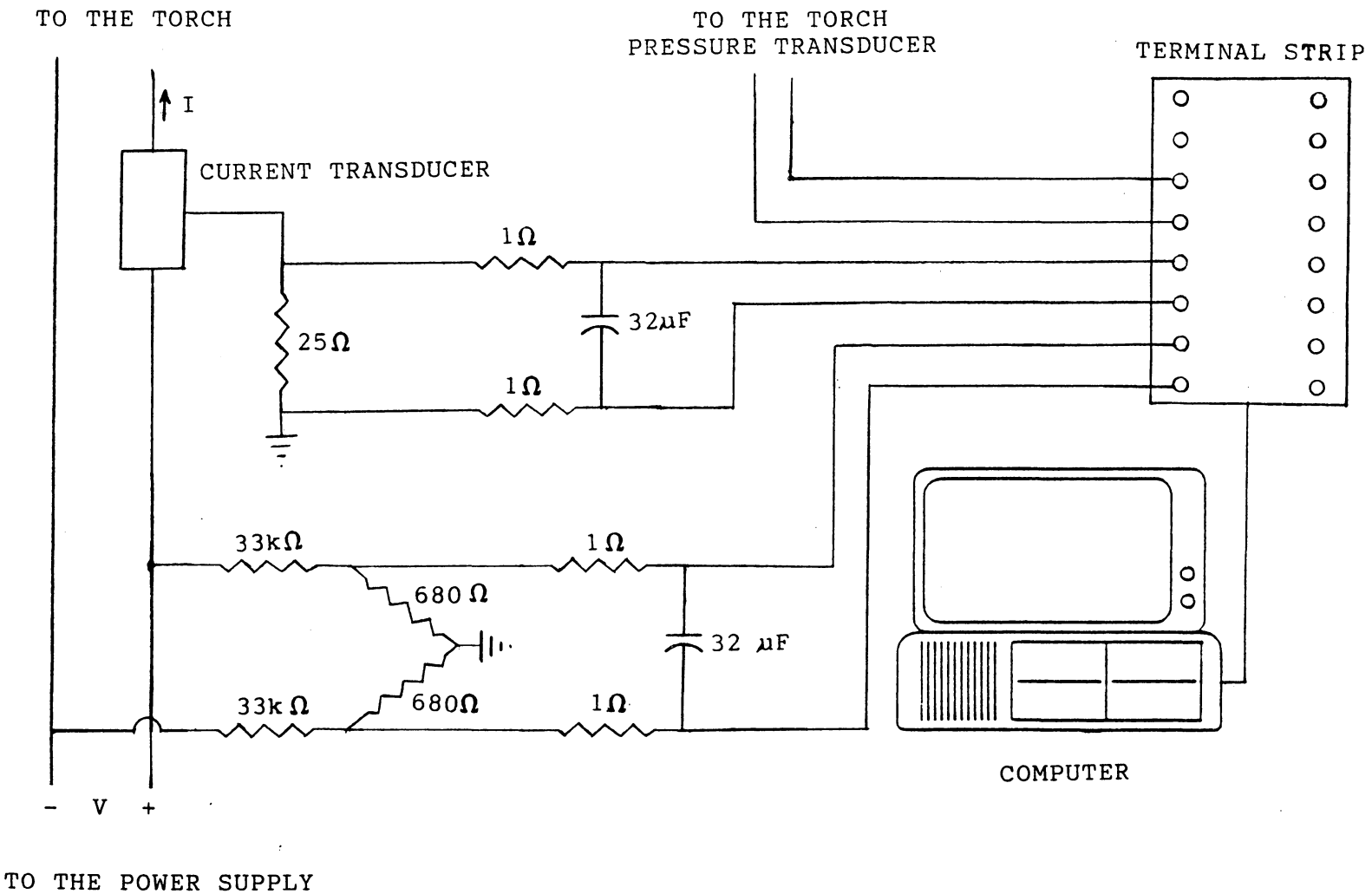

Figure 16. Data Acquisition System.

6.6 *Flow Measurements*

The flow measurement and regulation system is shown in figure 14. Gases are supplied by high-pressure gas cylinders. All of the feedstock gases used were commercial grade (99 percent pure). Copper tubing is used for all of the gas lines except for a short piece of rubber tubing to insulate the flow system from the torch voltage. The flow of the torch gases is regulated from the flow control panel inside the main lab building by changing the pressure in the control lines to the dome loaded regulators in the test cell. For safety, nitrogen is used in the control lines. The volumetric flow rates of the torch gases are calculated from measurements of pressure and temperature across calibrated orifices.

Nupro "S" series fine metering valves were used for the orifices. The temperatures of the gases were measured by iron-constantan thermocouples located upstream of the orifices. The pressures upstream of the orifices were initially measured with a pair of low voltage output pressure transducers and a digital readout mounted on the flow control panel. While this worked well for the tests of the torch operating on argon, the measurements were in error during tests with diatomic torch gases due to the associated EMI. For this reason, the upstream pressures were measured with analog pressure transducers and the readings were recorded by hand.

Due to the low flow velocity upstream of the orifice, the pressures and temperatures measured there are considered equal to the stagnation values. Because the distance from the downstream of the orifice to the torch is small, and the flow velocity is low, the pressure drop between the downstream of the orifice is negligible. Thus, the torch pressure is equal to the downstream pressure on the orifice.

A calibration of volumetric flow rate against upstream orifice pressure was made under the condition of a choked orifice. The flowmeter used (Singer DTM-115) was traceable to the National Bureau of Standards. The mass flow rate was calculated from the the measured pressure drop across the orifice by assuming steady, reversible, adiabatic flow along with the discharge coefficient obtained from the calibration. After the orifice becomes choked, the pressure ratio across the orifice is constant and the mass flow becomes a linear function of upstream temperature and pressure, independent of the downstream pressure. The volumetric flow rate at standard temperature and pressure (STP = 0 C and 1 atm) was calculated by dividing the mass flow rate by the density of the gas at STP.

During testing, the upstream pressures are set at a known value and are recorded by hand along with the temperatures of the gases. These data and the data file with the torch chamber pressure were used in a computer program to calculate the volumetric flow rate of the gases. When the pressure ratio across the metering orifice is such that the orifice is unchoked, the mass flow rate is corrected by the computer program assuming that the flow is the reversible, adiabatic flow of an ideal gas.

Chapter 7

Experimental Results and Discussion

7.1 Test Procedure

First, the torch was assembled and the gap was set to its initial position. This was done by decreasing the gap until electrical contact between the electrodes (gap = 0) was verified with a multimeter, and then turning the gap adjustment knob back until its angular position corresponded to the desired gap. After the gap was set, the torch was connected to the gas lines. Before each test, the hydrogen gas line was purged with nitrogen. The torch and gas lines were then checked for gas leaks with leak detection fluid, and the test cell fan was turned on to insure ventilation. Then the data acquisition system and all of the instruments were turned on.

The arc was always started with argon flowing through the torch. The open-circuit voltage (280 V) was used for arc ignition. To start the arc, the torch was first set to the

desired gap and the four supplies were turned on. In some of the tests the arc would start at the desired gap. When the arc did not start at the desired gap, the gap was decreased until the arc started. Immediately after starting, the gap was adjusted back to the desired setting. The electrode gap at which arc ignition would occur varied from test to test, presumably because of the changes in the electrode geometry, but was within the range of the normal operating gap. Electrical contact never had to be made in order to start the arc.

After arc ignition, the data acquisition system automatically began to record the data. After a warm-up operation period on pure argon, the nitrogen or hydrogen was mixed in with the argon and then the argon flow was decreased. When it was necessary to enter the test cell while the torch was operating, hearing and vision protection were required. Most of the time the torch was observed by video camera and the test cell was only entered to change the arc gap or to read a pressure gauge. Tests ended by the extinction of the arc or by turning off the power supplies. After tests with hydrogen-containing feedstocks, the hydrogen line was purged with nitrogen.

7.2 Overview of Tests

The final torch design was operated on feedstocks of argon, hydrogen, nitrogen, hydrogen-argon and nitrogen-argon mixtures. The nitrogen and hydrogen were chosen as feedstocks because both have shown chemical effects on combustion in the investigations reviewed in Chapter 2. Argon was used during torch start up and while the torch was warming up. Pure argon plasmas have been shown to be relatively ineffective as ignition and flameholding sources, but because arcs are difficult to maintain in diatomic gases, argon was mixed with the diatomic gases to stabilize the arc.

Two anodes and four cathodes were tested. The first anode was tested on hydrogen-argon mixtures and the second anode was tested on nitrogen-argon mixtures. For each anode, two cathodes were tested.

The objectives of the tests performed were:

1. To find combinations of current, gap, and gas flow rates which allowed stable operation of the torch.

2. To determine the lifetime of the torch on the two feedstocks with a goal of 20 hours operation on mixtures of argon with nitrogen or hydrogen.

3. To obtain stable operation of the torch on higher volume fractions of the diatomic gases than had been used in the original torch, with the goal of operating the torch on pure nitrogen or hydrogen at an input power of 1 kW or less.

4. To study the wear of the electrodes and the relation of the wear to the torch performance.

The testing was limited to currents of less than 15 A in order to reduce the power required to operate the torch. Also, since the heat transfer at the anode is known to be proportional to the current, it was thought that torch operation at the current range chosen would be compatible with the requirement of low anode erosion. Each test is defined as the time that the torch was operated between determining the mass change of the electrodes. The length of each test varied and lasted up to 5.5 hours. Some of the tests included more than one start and extended period of operation.

Graphs of the average torch data-verus-time are presented below for tests of significant length. The experimental data (average measurements collected at a frequency of one per second) were further reduced to the average value over six seconds before plotting, so that ten points are plotted each minute for each variable. The data files from each test have been split into two parts. The first part corresponds to the period of time that the torch was operated on pure argon, while the second part of the

data file corresponds to the period of time that the torch was operated on mixtures of argon with the diatomic gases. For convenience, the time scale of the data plotted for the argon-diatomic mixtures has been set to zero.

There are six measurements which are plotted: voltage, current, power, pressure, total flow, and volume fraction. The voltage and the current are those measured at the input leads to the torch. The torch power is the electrical power input to the torch, and is calculated as the product of the voltage and the current. The pressure graph is the gage pressure in the torch chamber measured upstream of the flowswirler. The total flow rates plotted are the total volumetric flow rates of the feedstock gases corrected to standard temperature and pressure. The final plot presented for each test with hydrogen- or nitrogen-containing feedstocks is the volume fraction of the diatomic gas. The total flow rates and volume fractions plotted in the graphs are correct except during the flow adjustment periods. The pressures in the gas supply lines upstream of the metering orifice were monitored by analog pressure gages which were read before and after the flow rate was adjusted; therefore, there was no way to record the upstream pressures on the orifices during a flow transition. A straight line was used to interpolate between the values of the volume fraction and the total flow rates on the two sides of the flow adjustment.

7.2.1 Starting and Warm-up on Argon

During many of the tests, tungsten particles were observed exiting the nozzle at arc ignition. It is thought that the loss of tungsten during arc ignition may have been due to the presence of a large current spike at the start of the test. Evidence of a current spike was seen at the start of each test; however, because the current signal had a low-pass R-C filter on it, the starting transient could not be accurately captured. But,

the data for the current did show the decay of a first-order system from a large initial value, which would indicate the presence of a large initial current.

After starting, torch operation on argon was always steady. The torch was usually operated on argon until the temperature of the torch stopped increasing. This could take up to 25 min, depending on the current setting. The temperature of the torch after the warm-up was usually between 160 and 180 C. The current after the initial transient was usually set between 7 and 11 A. The initial flow rate of argon was around 150 ml/s for most of the tests. The voltage required to run the torch ranged from 25 to 35 V, and varied from test to test.

Figure 17 shows the torch data during the warm up period of test 6. The data shown in this figure are typical of the warm-up periods for the rest of the tests. The graph of the current shows the presence of a large initial current. The first data point for the current in this test is 33 A. The voltage, current, and power show small fluctuations. It will be seen later that the magnitude of the fluctuations is less for operation on argon than for that on mixtures of hydrogen or nitrogen with argon. Also, the voltage and the power required to run the torch is much less on argon.

7.2.2 Hydrogen-Argon Tests

Summaries of the tests conducted on the anode and the two cathodes which were operated on hydrogen-argon feedstocks are presented in tables 1 and 2. The electrode gap as defined in figure 7 is tabulated in table 3. A total of 1054 min of choked operation of this anode were recorded during tests 1-7. The torch was operated on pure argon for 352 min of this time while the torch was warming up. The other 700 min (11.67 hours) of operation was on hydrogen-argon mixtures. During two of the tests, the torch was briefly operated on pure hydrogen. Tests with hydrogen-argon mixtures were

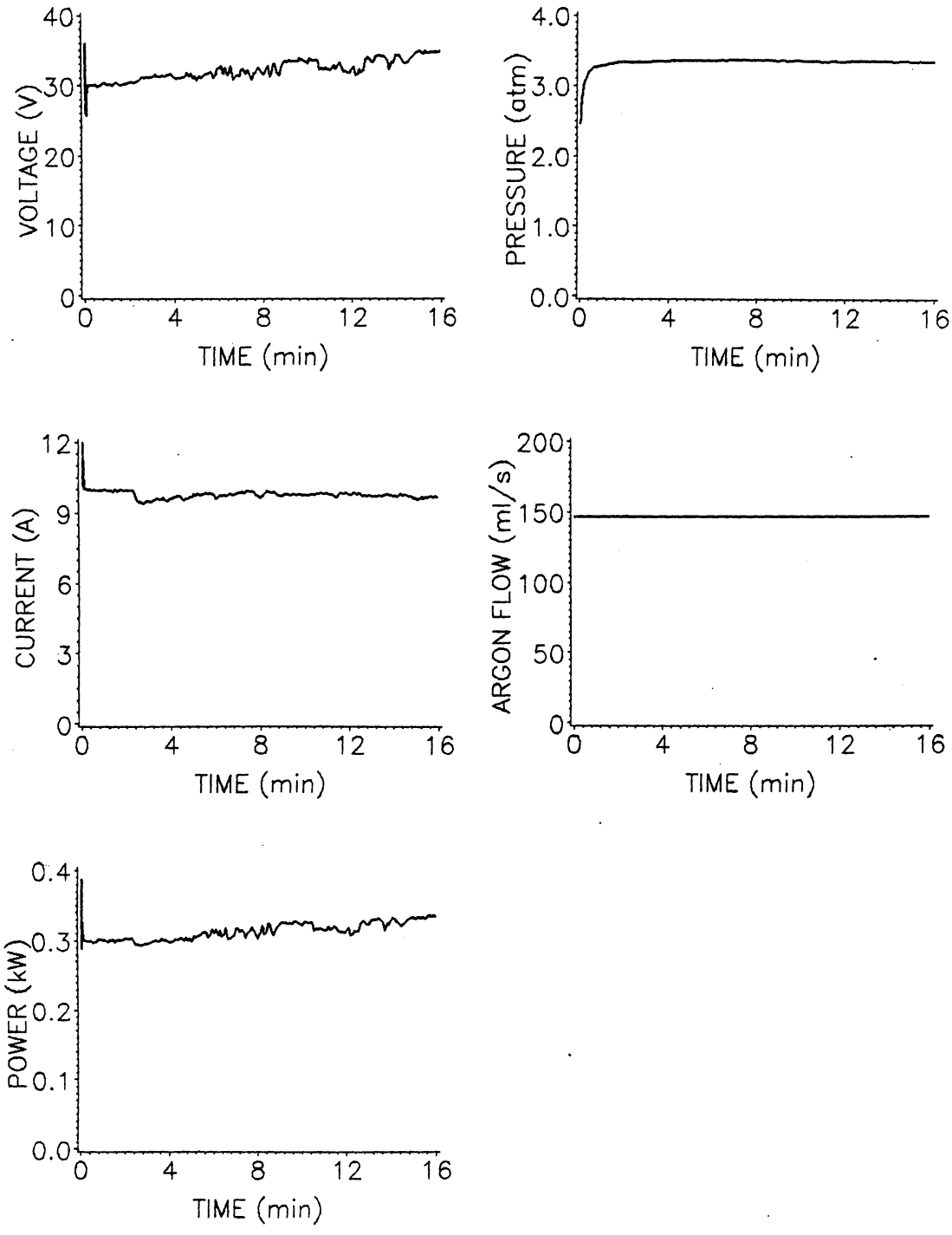

Figure 17. Torch Data During the Argon Warm-up Period of Test 6

halted after test 7 because of difficulty in maintaining a sealed torch with hydrogen feedstocks.

Figure 18 shows the torch data from test 1 during operation of the torch on hydrogen-argon mixtures. After the warm-up period on argon, hydrogen was slowly mixed with the the argon flow (which was kept constant throughout the test) until its volume fraction reached 45 percent. At 12 min the current was reduced to the lowest setting on the power supplies, which was an average of 4.5 A. More hydrogen was added to the torch as the time increased, as shown in the graphs of the total flow and the volume fraction of the hydrogen.

The torch pressure increased with each increase in the hydrogen flow rate. Because of the high torch pressure, the pressure ratio across the orifice in the hydrogen gas line was not choked. The unchoked flow orifice is reflected in the the fluctuations of the graphs of the total flow and the volume fraction of hydrogen with the fluctuations in the torch pressure. The average torch voltage increased as the hydrogen flow rate increased. This result was expected. As noted in chapter 3, the resistance of an arc is known to be greater for an arc in a diatomic gas than that in a monatomic gas. Also, the increase in the total flow increases the convective cooling of the arc column, which further increases the column resistance.

There were several fluctuations in voltage which were accompanied by small fluctuations in current in the opposite direction. The average current in this test, as in most of the other tests, drifted away from the initial setting during the test, and was difficult to adjust precisely to the desired value while operating in the low range of current which was used during the tests. As the hydrogen flow was increased, the torch power also increased because of the increase in the voltage. At 122 min, the current was increased intentionally, and the voltage decreased. This was expected because the resistance of a constant length arc is known to decrease as the current is increased. The

Table 1. Summary of Hydrogen-Argon Tests With Cathode One

Test Number	Number of Starts	Pure Ar Time (min)	H_2-Ar Time (min)	Pure H_2 Time (min)
1	1	25.3	138.0	0.0
2	2	48.6	180.6	0.0
3	2	28.6	85.2	10.4
4	2	73.9	103.4	0.0
5	3	119.6	53.4	0.0
Total	10	296	603.5	10.4

Table 2. Summary of Hydrogen-Argon Tests With Cathode Two

Test Number	Number of Starts	Pure Ar Time (min)	H_2-Ar Time (min)	Pure H_2 Time (min)
6	1	15.9	96.3	0.0
7	3	40.7	29.1	3.2
Total	4	56.6	125.4	3.2

Table 3. Electrode Gap During Hydrogen-Argon Tests

Test Number	Time Period (min)	Gap (mm)
1	0-End	0.152
2	0-End	0.152
3 (first start)	0-End	0.152
3 (second start)	0-End	0.162
4 (first start)	0-End	0.127
4 (second start)	0-End	0.152
5 (third start)	0-End	0.127
6	0-22.0 22.5-End	0.152 0.203
7	0-End	0.203

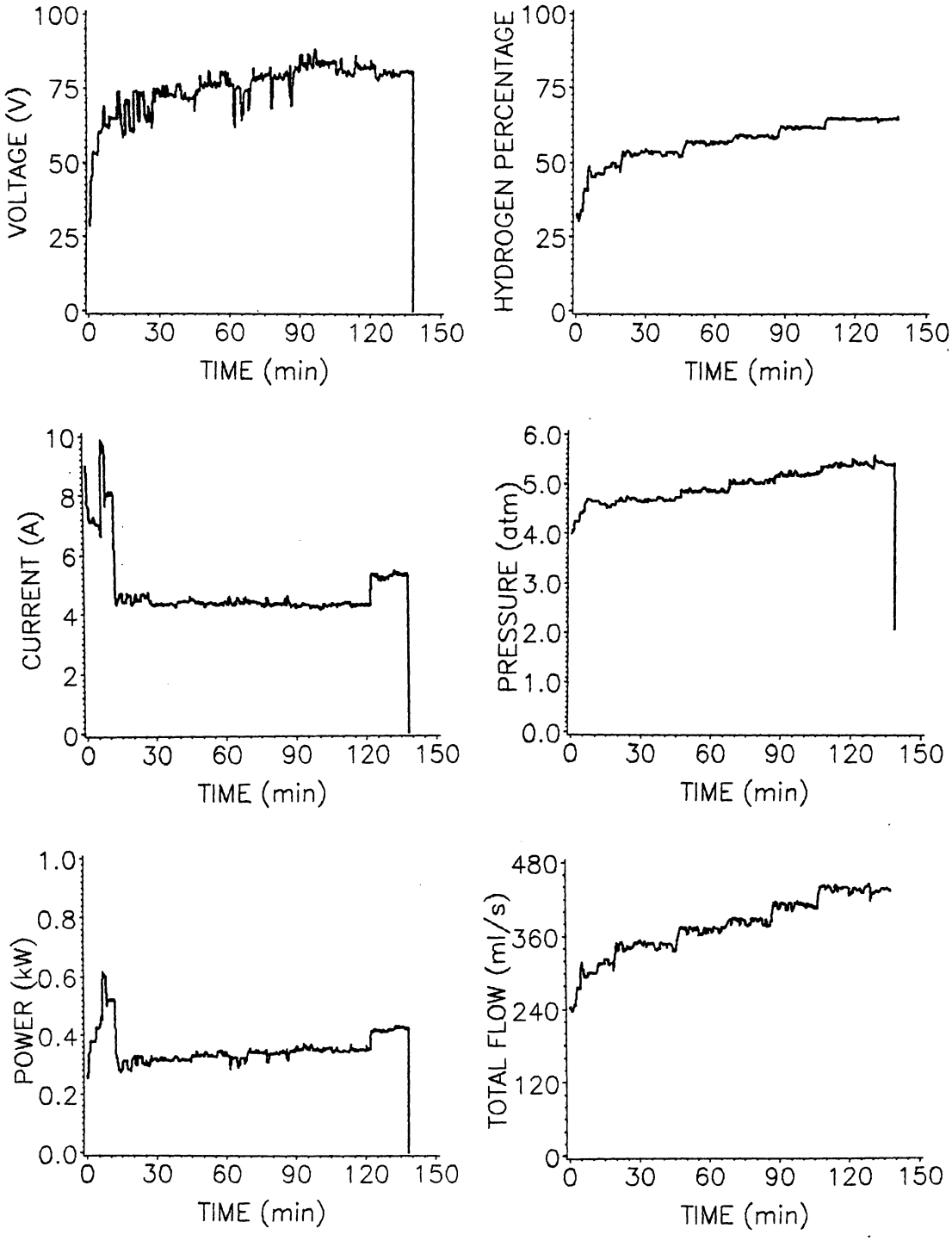

Figure 18. Torch Data During Test One

torch power increased with the increase in the arc current. After 138 min of operation on hydrogen-argon mixtures, the torch was turned off. The electrodes showed little damage.

In the second test there were two extended operating periods of the torch on hydrogen-argon mixtures. The torch data for the first start of this test is shown in figure 19. The average current through most of the test was kept at 6.3 A. The gap was kept constant at 0.152 mm through the entire test, but the flow rates were varied.

For the first 10 min the hydrogen flow rate was slowly increased until the total flow rate and hydrogen fraction reached 360 ml/s and 58 percent, respectively. The flows were left at this setting for the next 28 min. During this time the average voltage was 84 V. The fluctuations in voltage were less than those in test 1. The hydrogen flow rate was slowly increased between 38 min and 43 min, increasing the total flow rate and the hydrogen fraction to 397 ml/s, and 62 percent, respectively. The average voltage increased slightly to 89 V and fluctuated little from this value. Also, the addition of hydrogen to the arc caused the average power to increase from 530 to 560 W. From 74 to 81 min, the total flow was reduced slightly while keeping the hydrogen fraction constant. Little change was seen in the average voltage after the flow rate was decreased, and the voltage again showed little fluctuation. The hydrogen flow rate was turned off at 109 min and arc operation continued on pure argon for the next 2 min. Hydrogen flow was quickly mixed in with the argon flow until a mixture of 63.5 percent hydrogen at 370 ml/s was established. The average voltage increased to 97 V and showed larger fluctuations. The torch was turned off at 148 min, and the electrodes showed little damage.

The current was higher in test 2 than in test 1, but the voltage was higher for similar hydrogen fractions. At first glance this result is unexpected, since the resistance of the arc column is known to drop as the current is increased. It is thought that the higher

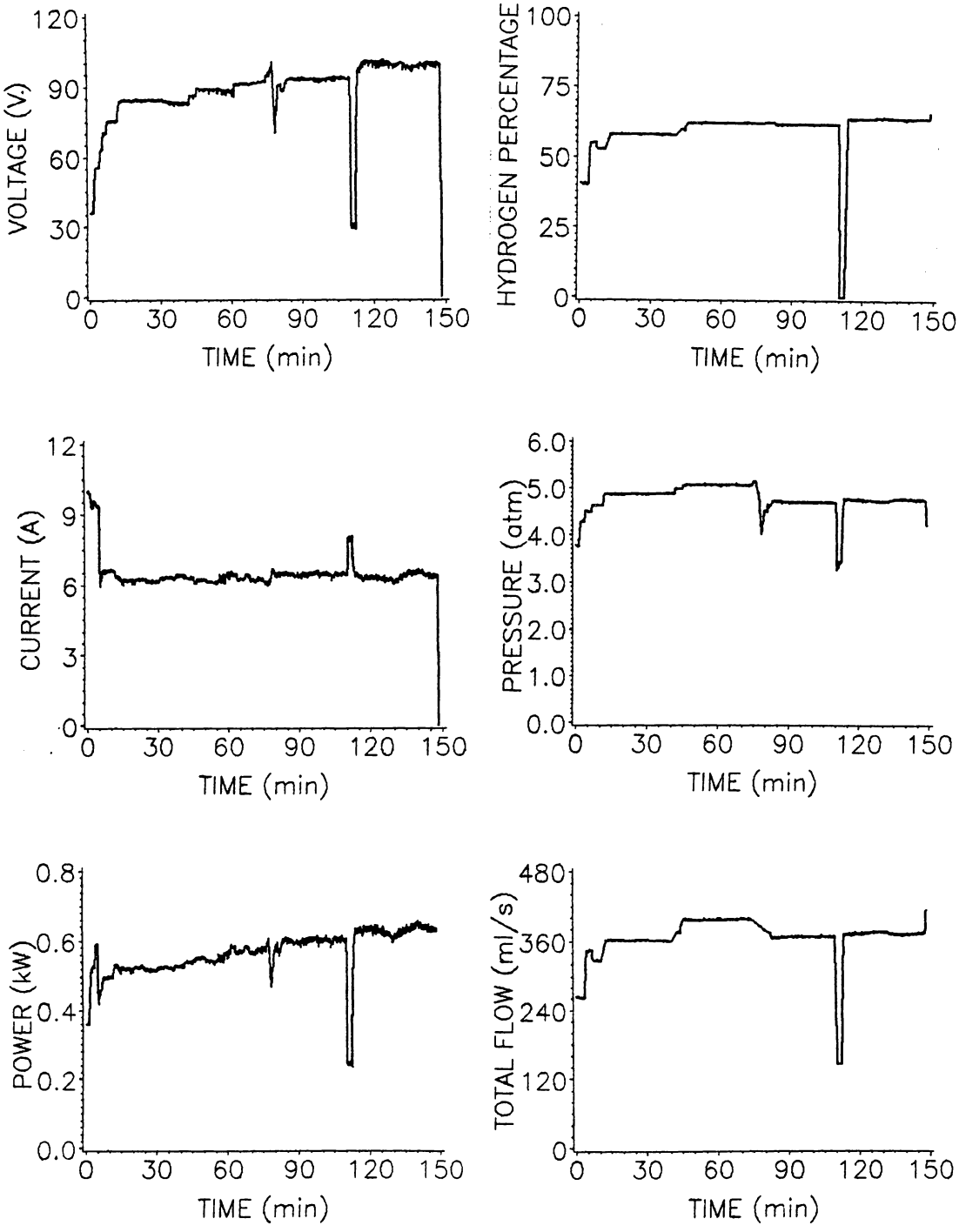

Figure 19. Torch Data During Test Two (First Start)

voltage in the second test was caused by a longer arc length than that in the first test. At low currents, column conductivity is low; therefore, small changes in the column length can cause large changes in the arc resistance. A longer arc length could be caused by the movement of the arc attachment point to a location further downstream in the anode. As will be shown later, the cathode length decreases with time, which also causes the arc length to change.

After the second start of test 2, the current was set at 7.8 A at the beginning of the hydrogen addition and was not changed throughout the test. Unfortunately, the current tended to drift down from this setting as the test progressed. The current at the end of the test was 6.0 A. Hydrogen was added to a constant argon flow rate throughout the test. As in the other tests, increases in the hydrogen flow rate produced increases in the torch voltage and power throughout the test. The voltage fluctuations were small throughout the test and corresponded to current fluctuations in the opposite direction. The final flow rate of the test was 390 ml/s, of which 66 percent was hydrogen. The voltage after the final increase in hydrogen climbed to over 115 V, and the arc blew out a few minutes later.

In test 3 there were two operating periods. In the first operating period the torch was operated on hydrogen-argon mixtures for 18 min before the arc stopped. The final flow rate of the first operating period was 350 ml/s, of which 66 percent was hydrogen. The final current of the first operating period was 7.0 A.

The torch data for the second operation period of test 3 is shown in figure 20. The gap was 0.162 mm through all of the test. After the second start of test 3, the current was increased because it was thought that higher currents would allow torch operation with higher hydrogen fractions, due to the lower arc resistance at high currents. As shown in figure 20, the average current during this test was between 9.5 and 11.5 A.

There were 3 different flow settings during the test. After the warm-up period on pure argon, the gas mixture was changed to 71 percent hydrogen at a total flow rate of 345 ml/s. At 32 min the argon flow rate was decreased and the hydrogen flow rate was increased, so that the hydrogen fraction was increased to 78 percent. The total flow rate was also increased, but the pressure dropped after the increase in the total flow rate. This indicates that the torch was leaking and that hydrogen leaked more than the argon. From 65 to 66 min, the hydrogen flow rate was kept constant and the argon flow rate was decreased to zero so that the arc was running on pure hydrogen. The total flow rate decreased by 80 ml/s and the pressure dropped to less than 2 atm. The torch was operated on pure hydrogen until the end of the test.

As shown in the graphs, the torch voltage and power gradually increased throughout the test while the current slowly decreased. The voltage during the test was between 65 and 95 V, and the total torch power ranged between 750 and 1050 W. The voltage and the power actually decreased after the mixture was switched to pure hydrogen. It is thought that this was due to a shift in the arc attachment point to a location further upstream in the anode, thus leading to a shorter arc. The power during the period of operation on pure hydrogen was about 1 kW. The torch operation on pure hydrogen was stable, but the test had to be terminated because the hydrogen supply tank was becoming empty. The decrease in the flow rate and the pressure are shown in the last few min of the graphs.

After the test, it was determined that the torch was leaking from the dynamic seal (component P in figure 8). Examination of the seal showed that the outer diameter of the seal decreased during the test so that the fit between it and the outer edge of the gland was not as tight as it was at the start of the test. It is thought that this deformation of the dynamic seal was due to the high temperatures that the seal was exposed to. For the rest of the tests a new dynamic seal was used for each test, and graphoil graphite

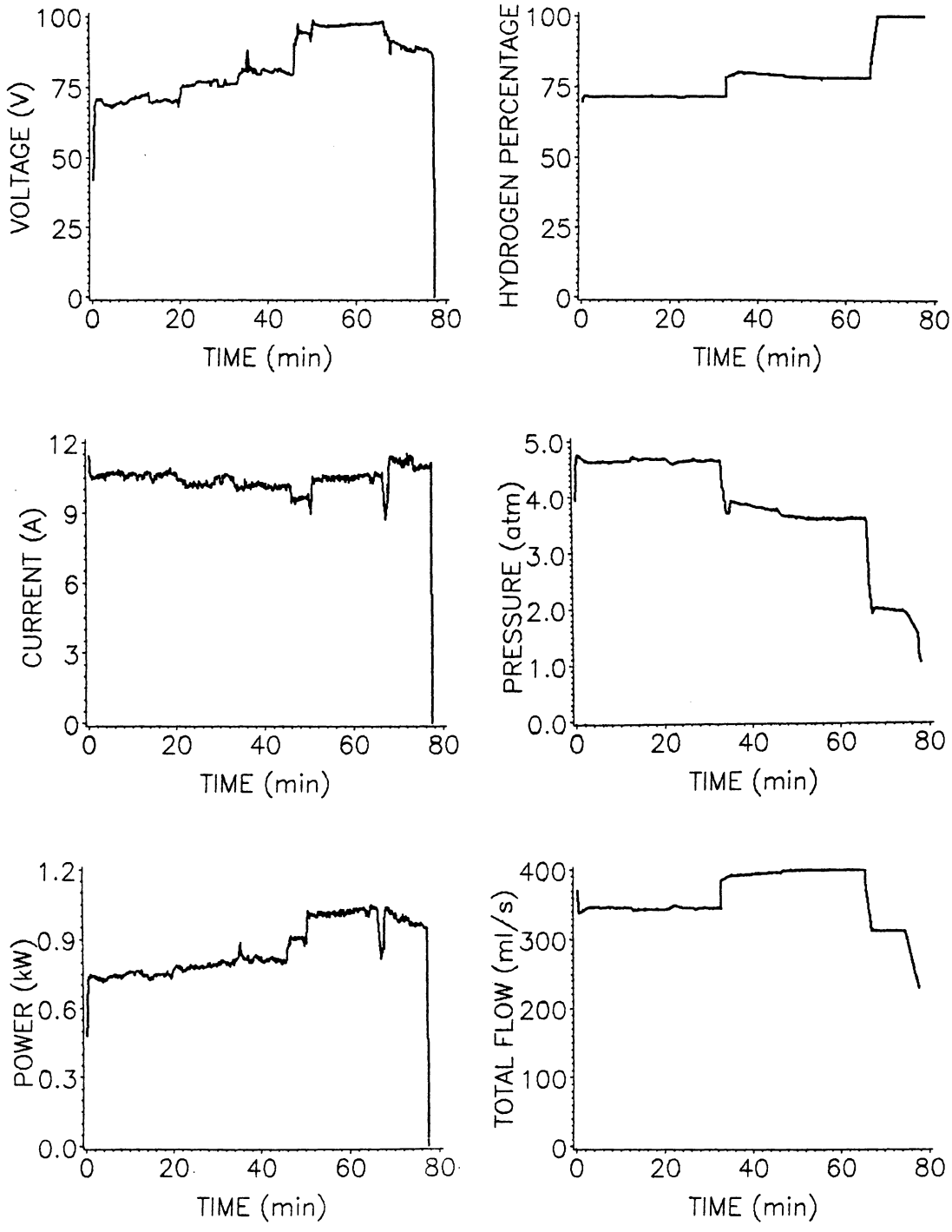

Figure 20. Torch Data During Test Three (Second Start)

sealing paste was placed on the threads of the cathode adjustment knob to aid the dynamic seal.

Test 4 consisted of two operating periods. During the first period of operation the torch was run on a constant argon flow at various hydrogen fractions from 35 to 55 percent hydrogen. The test was terminated after 50 min to check the seals. It was determined that there was a small leak. Inspection of the dynamic seal showed that the new seal was deformed in the same manner as the old one.

The leaking seal was replaced before the second start, and an attempt was made to slowly bring the hydrogen fraction to 100 percent during the test so that there would be no uncertainty in the volume fraction of hydrogen which actually passed through the anode. The torch data for the second start of test 4 is shown in figure 21. The hydrogen flow was increased throughout the test while the argon flow was left constant. During most of the test, the current was lower than that in test 3 in order to try to keep the temperature of the dynamic seal low. The current was raised to 10.5 A during the last 15 min of the test when the hydrogen fraction was over 65 percent and the total flow was over 330 ml/s. As before, the torch voltage increased as the hydrogen flow rate increased. Torch operation was stable on fractions of hydrogen up to 70 percent. When the hydrogen fraction was increased past 70 percent the arc blew out.

During test 5 there were two unsuccessful attempts to transfer to operation on pure hydrogen while operating on currents in the range of 5-6 A. After this, the torch was started a third time and the hydrogen addition was carried out gradually with the current set at a higher average value. Figure 22 shows the torch data after the third start of test 5. During the flow adjustments, the argon was decreased while the hydrogen was increased. Although the total flow rate supplied to the torch was increased, the torch pressure decreased slightly with each flow addition, again indicating preferential leakage of the hydrogen.

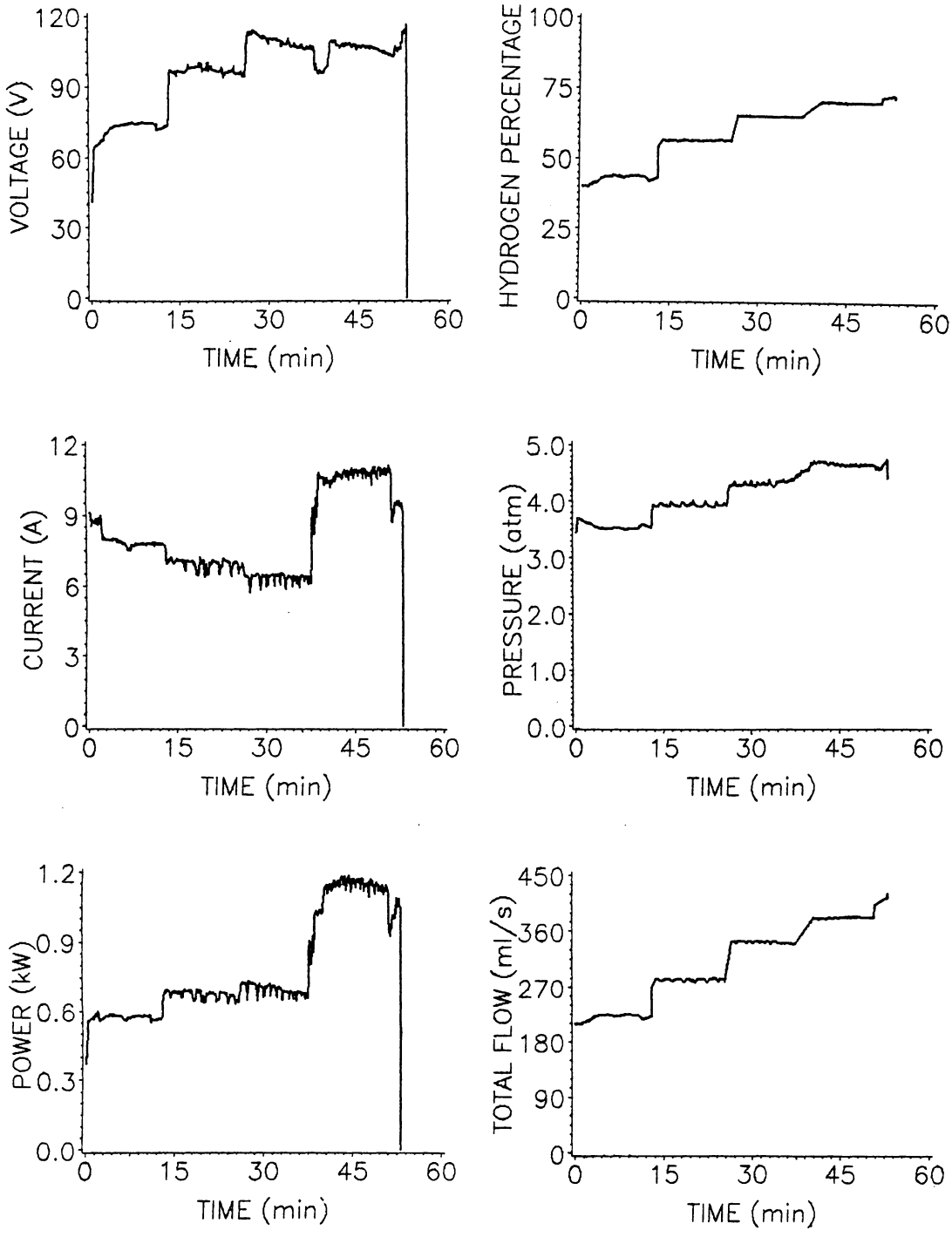

Figure 21. Torch Data During Test Four (Second Start)

The voltage increased as the hydrogen fraction increased. The current during the test was above 8 A for most of the test. Both the current and voltage showed large fluctuations. The positive fluctuations in the voltage were associated with negative fluctuations in the current and vice versa. In this, and following tests which showed fluctuations in the voltage, the fluctuations in the voltage were accompanied by fluctuations in the visible light which was emitted from the torch. The peaks in the voltage generally corresponded to peaks in the brightness of the visible light output of the torch as observed on the video monitor. This fluctuation in brightness was qualitative and was not actually measured. The voltage and the power were higher than in the previous tests. Some of the voltage peaks were as high as 150 V. After the flow rate was adjusted to 65 percent hydrogen the arc blew out.

After test 5 the cathode was replaced because it was thought that with a sharper cathode tip it would be possible to run at higher fractions of hydrogen. The torch data for test 6, are shown in figure 23. During the flow adjustments, the hydrogen flow rate was increased while the argon flow rate was decreased. As in some of the previous tests, although the total flow rate was increased the torch pressure decreased. The average current was about 10 A during the test. The voltage and the torch power slowly increased throughout the test. At the last flow setting, the mixture ratio of the gas supplied to the torch was about 85 percent. The torch blew out after 12.5 min at this setting.

During test 7 there were 3 attempts to switch operation of the arc over to pure hydrogen. The first two tries were at an average current of 13 A and were unsuccessful. After the third start the current was raised to 16 A and the mixture was easily switched to pure hydrogen; however, due to the leaking seal, the gage pressure on the torch was only 0.4 atm. Because of the low chamber pressure, the torch was turned off. The constrictor showed considerable erosion after this test, but the torch could still be

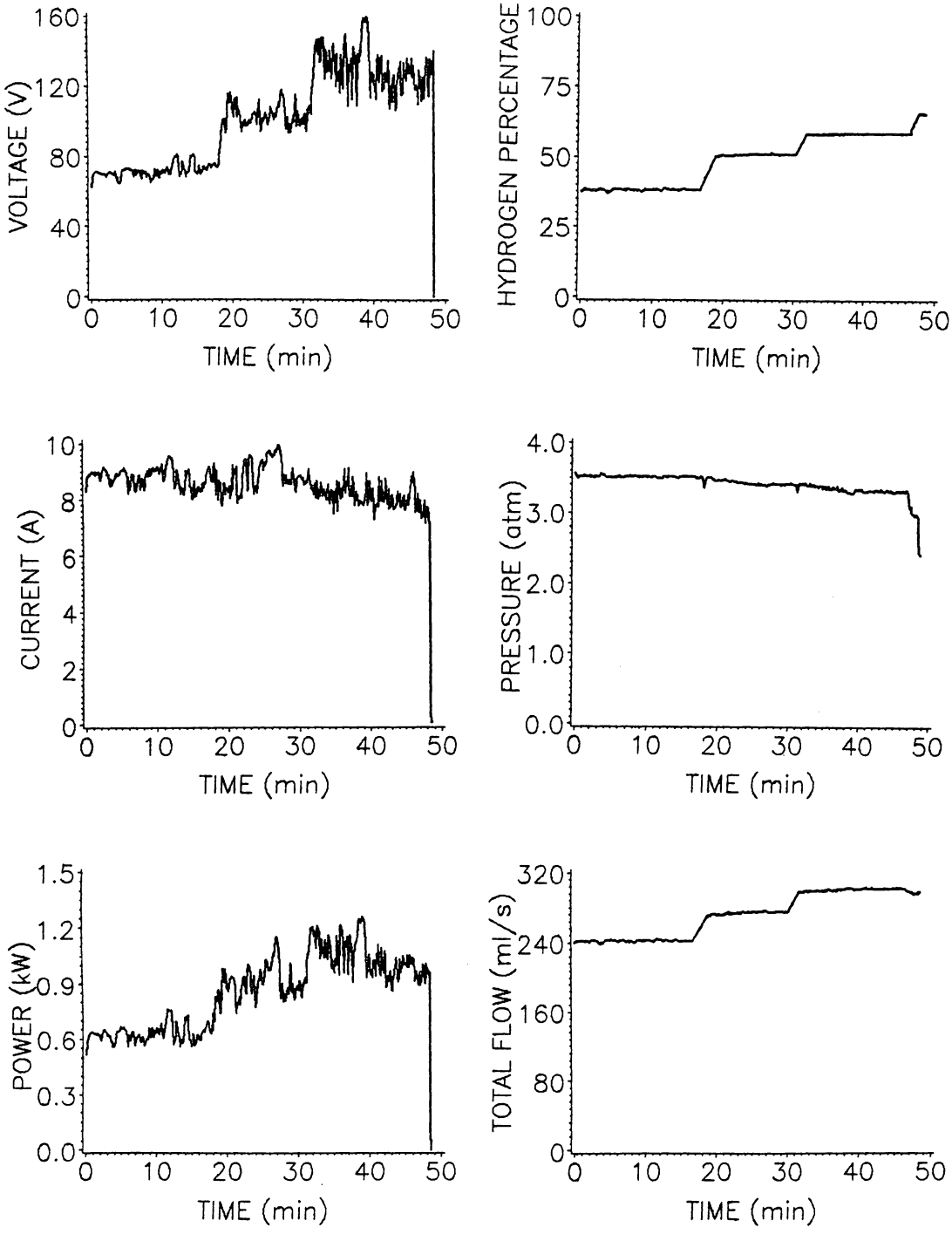

Figure 22. Torch Data During Test Five (Third Start)

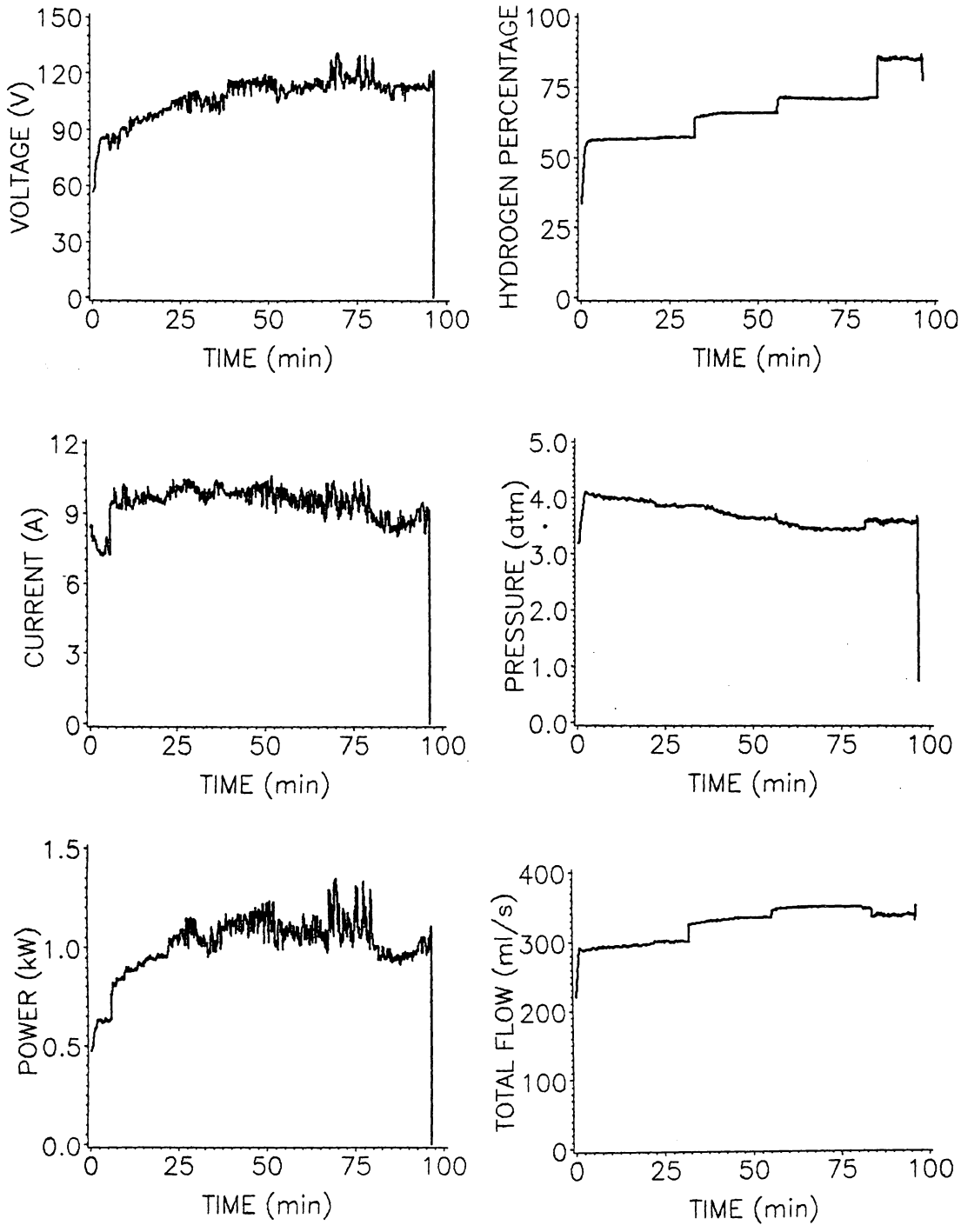

Figure 23. Torch Data During Test Six

choked on mixtures of argon and hydrogen. However, testing of the first anode was concluded after this test due to the sealing problems.

7.2.3 Nitrogen-Argon Tests

Summaries of the tests conducted on the anode and the two cathodes which were operated on nitrogen-argon feedstocks are presented in tables 4 and 5. The electrode gap as defined in figure 7 is tabulated in table 6. A total of 1445 min (24.1 hours) of choked operation with this anode were recorded during tests (8-17). The torch was operated on pure argon for 223 min of this time while the torch was warming up. The other 1202 min (20.0 hours) of operation was on pure nitrogen and nitrogen-argon mixtures. During five of the tests the torch was operated on pure nitrogen for a total of 393 min. The testing of the anode was voluntarily concluded after attaining the goal of 20 hours of torch operation on mixtures containing nitrogen. The torch was still choked at the end the tests.

The same orifice that had been used for the measurement of hydrogen flow was used for the measurement of nitrogen flow. For this reason the volume flow rates of the nitrogen in the tests were typically lower than those of hydrogen in the previous tests. Because of the problems with the dynamic seal, the average current was set at 7 A for most of the tests with nitrogen in order to keep temperature of this seal low.

Figure 24 shows the data from test eight. After the warm-up period on argon the mixture was changed to 52 percent nitrogen. For the first 15 min, the current along with the voltage, slowly decreased. After 15 min, the electrode gap was increased from its initial setting of 0.152 mm to 0.203 mm. Both the voltage and the power increased immediately, and leveled off at higher values. The nitrogen flow was increased at 29 min.

Table 4. Summary of Nitrogen-Argon Tests With Cathode Three

Test Number	Number of Starts	Pure Ar Time (min)	N_2-Ar Time (min)	Pure N_2 Time (min)
8	1	32.0	60.9	0.0
9	4	34.4	37.0	0.0
10	1	12.0	34.5	33.8
11	5	39.2	41.6	13.7
12	1	33.0	59.1	0.0
13	1	25.0	219.7	0.0
14	1	22.0	48.8	0.0
Total	14	198.5	501.6	47.5

Table 5. Summary of Nitrogen-Argon Tests With Cathode Four

Test Number	Number of Starts	Pure Ar Time (min)	N_2-Ar Time (min)	Pure N_2 Time (min)
15	1	12.0	15.0	303.9
16	1	20.0	28.7	19.1
17	1	13.6	264.4	22.0
Total	3	45.6	307.7	345.0

Table 6. Electrode Gap During Nitrogen-Argon Tests

Test Number	Time Period (min)	Gap (mm)
8	0-15 16-End	0.152 0.203
10	0-End	0.152
11 (last start)	0-End	0.152
12	0-End	0.152
13	0-68.0 68.5-85.0 86.0-117.0 118.0-End	0.152 0.178 0.152 0.127
14	0-End	0.152
15	0-End	0.152
16	0-End	0.152
17	0-74.5 75.5-88.0 90.0-106.5 107.5-122.5 123.5-End	0.152 0.127 0.152 0.165 0.152

The initial effect was a step increase in the voltage and a smooth operating period of about 3 min. Then, the voltage started to steadily increase. The current was increased in an effort to lower the voltage. After the current increase, the voltage began to decrease. The current was then decreased and the voltage continued to decrease. The argon flow rate was decreased and the nitrogen flow was increased at 48 min, so that the nitrogen fraction and the total flow rate were increased to 75 percent and 275 ml, respectively. The voltage showed fluctuations and continually increased until it reached 140 V and the arc was extinguished.

During test 9 the arc voltage became erratic and the arc went out while operating on 54 percent nitrogen. This was a lower fraction of nitrogen than the maximum that had been run through the torch in the last test. Several more attempts to run the torch on mixtures of 50 to 60 percent nitrogen failed after only a few min of operation. After disassembly of the torch it was discovered that the flow swirler had broken into several pieces.

The broken flow swirler was replaced before test 10. Figure 25 shows the torch data from this test. The torch pressure was lower in this test than in test 8 due to the erosion of the anode. At 15 min the total flow and nitrogen fraction were increased, and the voltage also increased as it did in test 8. At 33 min the mixture was slowly changed to pure nitrogen, by increasing the nitrogen flow and decreasing the argon flow. The pressure during the transition period first increased, and then decreased to the value corresponding to the final flow rate. This indicates that the nitrogen flow rate was increased faster than the argon flow rate was decreased. Therefore, the total flow during the transition period was greater than the initial flow rate. The voltage rapidly increased to 145 V during the flow adjustment, and then decreased at the end of the flow adjustment to 120 V, which was higher than the voltage on nitrogen-argon mixtures in this test. It is thought that high voltage during the flow adjustment is due to an increase

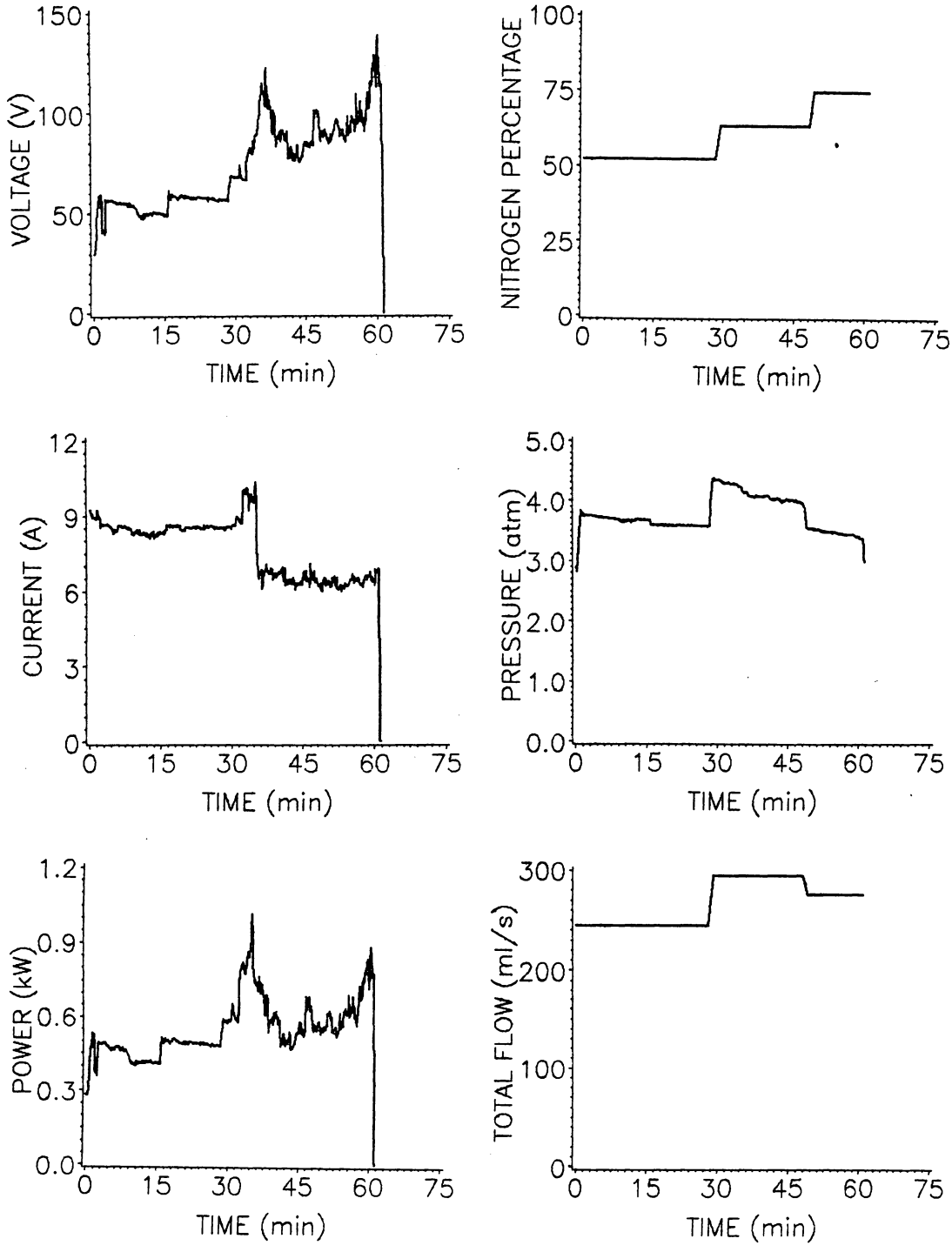

Figure 24. Torch Data During Test 8

in the arc length due to the high flow. The voltage and the current fluctuations were also larger during operation of the torch on pure nitrogen.

The nitrogen flow rate was increased at 44 min, and the power and voltage also increased. The current was increased at 60 min. This caused the voltage to decrease and the power to increase. A minute later, the nitrogen flow was increased and the voltage also increased. Operation at the higher flow rate was unsteady, and the arc was broken a few min after increasing the flow.

During test 11 several unsuccessful attempts were made to operate the torch on pure nitrogen at a current of 5 A. The current was increased to 7 A after the last start and stable operation of the torch on pure nitrogen was again accomplished. The torch data for the last operating period of test 11 is shown in figure 26. After the mixture was adjusted to pure nitrogen, the torch voltage was between 90 and 120 V. The fluctuations of the voltage corresponded to fluctuations of current in the opposite direction. The flow rate of pure nitrogen was less than that in the last test. The flow rate was increased at the end of the test to 179 ml/s, which was still less than the lowest flow rate of pure nitrogen in test 10. Less than two min after the flow was increased, the arc was extinguished.

Figure 27 shows the torch data during test 12. The total flow and nitrogen fraction for this test were a constant 216 ml/s and 57 percent respectively. The pressure remained relatively constant through the test. The current was set at an average of 7 A in the beginning of the test, but it drifted from this initial value during the test. The voltage fluctuated throughout the test. As in the previous tests with argon-nitrogen feedstocks, the fluctuations of the voltage corresponded to fluctuations of the current in the opposite direction. For the first 45 min the voltage was between 70 and 90 V. After 45 min, the voltage started to climb from 80 to 150 V. After the voltage increased past 150 V, the arc blew out.

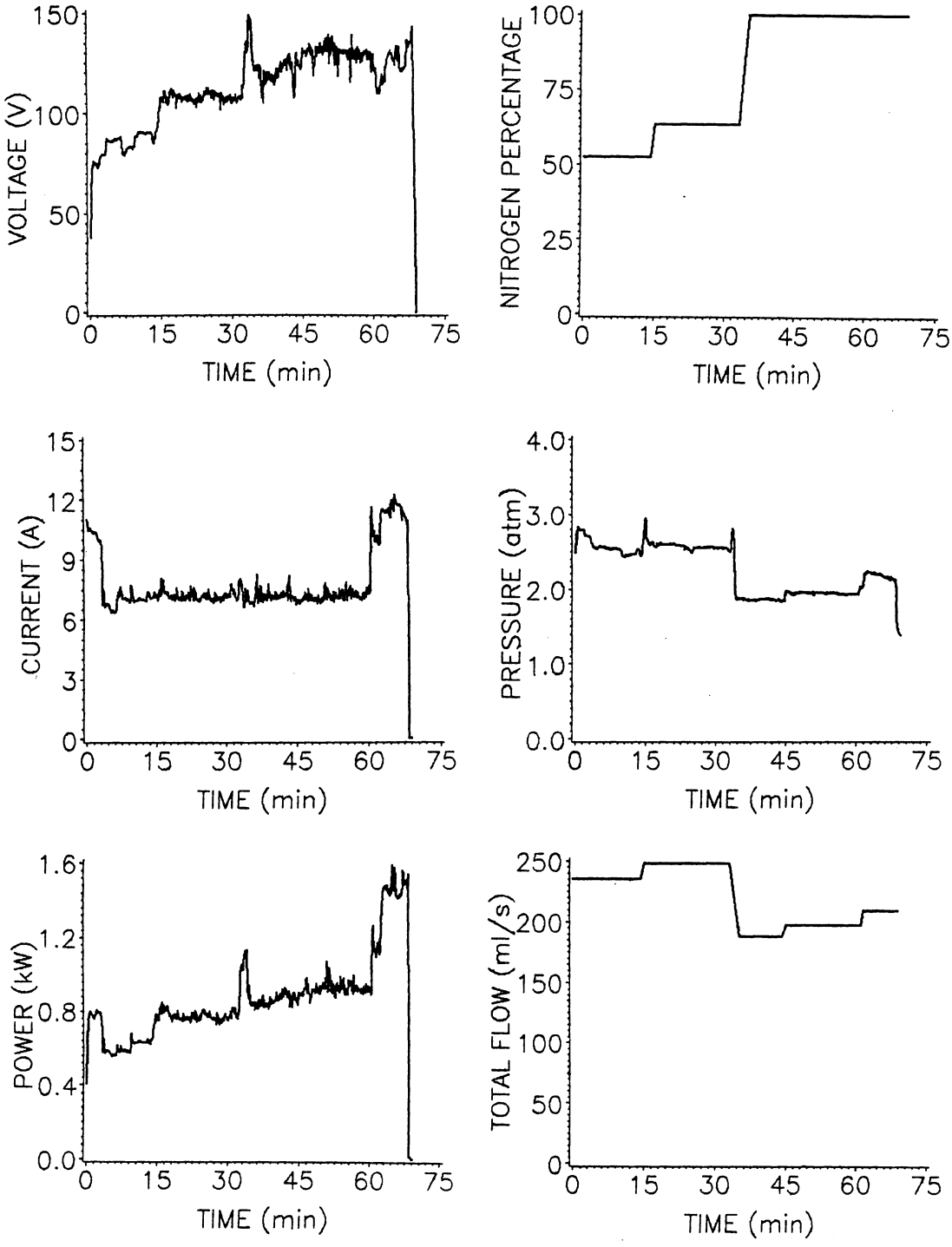

Figure 25. Torch Data During Test 10

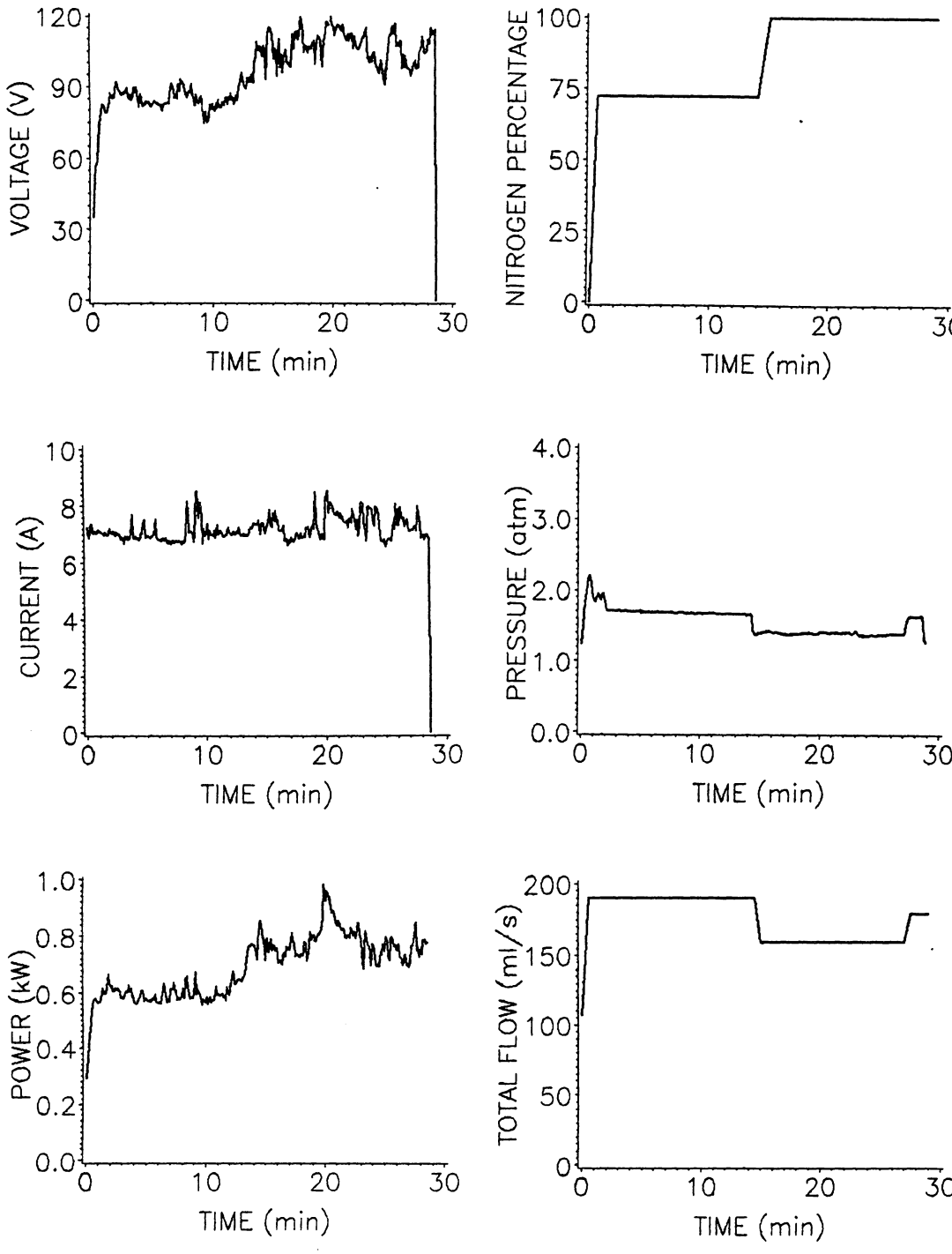

Figure 26. Torch Data During Test 11 (Last Start)

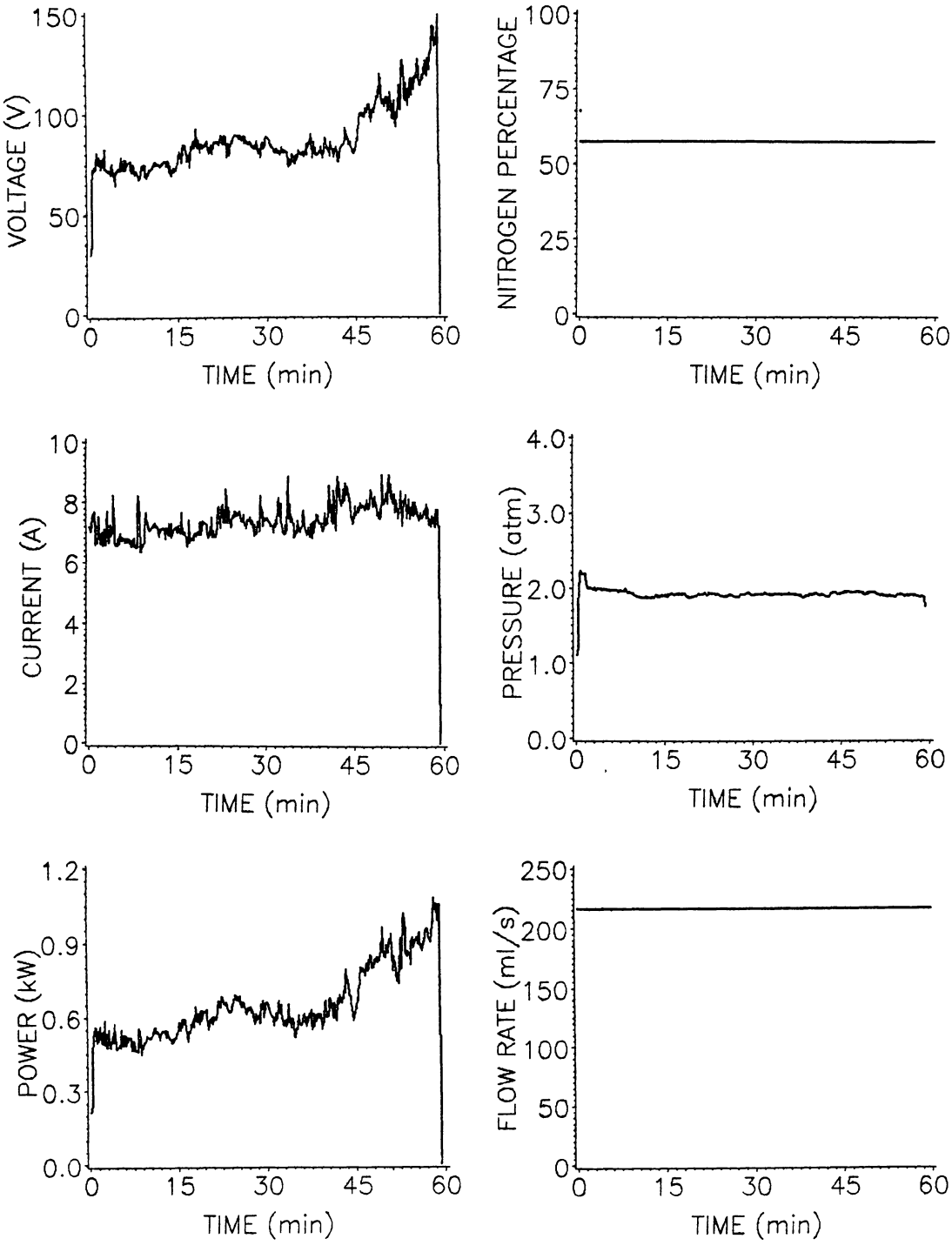

Figure 27. Torch Data During Test 12

The data for torch operation during test 13 is presented in figure 28. The total flow rate and nitrogen fraction for this test were constant at 196 ml/s and 54 percent, respectively. The current was initially set at 6.5 A, but drifted from this value throughout the test. The voltage increased throughout the test, changing from 80 to 150 V at the end of the test. As shown in table 6, the electrode gap was adjusted throughout the test. At 68 min the gap was adjusted from 0.152 mm to to 0.178 mm. The initial effect of this was a step increase of 15 V in the voltage. After the gap increase the voltage continued to slowly increase, as it had before.

At 85 min the electrode gap was decreased to its initial setting and there was a step decrease in the voltage. After the gap adjustment the voltage continued to increase. At 117 min the gap was decreased further to 0.127 mm, and there was another step decrease in the voltage. After this adjustment, the voltage decreased further until 140 min, and steadily increased thereafter. At the end of the test the current was intentionally decreased to its original value. The voltage immediately increased and the arc became unstable and was broken.

Test 14 consisted of running the torch at a fixed gap, and varying the total flow rate at almost constant nitrogen fraction. The nitrogen fraction during this test varied from 54 to 51 percent nitrogen. The average current for this test varied on its own between 6 and 9 A. Torch operation was stable for flow rates below 200 ml/s. At the last flow setting of the test (228 ml/s total) the torch operation became unstable and the arc was broken.

It will be shown later that the large voltages in tests 12-14 are thought to be caused by an increase in the arc length, which is caused by changes in the electrode geometry.

A new cathode was used for tests 15 through 17. The torch data during test 15 is shown in figure 29. The torch was operated on a 48 percent nitrogen mixture for the first

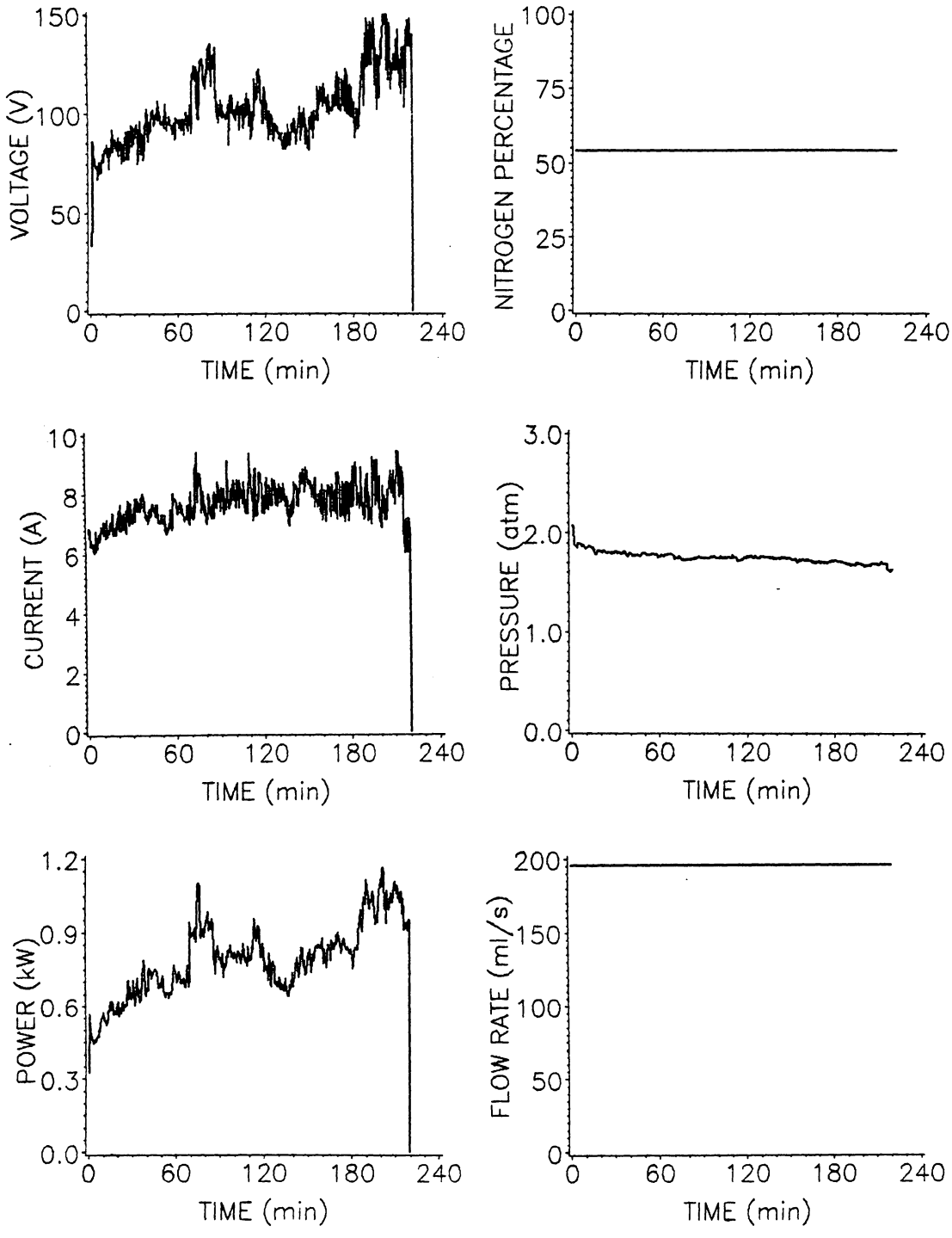

Figure 28. Torch Data During Test 13

13 min, and operated on pure nitrogen for the rest of the test. The flow rate of nitrogen was increased at 32 min from 168 ml/s to 187 ml/s.

After 32 min all of the torch controls were left untouched until 315 min. During this time the average current drifted between 7.4 and 6.6 A, and the average voltage was about 95 V with voltage fluctuations ranging between 70 and 110 V. The average torch power was between 700 and 600 W, with temporary fluctuations up to 800 W and down to 500 W. Over 4.7 hours of stable "hands off" operation of the torch with a diatomic feedstock were demonstrated. At 315 min the flow rate of nitrogen was increased to 208 ml/s. This caused the arc to become unstable and blow out in less than 4 min.

In test 16 torch operation was again established on pure nitrogen at a current of 7 A and a flow rate of 183 ml/s. However, after 22 min of stable operation on pure nitrogen the arc suddenly blew out.

Test 17 consisted of one continuous run which consisted of three parts. The data for this test is plotted in figure 30. In the first part of the test, which lasted from 0 to 75 min, the gap, total flow rate, and nitrogen fraction were held constant at 0.152 mm, 257 ml and 52 percent nitrogen, respectively. The current was adjusted several times in this part of the test. The immediate effect of any current decrease was to decrease the power and to increase the voltage. After the adjustment of the current, the voltage tended to drift again.

The second part of the test lasted from 75 to 155 min. The flow rates were kept the same for the second part of the test as they were in the first part, but as shown in table 6, the gap was varied. The first gap adjustment was a decrease from 0.152 mm to 0.127 mm, which caused a voltage drop of 8 V. In the second adjustment the gap was set back to 0.152 mm and the voltage decreased by 3 V, however, during this adjustment period the current increased instead of remaining constant. The gap was increased to 0.165 mm at 107 min, and the voltage decreased 2 V, but again, there was a small increase in the

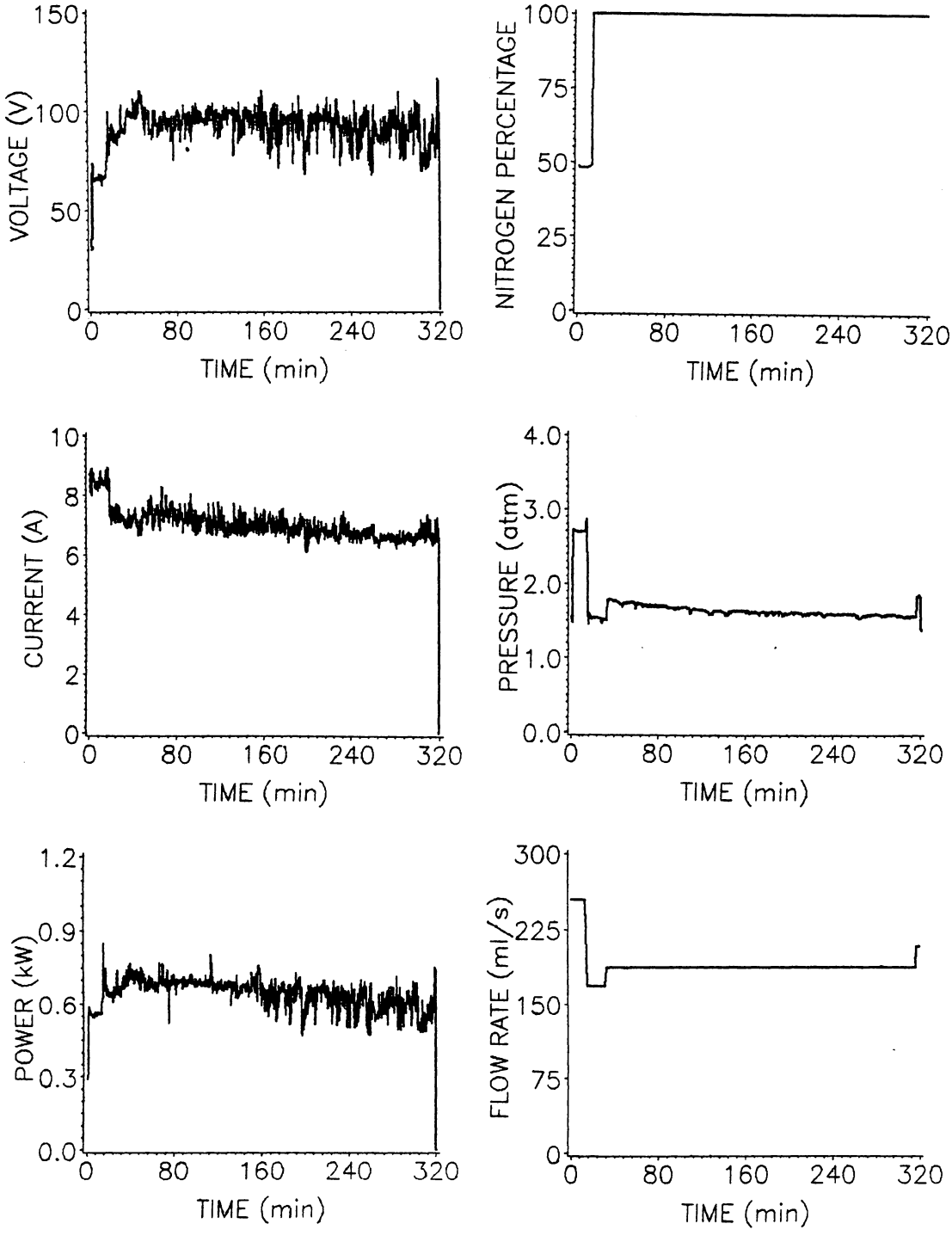

Figure 29. Torch Data During Test 15

current. The final change in gap was a decrease to restore the gap to its original position of 0.152 mm. The voltage decreased 21 V during this adjustment, and the current remained constant during the transition.

The third part of the test lasted from 155 min to the end. The gap was kept constant and the gas flow rates were varied. From 150 to 227 min the current was about 7 A and the voltage ranged between 75 and 95 V for mixtures of ranging from 68 to 52 percent nitrogen. At 227 min the mixture was adjusted to 100 percent nitrogen and the arc was stable with a flow rate of 184 ml/s. Operation on pure nitrogen had to be halted because the nitrogen tank was running out, so the mixture was changed to 50 percent nitrogen for the last part of the test. The severe drop in torch pressure and total flow rate at the end of the test was a result of the decrease in tank pressure. When the gas flow into the torch became too low, the torch was turned off.

After test 17, over 20 hours of choked operation of the torch had been demonstrated on nitrogen and nitrogen-argon mixtures. This was one of the major goals of the test program. After test 17 the torch was still capable of further choked operation, but testing was halted because sufficient torch life had already been demonstrated.

7.3 Electrode Erosion

The mass change of the electrodes was determined by weighing them on a balance (Mettler AE 163) before and after each test. With this balance it was possible to determine the mass of the anode within ± 0.2 mg and that of the cathode ± 0.03 mg. The uncertainty of the mass changes were ± 0.3 mg and ± 0.04 mg for the anode and cathodes, respectively. The change in the total cathode length, measured from the tip of the cathode, was also measured. This change in length was determined by measuring

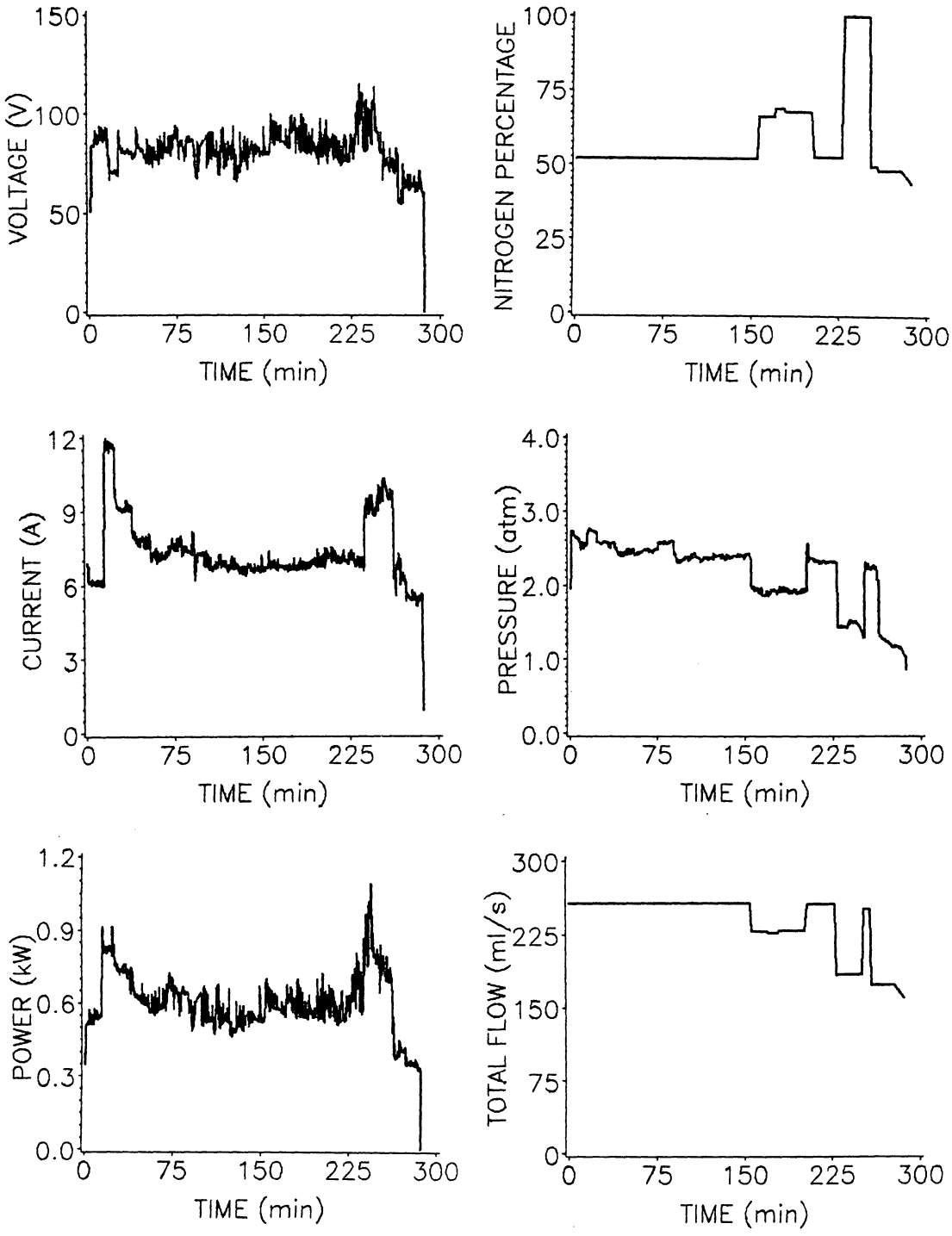

Figure 30. Torch Data During Test 17

the cathode from the flat end to the extreme tip with a pair of vernier calipers before and after each test.

The electrode mass changes and the cathode length changes are shown in tables 7 and 8 for the tests with hydrogen-argon and nitrogen-argon respectively. In addition to the mass loss and length changes, the electrodes were studied and photographed with a microscope which was capable of 80X magnification.

7.3.1 Cathode Mass Loss

In the study of the original version of the torch by Barbi et al. [8], cathode erosion was negligible compared to the anode erosion. In contrast, the results shown in tables 7 and 8, show that in most of the tests the anode erosion has been reduced to the level of the cathode erosion, and in many of the tests the erosion is less than the cathode erosion. Thus, the rate of cathode erosion is also important when considering the endurance of the improved torch.

The cathode mass loss was compared with the total electric charge passed through the torch while it operated on diatomic-argon mixtures for each test. This comparison neglects the possibility that some of the mass lost from the cathode could occur during warm up periods while the torch was operated on pure argon. However, past experience with torch operation indicated that the cathode mass loss on argon was negligible compared to that which occurred on mixtures of diatomic gases and argon.

The charge passed through the torch was calculated by numerically evaluating the integral

Table 7. Electrode Changes for Hydrogen-Argon Tests

Test Number	Cathode Number	Cathode Δm mg	Cathode ΔL mm	Anode Δm mg
1	1	-0.83	-0.13	+0.6
2	1	-0.79	-0.13	-1.9
3	1	-0.36	-0.13	-0.5
4	1	-1.43	-0.20	-1.1
5	1	-1.58	-0.20	-6.0
6	2	---	-0.66	
7	2	-1.64	-0.15	-5.7

Table 8. Electrode Changes for Nitrogen-Argon Tests

Test Number	Cathode Number	Cathode Δm mg	Cathode ΔL mm	Anode Δm mg
8	3	-1.38	-0.40	-1.3
9	3	-1.34	-0.30	-5.7
10	3	-1.64	+0.03	-1.9
11	3	-0.95	-0.10	-1.8
12	3	-1.34	-0.13	0.0
13	3	-3.24	-0.13	-1.4
14	3	-0.61	-0.05	-0.2
15	4	-4.50	-0.89	-1.1
16	4	-0.84	-0.08	-0.5
17	4	-4.05	---	-1.4

$$C = \int_0^t I \, dt$$

with a simple trapezoidal integration routine. The cathode mass loss is plotted against the charge that was passed through the torch while operating on diatomic and diatomic-argon mixtures, in figure 31. The numbers next to the data points correspond to the test number.

As shown in figure 31, the cathode mass loss during the nitrogen tests is a strong function of the charge. The greatest mass loss per charge was that for test 9, which was the test with the broken swirler. The straight line drawn through the data is a linear regression of the data for all of the nitrogen tests except test 9. During test 15 the nitrogen fraction was 100 percent for most of the test, but the value of the mass loss per charge was within the range of that for the tests with nitrogen argon mixtures of lower nitrogen fractions.

The average current while operating on nitrogen containing mixtures was 7.38 A for cathode 3 and 7.12 A for cathode 4. The average cathode mass loss rates were 0.0179 mg/min and 0.0141 mg/min for cathodes 3 and 4, respectively. These rates may be compared to two studies of the mass loss of cathodes operated on pure nitrogen at atmospheric pressure. In a study by Hardy and Nakanishi [38], the mass loss of a 2 percent thoriated tungsten cathode, which had a 45 degree cone at the tip, was investigated. In this study the arc was started on pure argon and the gas was switched to pure nitrogen. The mass loss during the operation on argon was considered to be negligible. The mass loss rates obtained in this study were 0.62 mg/min at 5 A, and 0.55 mg/min at 10 A. These mass loss rates were over an order of magnitude greater than those in the present study, however, the nitrogen flow rate in this study was 300 ml/min,

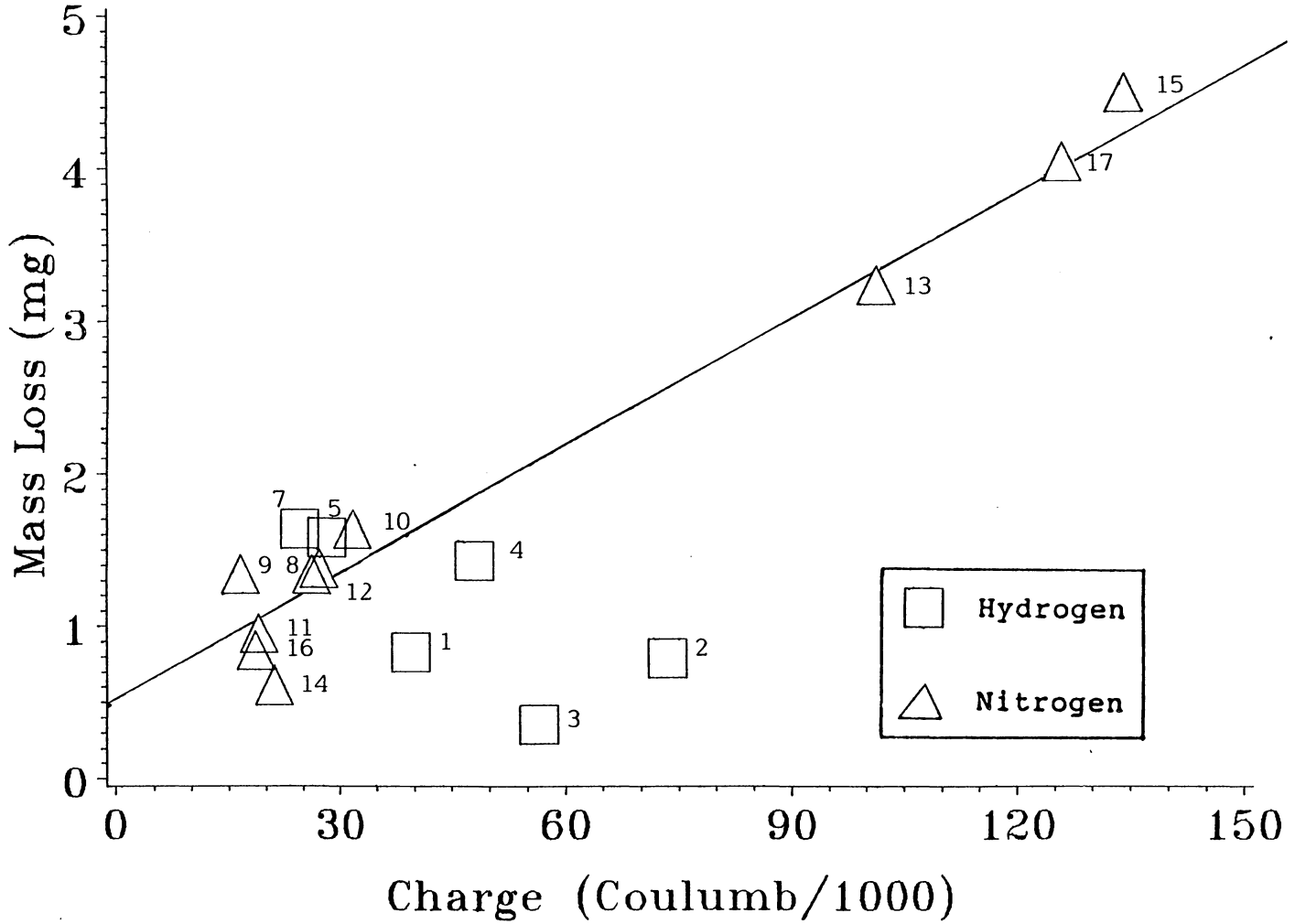

Figure 31. Cathode Mass Loss vs Charge Passed on Diatomic-Argon Mixtures

which was much less than the the flow rates in the present investigation. One interesting finding in the study by Hardy and Nakanishi was that the mass loss of the cathode while operating on 99.5 percent pure nitrogen was more than 4 times that of a cathode which was operated on 99.95 percent pure nitrogen. All of the gases used in the present investigation were commercial grade (99 percent pure).

The mass loss of a cathode at a pressure of 600 torr in high purity nitrogen was determined by Hardy [44]. As in the other study, the arc was started on pure argon and switched over to operation on pure nitrogen, and the mass loss during operation on argon was neglected. At a current of 10 A, and a flow rate of 4000 ml/min, the mass loss rate of the cathode was found to be 0.13 mg/min, which is still much greater than that the present investigation. However, it should be noted that the flow rate of nitrogen used was about a third of the average total flow rate during the present investigation with nitrogen-argon mixtures.

As shown in figure 31, the cathode mass loss while operating on hydrogen-argon mixtures could not be simply related to the charge passed. The points which are plotted below the regression of the mass losses for the nitrogen test were for tests 1-4 and the the two points that were above the regression line were for tests 5 and 7. While the average current in the tests with nitrogen argon mixtures was around 7 A for all of the tests with nitrogen, the average current during the hydrogen-argon tests ranged from 4.7 to 12.5 A. However, the difference between the mass loss rates for tests with hydrogen mixtures and those with nitrogen mixtures can not be explained by the current, since the values plotted below the regression line were obtained for tests with average currents that were both less than and greater than 7 A.

One explanation for the scatter in cathode mass losses for the hydrogen-argon tests is the differences in the total flow rates which actually passed through the torch. The later tests with hydrogen, which had higher cathode mass losses per charge than the

nitrogen tests, probably also had lower flow rates past the cathode because of the leaking seal. Also, the total flow rates for the first four tests with hydrogen, which had much lower cathode mass losses than the nitrogen tests, were much higher than those in the nitrogen tests. This indicates that higher flow rates through the torch, possibly by providing more cooling of the cathode and/or a higher pressure at the cathode tip, may be responsible for the reduced cathode mass loss. The argon warm-up period during the first four tests were comparable to those in the nitrogen tests, yet the mass loss was much less for the first four tests. This tends to confirm the assumption of negligible cathode mass loss during the torch warm-up on argon.

7.3.2 Anode Mass Loss

The anode mass losses were plotted against the charge passed while operating on diatomic gas mixtures in figure 32. As shown in this plot there is considerable scatter in the data. Part of the scatter may be due to the uncertainty of the anode mass loss measurements, which was ± 0.3 mg. The worst anode mass loss per charge was that for test 9, which was the test with the broken swirler. Since the cathode loss rate for this test was also the largest out of all the tests, this tends to point out the importance of swirl in reducing the electrode erosion. The other two data points which indicated high mass losses correspond to the last three hydrogen-argon tests. In these tests, the current was high and leakage was a problem. All of the other tests had anode mass losses which were less than 2.0 mg. In many of the tests, the anode lost less mass than the cathode. One data point which is not shown in figure 32 is that for test 1, which had a measurable gain of mass. It is thought that this gain in mass may be due to material lost from the cathode being deposited on the anode.

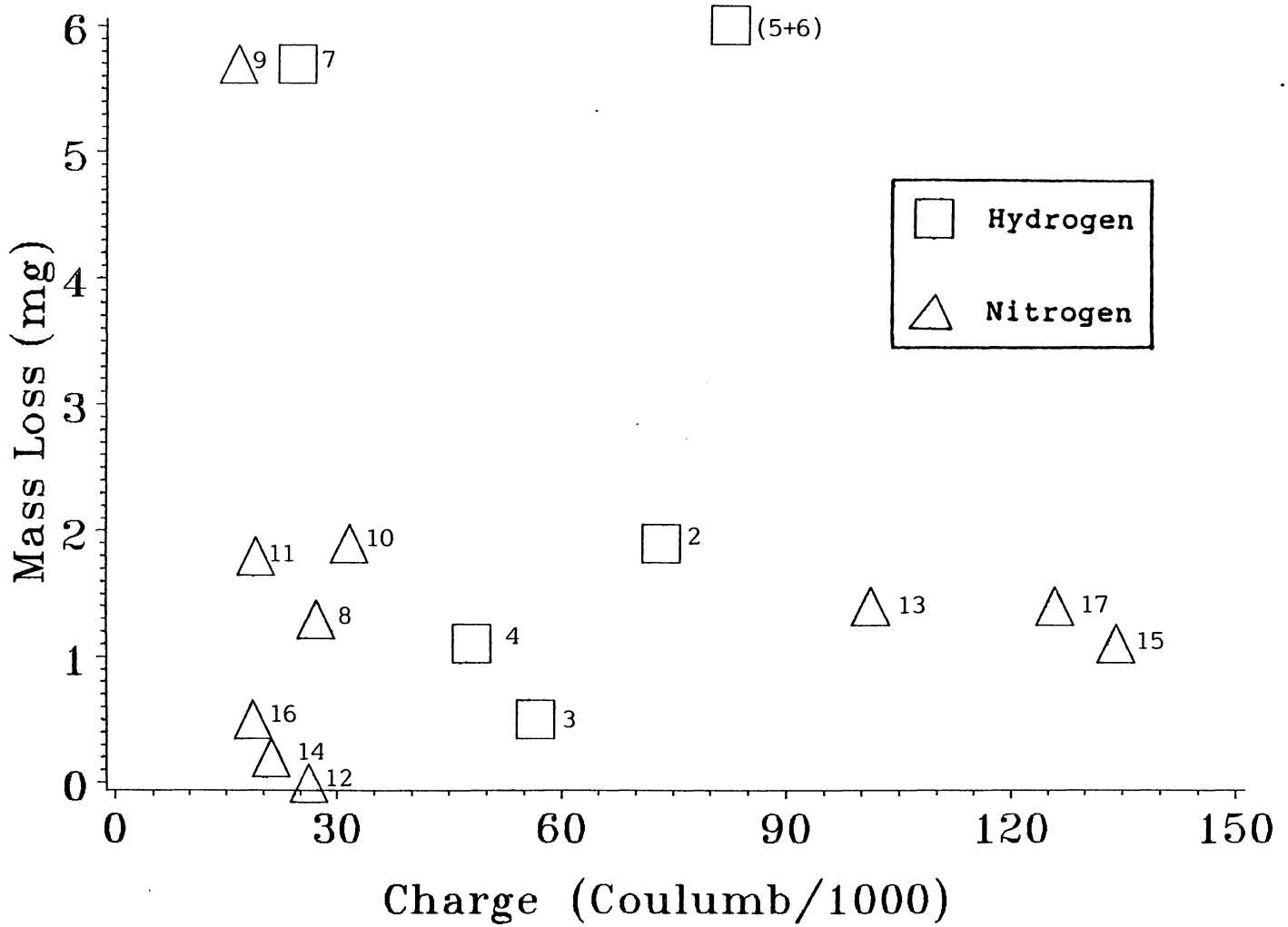

Figure 32. Anode Mass Loss vs Charge Passed on Diatomic-Argon Mixtures

The total mass loss for the first anode was 14.6 mg. Most of the mass loss (80 percent) took place during the last 3 tests. During the first 4 tests (507 min of operation on hydrogen-argon) the total anode mass loss was only 2.9 mg. The average anode mass loss rate during this time was only 0.00572 mg/min. This implies that high anode lifetimes are obtainable on argon-hydrogen and pure hydrogen for operation on hydrogen-argon feedstocks if the torch can be properly sealed.

The total mass loss for the second anode was 15.3 mg, which was less than the sum of the mass loss of the two cathodes which were tested with it. Over 37 percent of the mass loss occurred in test 9, which was the test with the broken swirler. Figure 32 shows that the mass loss per charge was much less for the last six tests with nitrogen than it was for the first four tests on nitrogen. As noted in the section on the torch characteristics, the voltage traces were rougher for the later tests with second anode than that for the earlier tests. It is thought that part of the cause of the voltage fluctuations may be movement of the anode attachment point to higher and lower positions along the diverging portion of the nozzle. If the arc does move in this way, the anode heat transfer would be distributed over a greater area, and thus the erosion would be expected to be less.

Assuming that all of the anode mass loss for the second anode occurred while operating on pure nitrogen and nitrogen-argon mixtures, the average mass loss rate was 0.013 mg/min. This may be compared to the 0.1 mg/min found in the study by Hardy [44], for a thoriated tungsten anode operating with a flow rate of 4000 ml/min of nitrogen, and a current of 10 A.

7.3.3 Electrode Geometry Changes

A photograph of the anode after test 3 is shown in figure 33. Little wear was observed upstream of the constrictor. Most of the anode wear was confined to one half of the downstream side of the constrictor. The length of the cathode, decreased 0.38 mm during this time. Photographs of the cathode are shown in figures 34 (a) and 34 (b). The cathode maintained its shape with some rounding of the tip. The cathode had small region at the tip which was molten. Near the tip of the cathode there were many small craters which were determined to be about 0.05 mm in diameter from the photograph.

During test 4 the anode continued to erode downstream of the constrictor. The erosion was still concentrated on one side of the anode. The cathode tip length decreased 0.20 mm during test 4, but the shape of the cathode changed during this test, with the creation of a large crater in the tip of the cathode. The formation of a crater in the cathode tip has also been seen in investigations of low power arcjet cathodes [45]. In the middle of the crater was a blob of tungsten which stuck out past the rim of the crater.

The cathode crater continued to broaden during test 5 and the number of tungsten blobs inside of the crater increased. A photograph of the cathode after test 5, which was the last test on the first cathode, is shown in figure 35. The final width of the crater rim at the tip of the cathode was measured from the photograph to be 0.60 mm. By the end of test 5 the length of the first cathode had decreased 0.78 mm.

After test 5, cathode 1 was switched to cathode 2. The length of the new cathode decreased 0.66 mm during test 6. The cathode tip of cathode 2 showed the formation of a crater with blobs of tungsten in the center similar to the crater on cathode one. During test 7, which was the last test with the second cathode, the length decreased another 0.15 mm. The crater rim was still present in this cathode after test 7 and there was a large blob of molten tungsten which protruded from the rim of the crater.

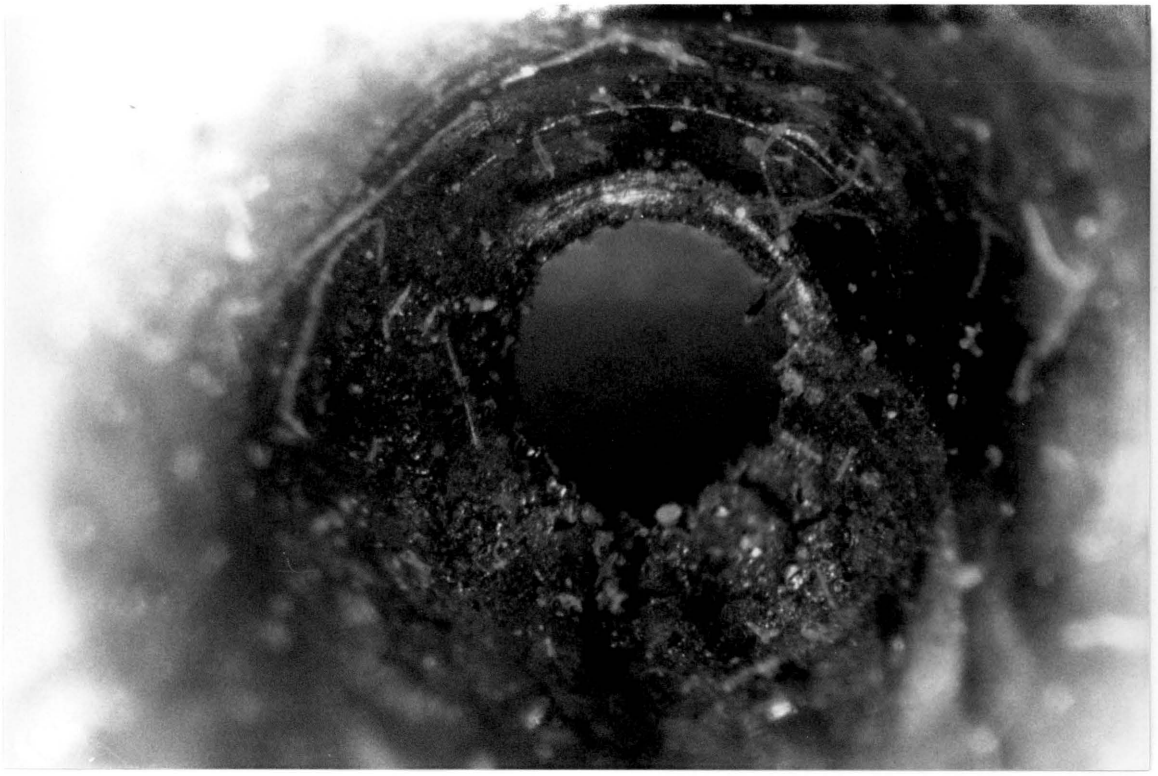

Figure 33. Anode Downstream After Test 3 (31.25 X)

(a)

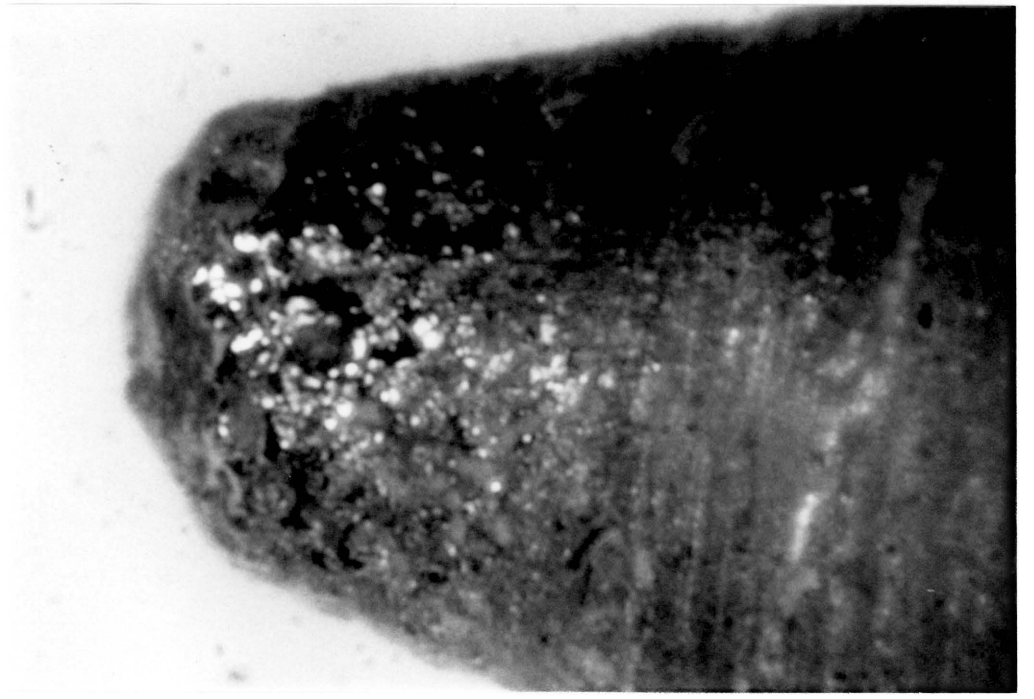

(b)

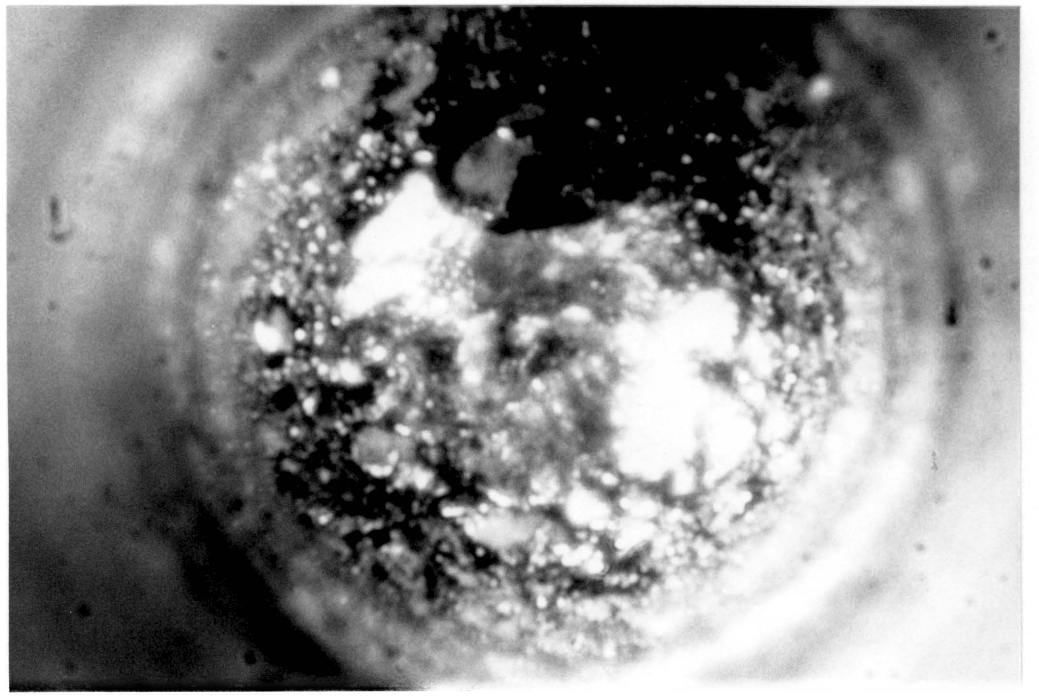

Figure 34. Cathode After Test 3: (a) Sideview (80 X) (b) End View (80 X)

(a)

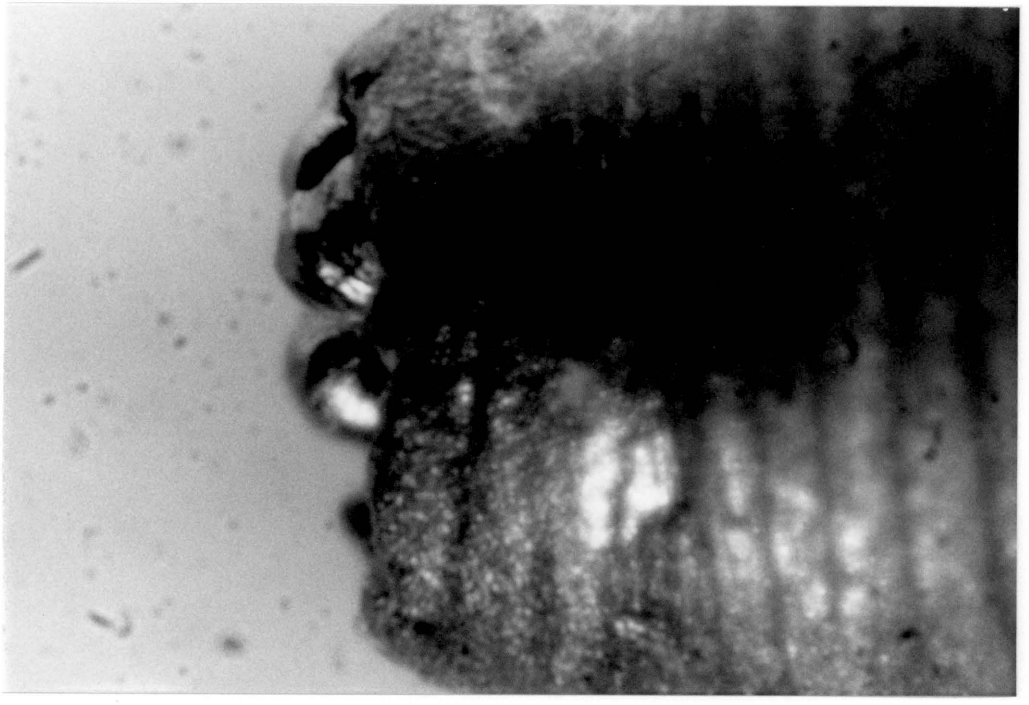

(b)

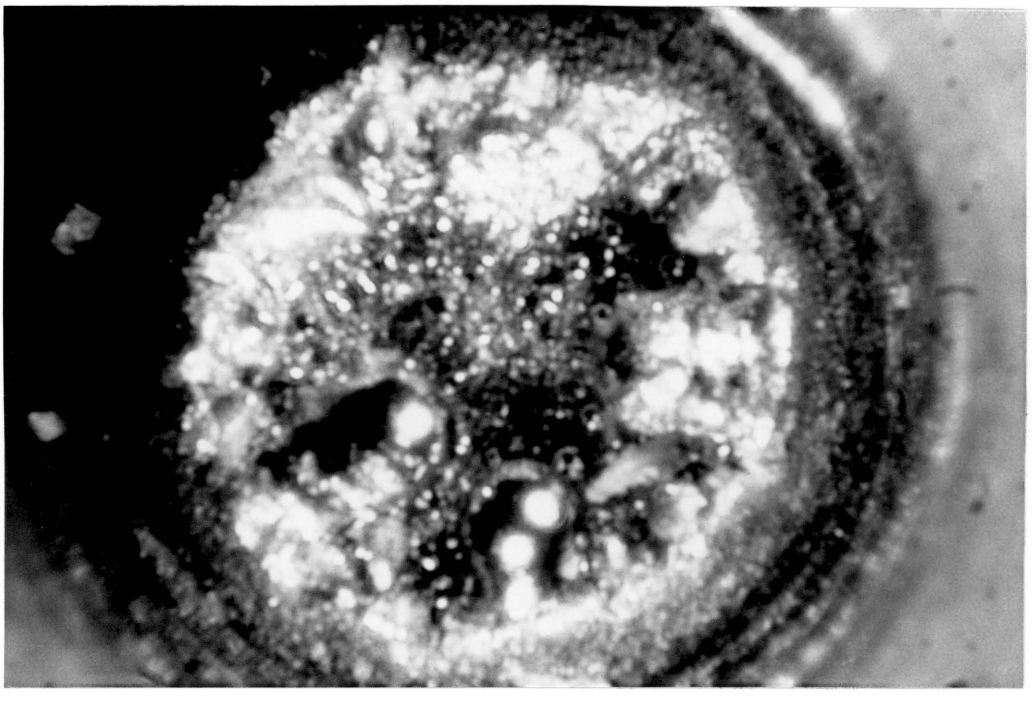

Figure 35. Cathode After Test 5 (80 X): (a) Sideview (b) Endview

A photograph of the anode after test 6 is shown in figure 36. The eroded region of the nozzle was spread further into the diverging section of the nozzle after this test, but there was still little damage upstream of the constrictor. Also, the constrictor itself showed little erosion through test 6. So, while the flow swirler was ineffective in turning the arc downstream of the constrictor, it was effective in anchoring the anode attachment point downstream of the constrictor. As noted in Chapter 3, anchoring the anode attachment point in the low pressure region of the nozzle, lowers the heat flux at the anode attachment point.

In test 7 there were severe problems with the dynamic seal, and the torch was operated at low chamber pressures and low chamber flow rates through the constrictor. The anode erosion for test 7 was concentrated in the constrictor. The entire constrictor showed evidence of melting after this test, and the diameter of the constrictor had increased during this test. Apparently, the actual flow rate through the constrictor was too low to force the arc through the constrictor. Also, with the low flow rate through the constrictor, there was little convective cooling of the constrictor.

A photograph of anode 2 taken after test 8 is shown in figure 37. This was the first test on nitrogen argon mixtures. This photograph shows that most of the damage to the anode is concentrated in a small region downstream of the constrictor. This indicates that little turning of the arc occurred downstream of the constrictor. Close observation of the torch during operation through a welding mask also confirmed this. During observation of the torch during this and other tests with nitrogen feedstocks, the anode was seen to glow in the region where the most damage had occurred. The cathode length decreased 0.406 mm, which was 40 percent of the initial length of the anode constrictor. The cathode is shown in figure 38. As in the tests with argon-hydrogen mixtures, the cathode had a crater with a blob of tungsten protruding from the center of it.

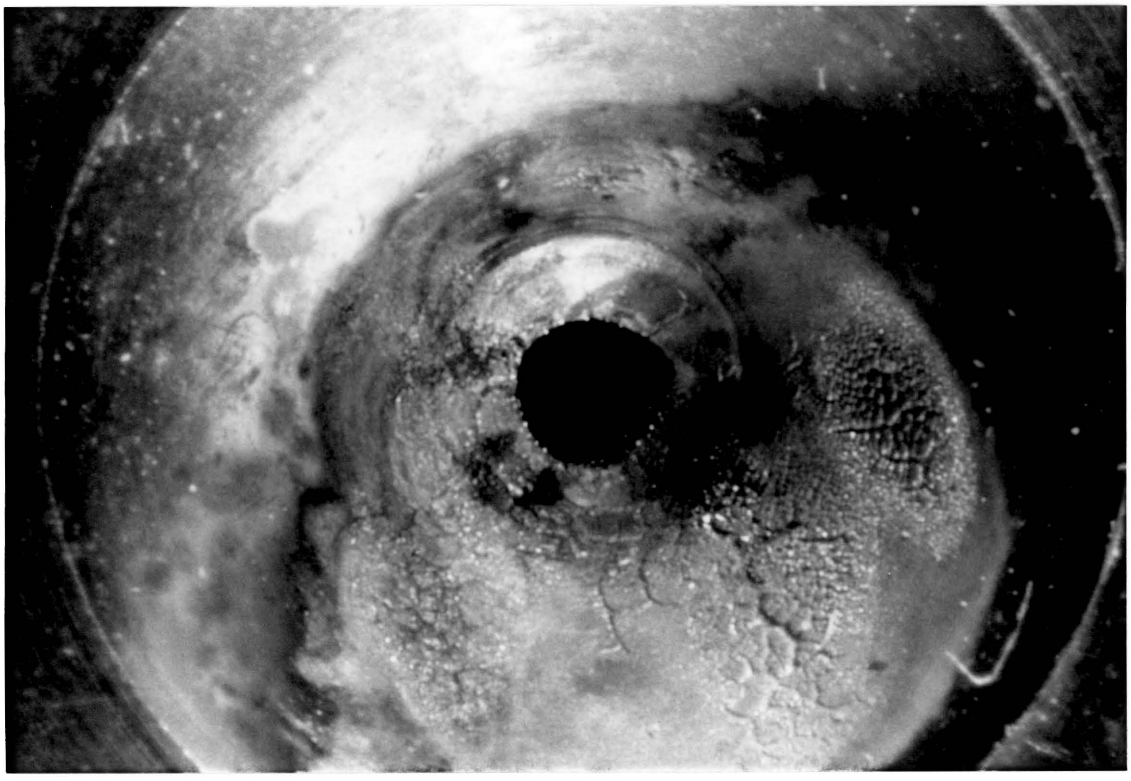

Figure 36. Anode Downstream After Test 6 (15.75 X)

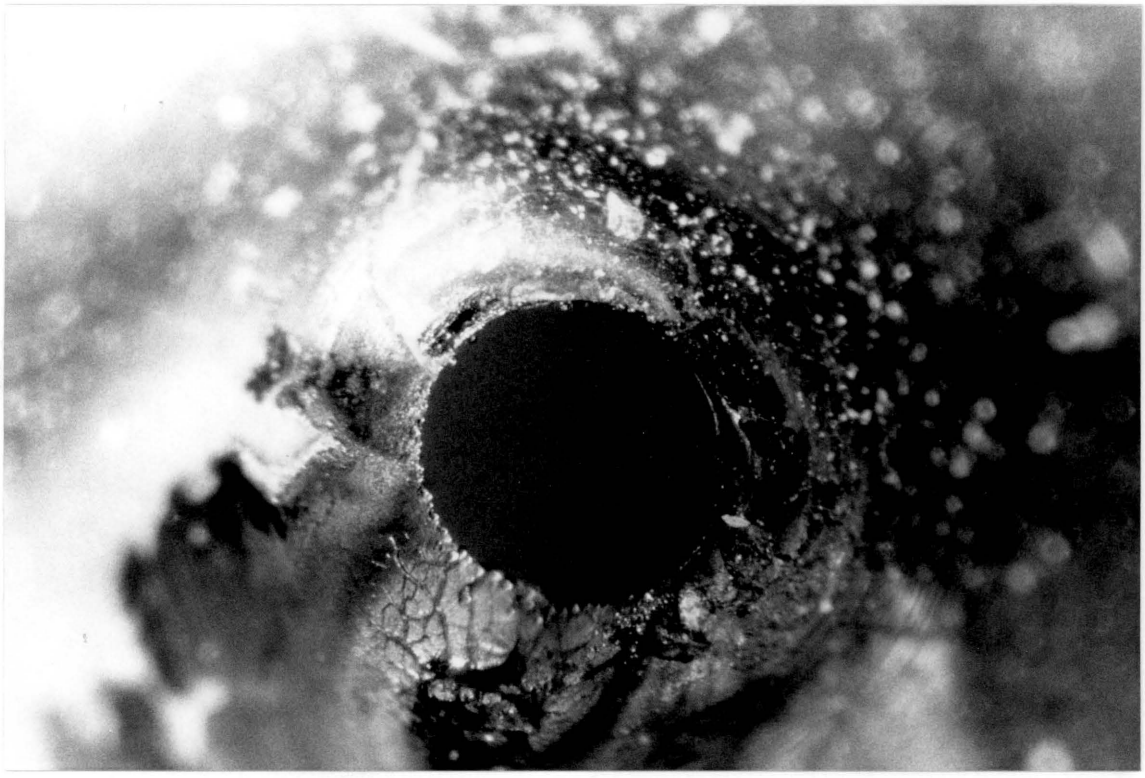

Figure 37. Anode Downstream After Test 8 (31.25 X)

(a)

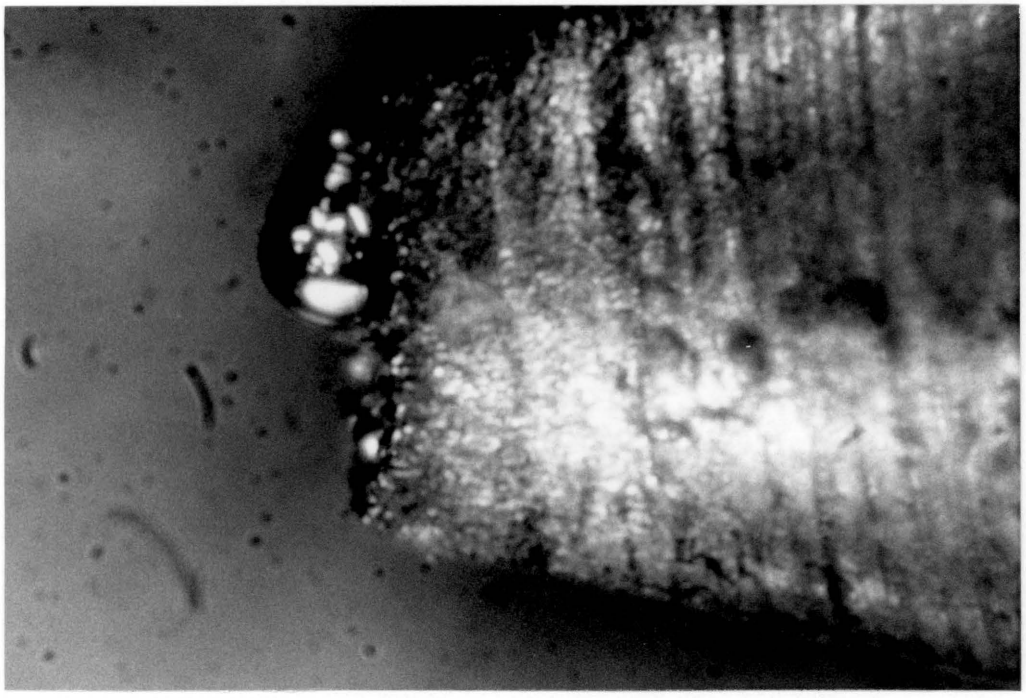

(b)

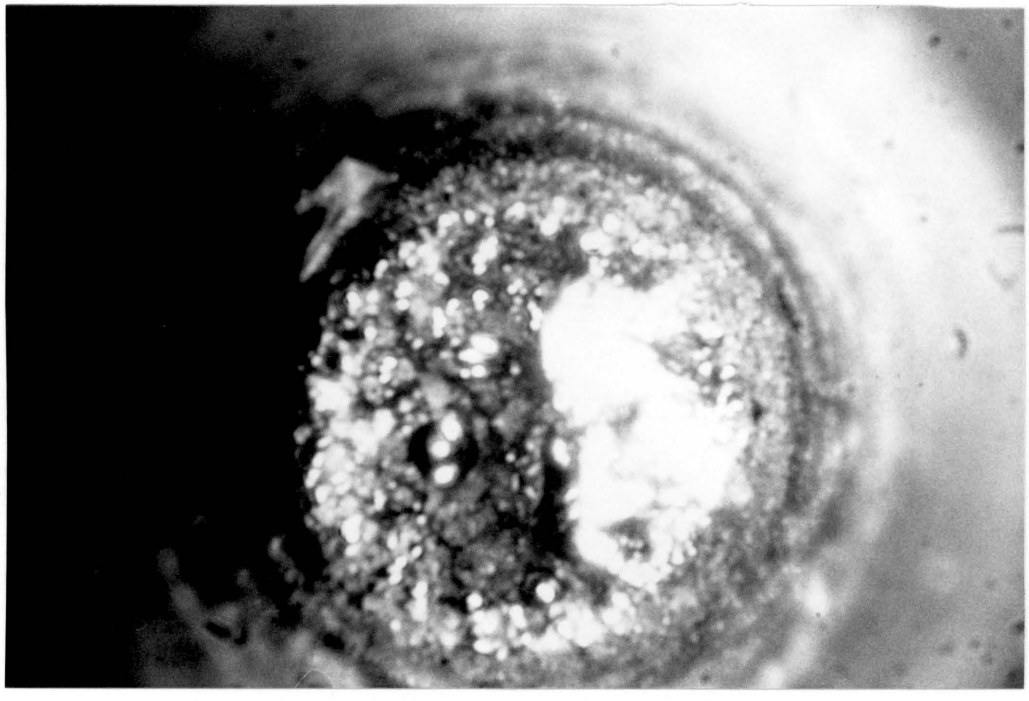

Figure 38. Cathode After Test 8 (80 X): (a) Sideview (b) Endview

Test nine was the test in which the flow swirler had broken. The mass loss rates of both electrodes were the worst out of all of the tests. A photograph of the anode after this test is shown in figure 39. The constrictor exit became wider and oval shaped. Also, the cathode tip recessed 0.30 mm more during the test, and the rim of the crater showed an increase in width. Also, the rim of the crater was worn more on one side than on the other.

A photograph of the anode after test 10 is shown in Figure 40. The constrictor exit had become more circular after this test. The cathode crater became larger during this test, and a large ball of tungsten had formed in the center of the crater. Although there was a cathode mass loss during this test, the length change, measured from the end of the cathode to the tip, was positive due to the presence of a tungsten ball protruding from the center of the cathode crater.

Throughout tests 11-14 the cathode continued to loose mass as shown in table 8. The crater became wider and the number and size of tungsten balls contained in the crater varied from test to test. During tests 8-14 the length of cathode 3 had decreased by 1.09 mm. The cathode is shown after test 14 in figure 41. The final cathode crater width as measured from this photograph was 0.78 mm.

The anode continued to loose more mass during tests 10 to 14 as shown in table 8. A photograph of the anode after test 14 is shown in figure 42 (a). Comparing this photograph with figure 40 taken after test 10 shows that little erosion of the constrictor had occurred during tests 11-14. Figure 43 (b) shows that some wear also occurred upstream of the constrictor.

For tests 15-17, cathode 3 was replaced by cathode 4. The erosion of cathode 4 was similar to that of cathode 3. A crater was formed in cathode 4 after test 15, and the number and size of the tungsten balls within the cathode crater varied for each of the tests with it. The length decreased by more than 0.967 mm (no measurement was taken

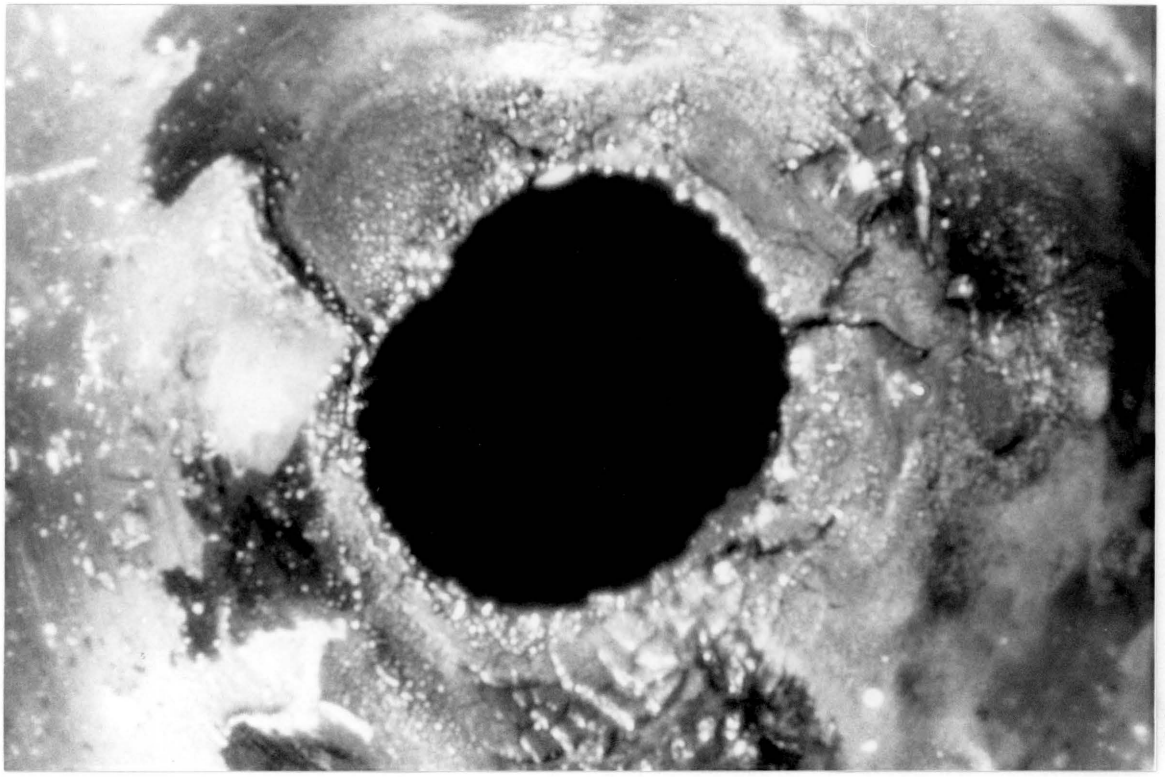

Figure 39. Anode Downstream After Test 9 (40 X)

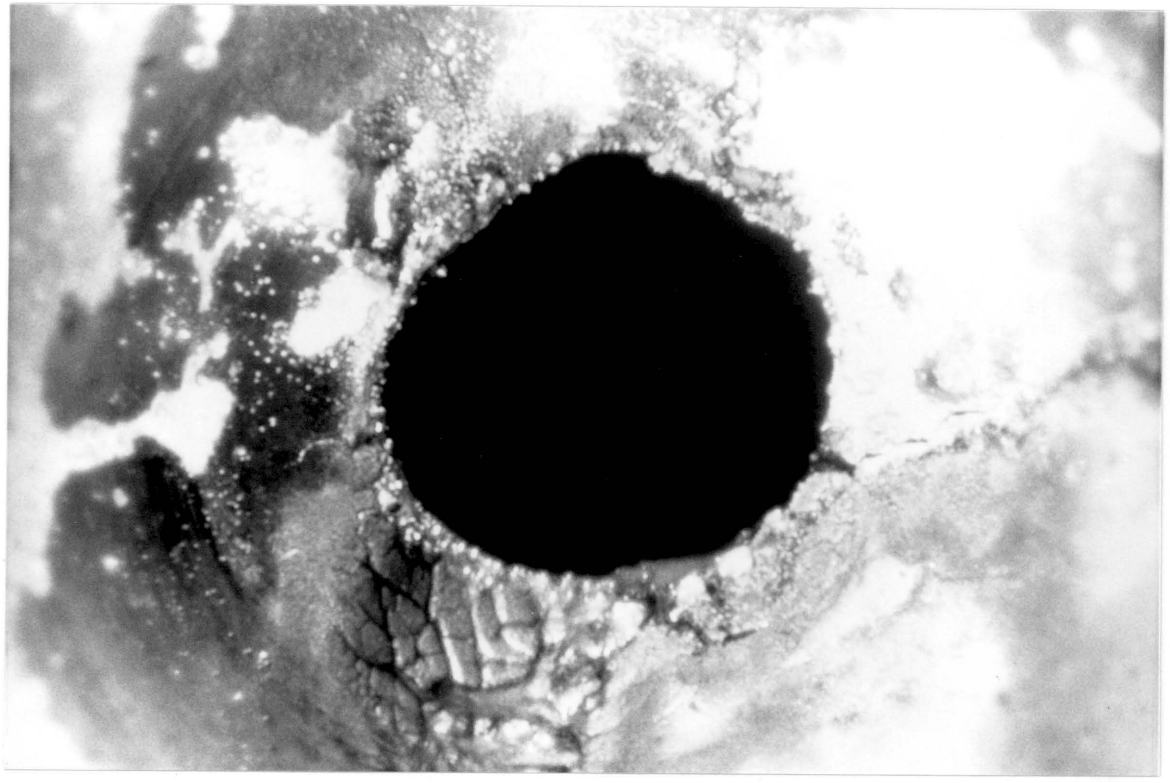

Figure 40. Anode Downstream After Test 10 (40 X)

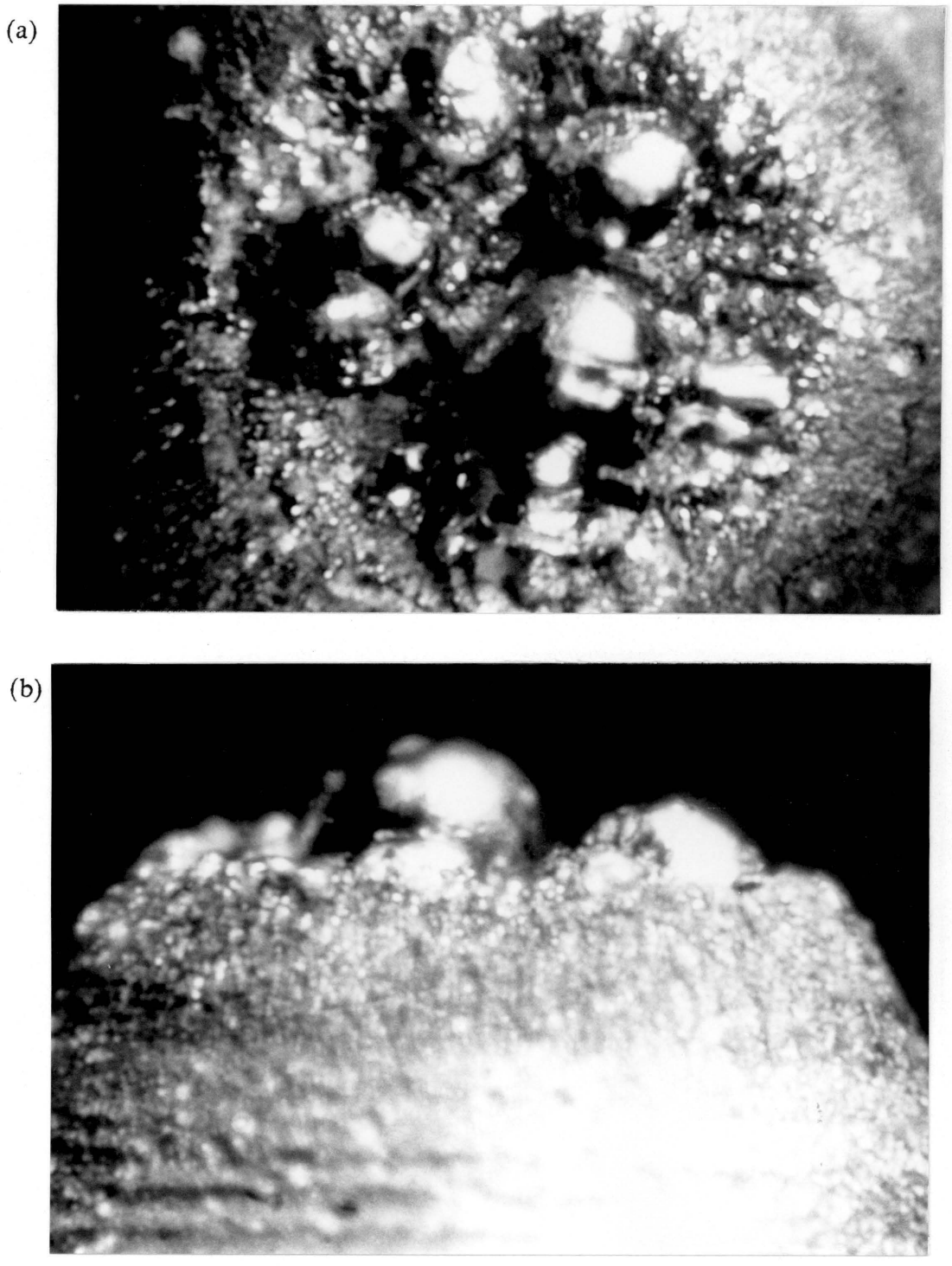

Figure 41. Cathode After Test 14 (80 X): (a) End View (b) Side View

(a)

(b)

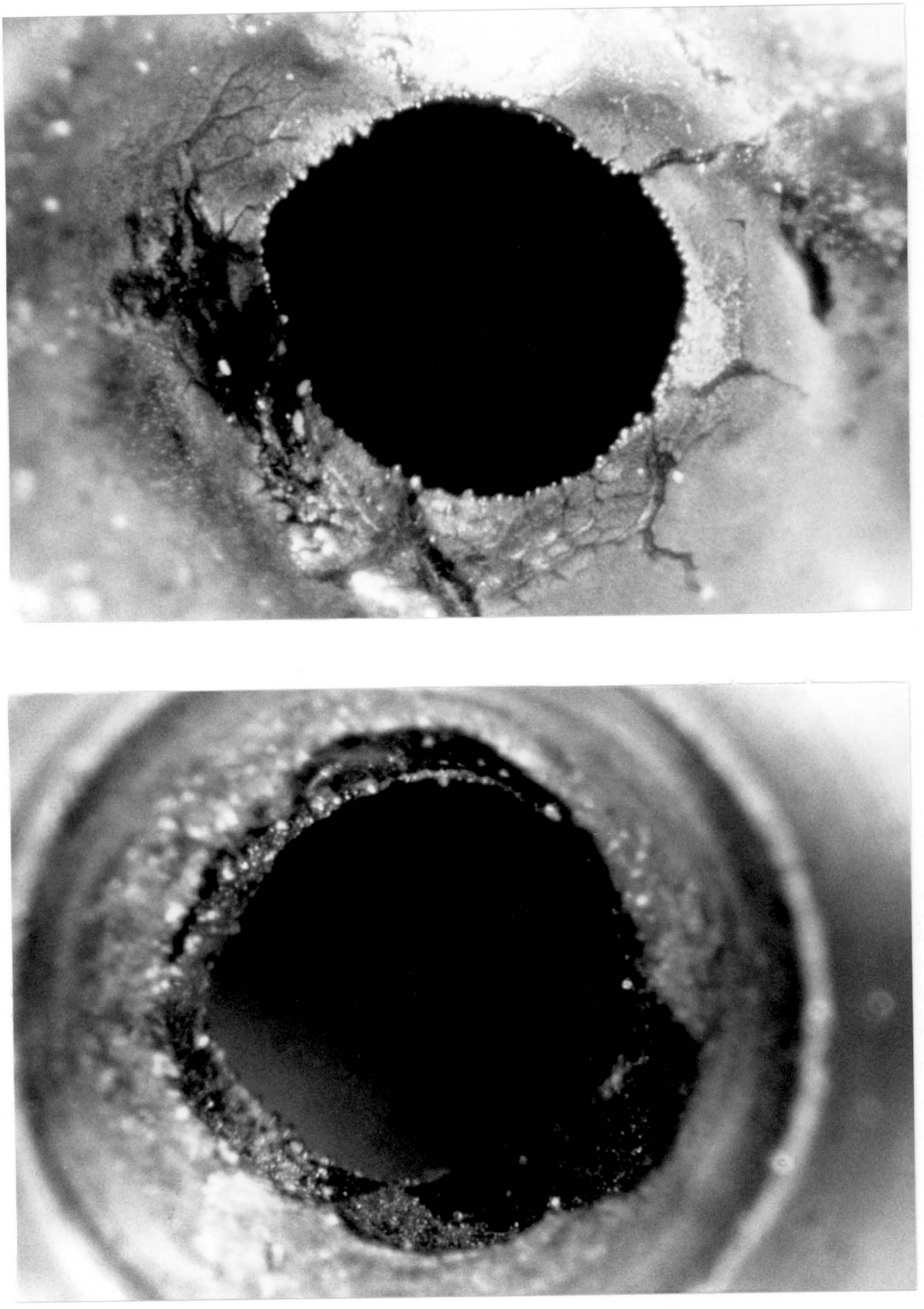

Figure 42. Anode After Test 14: (a) Downstream (40 X) (b) Upstream (40 X)

of the final cathode length) during tests 15-17. While the cathode erosion for tests with cathode 4 was comparable to that with cathode 3, the anode wear was significantly less for torch operation on the second cathode.

The photographs which have been shown of the anode show the increase in the radius of the anode constrictor from test to test, but they do not give an indication of the axial extent of the damage to the anode. Most of the anode erosion occurred downstream of the constrictor. The anode erosion started at the exit of the constrictor and eroded upstream. The erosion was uneven around the circumference of the constrictor exit so that one side was eroded severely while the other was left untouched.

Figure 43 shows a simplified sketch of anode erosion. On the side that was eroded severely the constrictor exit is at a smaller distance from the constrictor entrance. Also, the angle of the downstream portion of the severely damaged portion of the constrictor is more inclined to the cathode axis of the torch than the portion of the torch with low damage. This means that after the erosion has occurred, the arc has to turn less after exiting the constrictor. In a new anode (shown by the dotted lines in figure 43) the arc makes a sharp turn after exiting the constrictor, and is forced near the sharp edge at the exit of the constrictor, causing it to erode. During operation of both anodes the visible plume downstream of the torch was inclined toward the side of the torch which was damaged. This was especially true in the case of the anode used for the nitrogen tests.

7.4 Effect of Electrode Erosion on Torch Performance

As noted earlier, the torch performance during operation on both anodes changed with time. At similar levels of current and flow rates the voltage generally increased with each test. After the switch from cathode 1 to 2 between tests 5 and 6, for the same

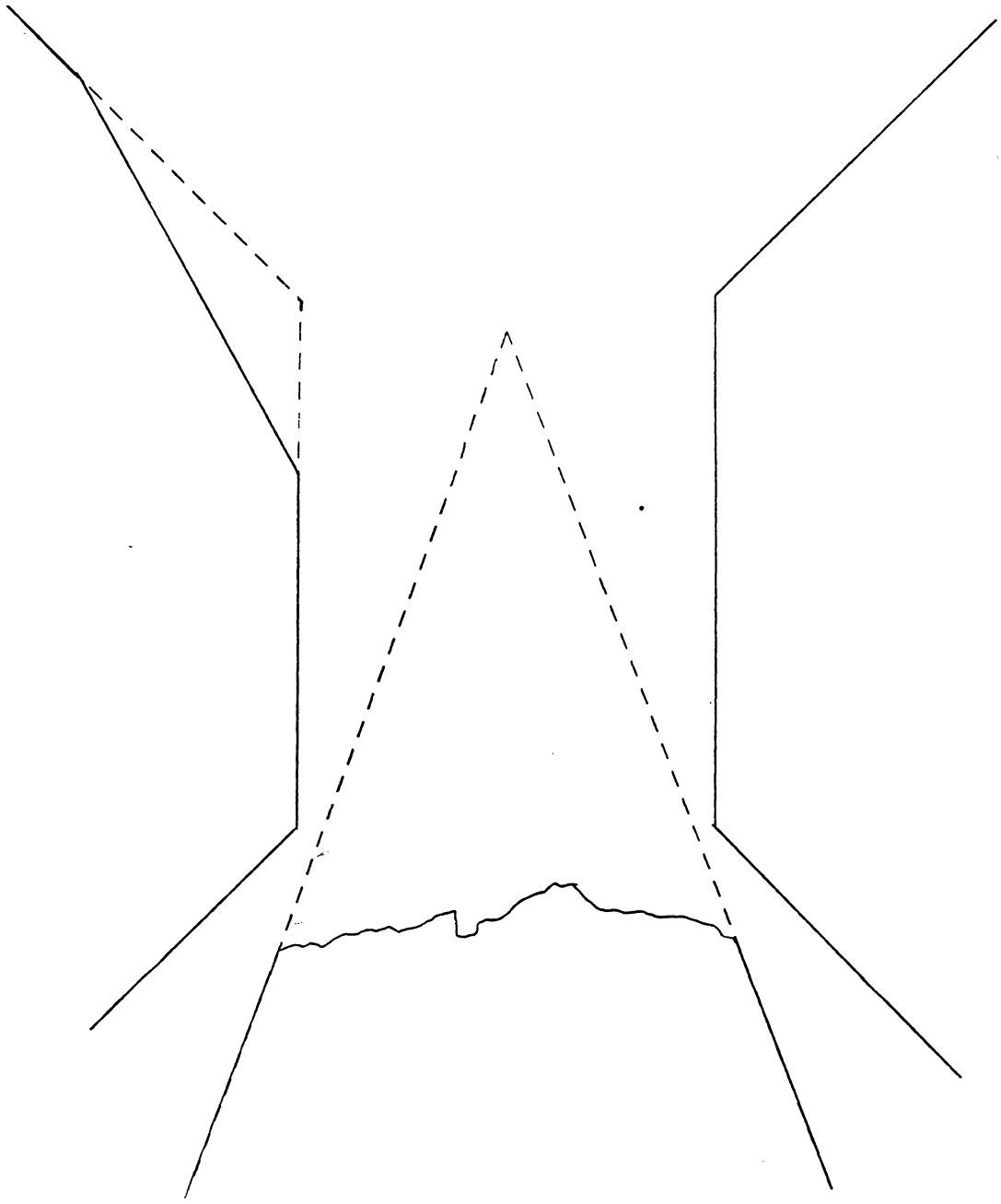

Figure 43. Sketch of the Anode Erosion During Tests 8-14

current it was possible to operate the torch at 85 percent hydrogen instead of only 57 percent hydrogen. A similar improvement in torch performance was noted between tests 14 and 15, when the cathode was switched. The first conclusion that one could make from this is that a new, and thus sharper cathode runs better than an old cathode with a blunted point. While this is probably true, it is thought that the change in the arc length may be largely responsible for the change in performance.

The side views of the cathode after some of the tests with cathode 1 were photographed at the same level of magnification. Each of the photographs was traced and the outlines were superimposed on a drawing of a perfect cathode, and a perfect anode at a gap of 0.152 mm, to illustrate the change in the cathode-anode geometry. The results are shown in figure 44. The line segment a_1 to a_2 represents the approximate region of anode attachment during test 1, while the segment a_1 to a_3 represents the approximate region of anode attachment during the latter tests after the slight erosion of the constrictor exit. The numbers on the outlines of the cathode represent the test after which it was photographed.

From figure 44 it can be seen that the arc length increased significantly during the tests. The cathode tip position has recessed from a position near the exit of the constrictor to one upstream of the constrictor. This had the effect of increasing the length of the arc. Since the arc column resistance is proportional to its length, the increase in the arc length led to a larger arc column resistance. Therefore, the total resistance, and thus the required voltage to operate the arc, was increased. After the cathode was switched the initial position of the cathode tip was once again at position 0, so that the arc length was decreased. The smaller arc length meant that for the same available voltage the arc column could have a higher resistance per unit length. Therefore, the torch could be operated on higher fractions of hydrogen after switching cathodes.

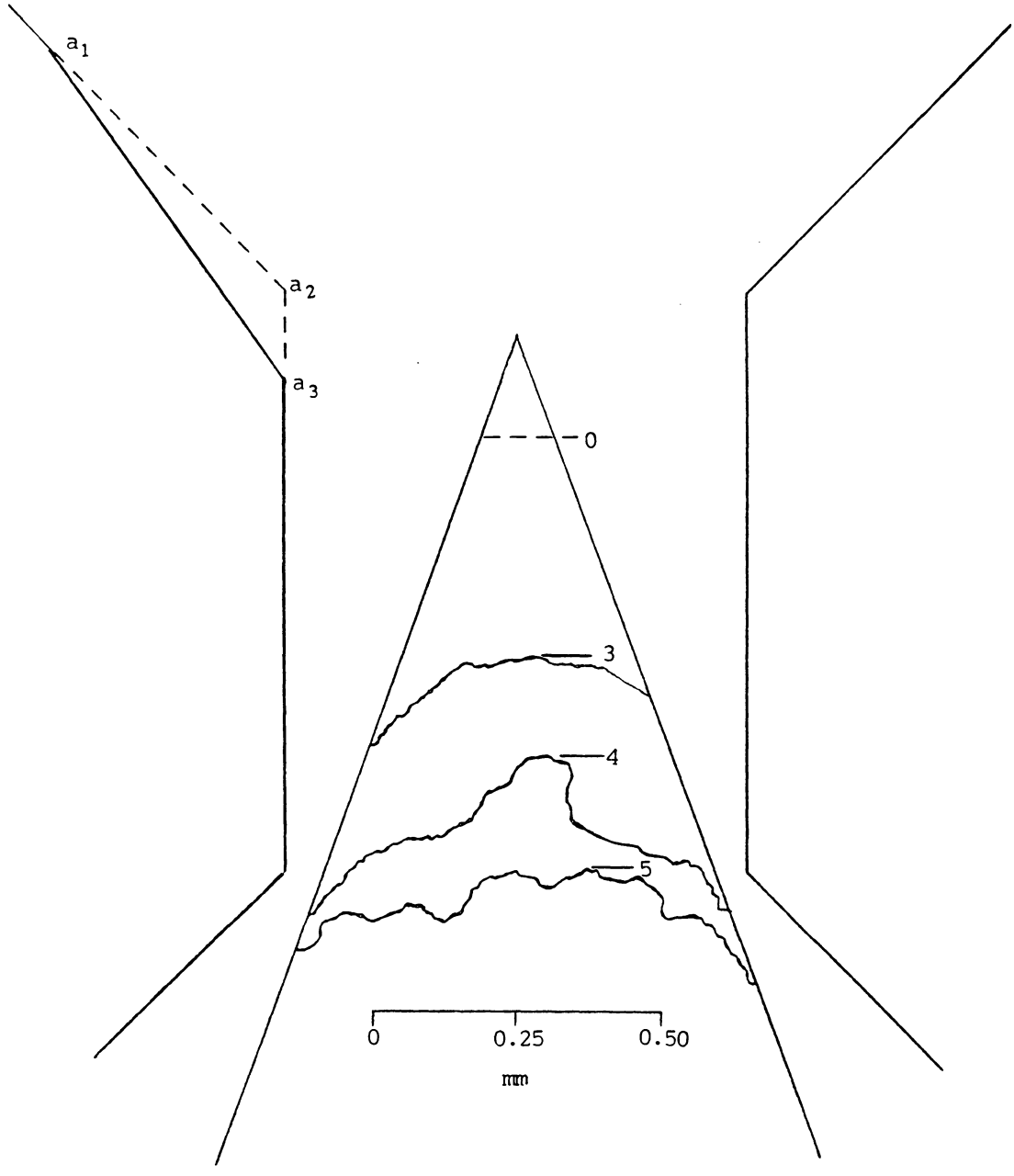

Figure 44. Electrode Geometry Changes for Cathode 1

Figure 45 (a) shows the side view of cathode 3 through tests 8-14. The torch was operated on pure nitrogen during test 10, and again, but with a higher voltage, in test 11. After test 11, each test was characterized by high voltages while operating on 50 percent mixtures of nitrogen-argon. The same argument about the increased arc length causing an increase in the voltage applies here as it did with cathode 1.

Both the cathode and the anode erosion were more rapid with this cathode operating on nitrogen than with the early tests on cathode 1. The anode erosion was more pronounced for the second anode than the first anode. That is, the anode attachment region a_1-a_2 is larger in the second anode than in the first anode. Also as shown in the photograph of the anode after test 14, figure 42 (b), the anode had eroded upstream of the constrictor. This is thought to have been caused by the presence of the blunted cathode upstream of the constrictor in tests 13 and 14. During tests 13 and 14 the width of the cathode is greater than the diameter of the constrictor.

After test 14, cathode 3 was replaced by cathode 4. Since the entrance to the constrictor was eroded. The position of the cathode upon making electrical contact was further into the constrictor. After making electrical contact the cathode position was moved back to 0.152 mm from the contact point. This is shown in figure 45 (b). The distance from the cathode to the anode attachment region is much much shorter than that during tests 13 and 14. After making this change of cathodes the torch was easily operated on pure nitrogen for over 5 hours, at a lower voltage than that during the periods of pure nitrogen operation during tests 10 and 11. This shows that low power operation on a pure diatomic gas is easily achieved if the arc length is small enough.

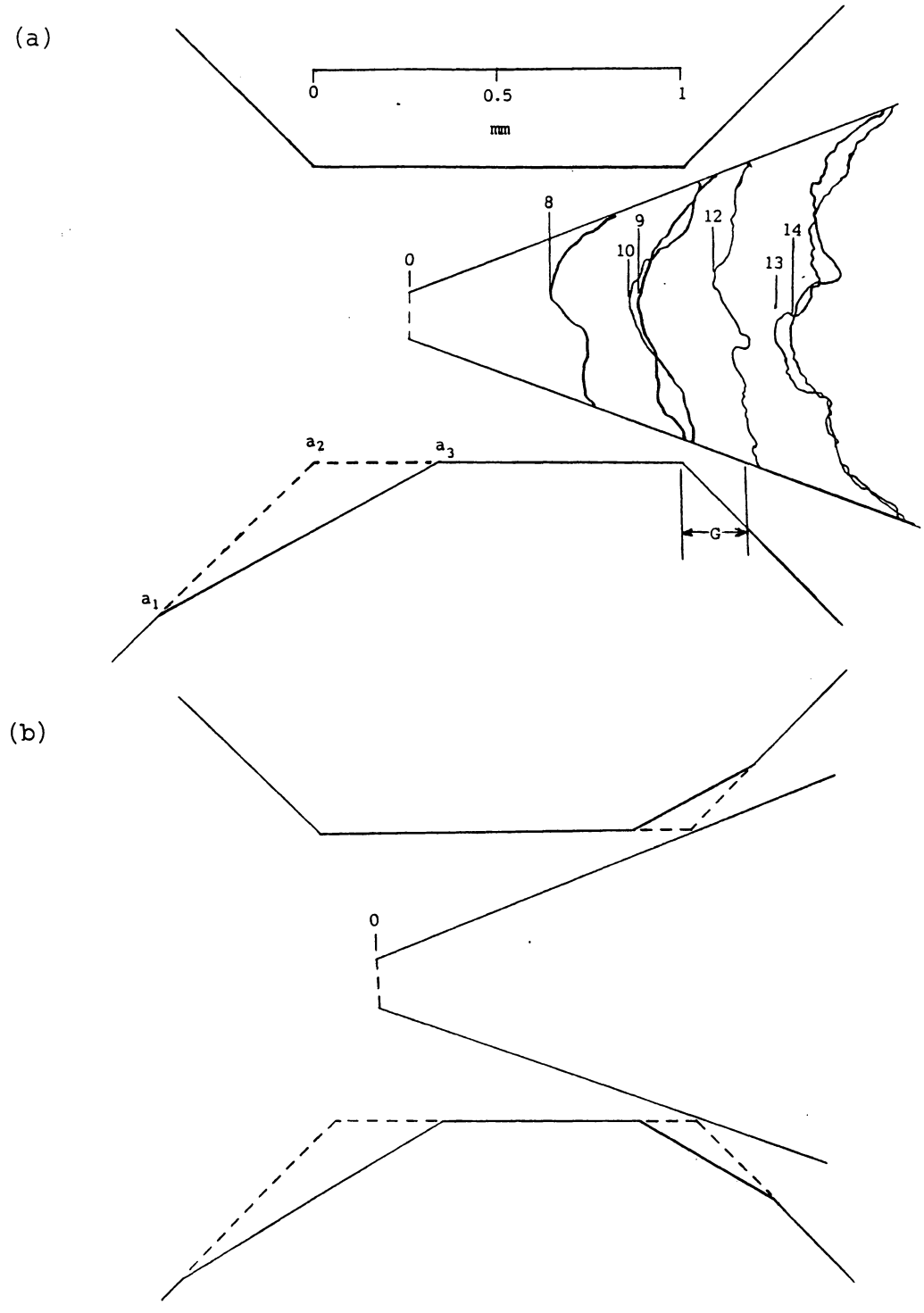

Figure 45. Electrode Geometry Changes During Nitrogen Tests: (a) Test 8-14 (b) start of test 15

Chapter 8

Summary,Conclusions and Recommendations

8.1 Summary and Conclusions

The design of the VPI plasma torch has been modified in order to decrease the erosion rates of the electrodes, and to improve the stability of the torch. The operational characteristics of the improved plasma torch were monitored by a microcomputer-based data acquisition system. Extended operation of the torch was demonstrated on feedstocks of argon, nitrogen, argon-nitrogen, and hydrogen-argon mixtures. Operation of the torch was also briefly demonstrated on pure hydrogen.

The rate of anode erosion, which had previously limited the choked lifetime of the torch to two hours, has been reduced significantly. In tests with nitrogen-argon mixtures the total anode mass loss was less than that of the cathode, so that the cathode wear has become the limiting factor in the lifetime of the torch on nitrogen-argon mixtures.

The cathode mass loss has been shown to be proportional to the charge passed through the torch, in the tests with nitrogen-argon mixtures.

The testing of the improved torch on hydrogen was concluded because of difficulty in maintaining a sealed torch on hydrogen. However, with the improved torch over 700 min of choked torch operation have already been demonstrated on a single anode, while operating on mixtures of hydrogen and argon. Also, the results of the first 500 min of testing on hydrogen-argon mixtures imply that anode lifetimes in excess of 20 hours on hydrogen-argon mixtures are obtainable with a properly sealed torch.

During tests with nitrogen-argon mixtures, testing of the anode was voluntarily halted after 20 hours of choked operation. During these tests, the torch was operated on pure nitrogen for 393 min. After the tests, examination of the anode showed that further operation in excess of the original goal of 20 hours per anode was indeed possible. Therefore, the improved plasma torch is a device capable of extended operation and may be considered as operational tool for future combustion research.

8.2 Recommendations

The major weakness in the present torch design is the dynamic seal. The problem of sealing the torch is especially important when using hydrogen gas in the torch. Development of a more reliable sealing technique for the sliding seal should be undertaken immediately. This may involve using the existing seals and moving the location of the seal back to a lower temperature region of the torch or using a seal which can withstand higher temperatures.

It is also suggested that the existing torch be operated on higher purity gases than the commercial grade (99 percent pure) feedstock gases in order to determine if the impurities in the gas have an effect on the electrode erosion.

The power supply unit, consisting of the four arc welding power supplies, was satisfactory for a preliminary investigation of the torch, however, the current regulation was awkward in the low current range used in this study, and the current usually tended to drift during tests. Also, the use of the four power supplies disabled the high frequency starter so that the arc had to be started by the open circuit voltage and the gap. The gap at which the arc started varied from test to test, so that the starting procedure was not repeatable. For these reasons, it is recommended that the existing set of power supplies be replaced by a single power supply unit for practical use of the torch. The new power supply should be designed for operation at low current and high voltage and offer fine control of the arc current. In addition, it would be desirable to have a more reliable and repeatable method of starting the torch.

Power processors which use pulse width modulation for control of the arc and pulsed, high voltage arc ignition have been developed for application to the control of low power arcjets [43]. It is suggested that a power supply of this type should be used for further studies.

Before any detailed development program is undertaken on the present torch it is suggested that chemical diagnostics of the reacting plasma-flame region should be performed in an actual combustor. The diagnostics are desired to characterize the radical production of the torch and the role of specific radicals in combustion enhancement. Another objective of such diagnostics could be to separate the fluid-mechanical effects from the chemical effects of the torch. Finally, chemical diagnostics of the torch could yield information about what the optimum set of torch parameters (flow rates, gap, current) is for a desired chemical effect.

After chemical diagnostics of the present torch have been performed, The suggestions in the following sections are expected to improve the torch.

8.2.1 Arc Rotation

One of the reasons that a flow swirler was designed into the torch was to insure that arc rotation occurred at the anode attachment point. As noted in chapter 8, with the present flow swirler and electrode geometry, arc rotation did not occur downstream of the constrictor. There are two known ways to produce arc rotation : magnetic and fluid mechanical.

If magnetic rotation was employed in the present torch, the expected effect of it would be to rotate the arc attachment point downstream of the constrictor. Since only the portion of the arc downstream of the constrictor, which has a radial component of current, would be rotated by the magnetic field, the radical output of the present torch would be expected to be the same whether or not rapid arc rotation occurs downstream of the constrictor. This is in contrast to the effect of the axial magnetic field on the arc in the plasma torch discussed in reference [21] in which the magnetic field rotates the entire arc column though the gas upstream of the constrictor, thus producing a more uniformly heated flow.

Magnetic rotation of the arc could be accomplished by a magnetic field aligned with the cathode of the torch. The torch temperatures, measured by the thermocouple shown in figure 9, was below 250 C, which is low enough that a small permanent magnet could be placed in the torch without reaching the Curie temperature of the magnet. One possible location of the magnet could be to replace the ceramic material used for component S in figure 8 by an electrically nonconducting magnet material.

The other known means of rotating the arc is to use vortex rotation. As noted above, the vortex failed to rotate the arc downstream of the constrictor. One way of strengthening the vortex at the constrictor upstream of the constrictor would be to increase the angular momentum of the flow exiting the flow swirler. There are two ways to accomplish this in the present device. The first way is to increase the the tangential component of the gas velocity exiting the swirler by decreasing the angle of the flow passages in the swirler with respect to the cathode axis. This is a manufacturing problem. The other way to increase the angular momentum of the flow is to use smaller flow passages in the flow swirler. However, it would be undesirable to have the flow choked at the swirler.

The amount of swirl present downstream of the constrictor is not only dependant on the amount of swirl upstream of the constrictor but also on the amount of viscous dissipation in the the constrictor region. The dissipation in the constrictor region is expected to be related to the geometry of the electrodes. The expected relation of proposed electrode geometry changes on the swirl present at the constrictor exit will be examined along with the other expected effects of such changes in the following Section.

8.2.2 Electrode Geometry

As noted in the introduction, the purpose of this work was to improve the performance of the existing torch without changing the electrode design. However, after conducting the tests reported in this thesis, several design changes to the electrodes are suggested. The first change to the electrodes is to decrease the length of the constrictor. This is expected to have several effects on torch operation. The first effect is that the voltage (which is related to the length of the arc) will be reduced. If the length, and therefore the voltage, required for an arc was reduced this would allow low power

operation of the torch on diatomic gases. Also, the dissipation of the swirl in the constrictor, which would be expected to be proportional to the length of the constrictor, would be less if the constrictor length were reduced.

The present divergence angle of the anode downstream of the constrictor is 45 degrees with respect to the cathode. It is suggested that this angle should be decreased. Since angular momentum is the product of the tangential velocity, mass, and the radius, the larger the wall radius at the point of arc attachment, the smaller the swirl will be. Thus the use of a smaller divergence angle would mean that the wall radius at the arc attachment point would be less and therefore the swirl there would be greater than that in the present design. Another reason that the switch to a smaller angle is thought to be beneficial is that the arc would not have to make as sharp of a turn at the exit of the constrictor.

As noted in chapter 3, the larger the constrictor diameter is with respect to the arc, the less stable it is. The diameter of the constrictor may be decreased to improve the stability on diatomic gases, but there are several trade-offs. The first is that any alignment errors will be amplified by the use of a smaller constrictor. Another possible trade-off would be the further heating of the constrictor due to the closer proximity to the arc. Also, the size of the constrictor may well affect the penetration of the plasma into the reacting region. In the case of the sonic fuel injection into a supersonic crossflow the penetration of the fuel is dependant on the diameter of the orifice [46]. If the penetration of the plasma is dependant on the constrictor diameter, a decrease of the constrictor diameter may be detrimental to intended application of the torch.

As noted in chapter 7, the decrease of the the cathode length produced significant changes in the relative electrode geometry and thus the torch performance. It is suggested that the cathode tip angle be increased so that the length change per amount of material removed is reduced. Another change which is recommended for the cathode

is to improve the surface finish so that there are no sharp edges other than the cathode tip at which arc attachment could be favored.

References

1. Jones, Robert A., and Huber, Paul W.,"Toward Scramjet Aircraft," *Aeronautics and Astronautics,* Vol. 16, No. 2, pp. 38-48, 1978.

2. Andrews, E. H., Northam, G. B., Torrence, M. G., and Trexler, C. A.,"Mach 4 Tests of a Hydrogen-Burning Airframe- Integrated Scramjet Engine,"Presented at the 18th JANNAF Combustion meeting, October 1981, CPIA Publication 347, Vol. IV, pp. 87-96, 1981.

3. Andrews, E. H., Northam, G. B., Torrence, M. G., Trexler, C. A., and Pickney, S. Z.,"Mach 4 Wind Tunnel Tests of a Hydrogen-Burning Airframe Integrated Scramjet engine," NASA TM-85688, 1984.

4. Jachimowski, Casimir, J.,"An Analytical Study of the Hydrogen-Air Reaction Mechanism With Application to Scramjet Combustion," NASA Technical Paper 2791, 1988.

5. Anderson, G. Y., and Mackely, E. A.,"Mach 7 Performance of the Langley Airframe Integrated Modular Scramjet," Presented at the 1983 JANNAF Propulsion Meeting, CPIA Publication 370, Vol. 5 , pp. 493-508, 1983.

6. Northam, G. B., McClinton, C. R., Wagner, T. C., and O'Brien, W. F.,"Development and Evaluation of a Plasma Jet Flameholder for Scramjets," AIAA-84-1408, Presented at the AIAA/SAE/ASME 20th Joint Propulsion Conference, June 1984.

7. Wagner, T. C., O'Brien, W. F., Northam, G. B., and Eggers, J. M., "Development and Evaluation of a 1kW Plasma Torch Ignitor for Scramjets," Presented at the 23rd JANNAF Combustion Meeting, October 1986.

8. Barbi, E., Mahan, J. R., O'Brien, W. F., and Wagner, T. C., "Operating Characteristics of a Hydrogen-Argon Plasma Torch for Supersonic Combustion

Applications," *AIAA Journal of Propulsion And Power*, Vol. 5, No. 2, pp. 129-133, 1989.

9. Lawton, J., Payne, K. G.,and Weinberg, F. J.,"Flame-Arc Combination," *Nature*, Vol 193, pp. 736-738, 1962.

10. Chen, D. C. C., Lawton, J., and Weinberg, F. J.,"Augmenting Flames With Electric Discharges," Tenth Symposium (International) on Combustion, The Combustion Institute, 1965.

11. Harrison A. J., and Weinberg F. J.,"Flame Stabilization by Plasma Jets," Proceedings of the Royal Society of London A, Vol 321, pp. 95-103, 1971.

12. Waterson, K.,"Some Operating Characteristics of Novel Ignition Devices For Hydrocarbon/Air Mixtures," Ph. D. Thesis, University of Oxford, September 1973.

13. Weinberg, F. J., Hom K., Oppenheim, A. K., and Teichman, K., "Ignition by Pulsed Plasma Jet," *Nature*, Vol. 272 , pp. 341-343, 1978.

14. Cetegen, B., Teichman K. Y., Weinberg, F. J., and Oppenheim, A. K.,"Performance of a Plasma Jet Igniter," SAE Paper 80042 1980.

15. Orrin, J. E., Vince, I. M., and Weinberg F. J., " A Study Of Plasma Jet Ignition Mechanisms," Eighteenth Symposium (International) on Combustion, The Combustion Institute, pp. 1523-1531, 1982.

16. Clements, R. M.,"Review of Plasma Jet Ignition," *The Chemistry of Combustion Processes*, ACS Symposium 249, American Chemical Society, pp. 193-204.

17. Vince, I. M. ,Vovelle, C., and Weinberg F. J. "The Effect of Plasma Jet Ignition on Flame Propogation and Sooting at the Rich Limit of Flammabilty," *Combustion and Flame*, Vol 56, pp. 105-112, 1984.

18. Weinberg, F. J.,"Electrical Discharge-Augmented Flames and Plasma Jets in Combustion," *Advanced Combustion Methods*, Edited By Weinberg F. J., Academic Press, London, pp. 277-330, 1986.

19. Hillard J. C., and Weinberg F. J.,"Effect of Nitrogen Containing Plasmas on Stability, NO Formation and Sooting Of Flames," *Nature*, Vol 259, pp. 556-557, 1978.

20. Behbahani, H. F., Fontijn, A., Muller-Dethlefs, K. , and Weinberg F.J.,"The Destruction of Nitric Oxide by Nitrogen Atoms From Plasma Jets," *Combustion Science and Technology*, Vol. 27, pp. 123-132, 1982.

21. Chan, A. K. F., Hilliard J. C., Jones, A. R.,and Weinberg F. J.,"An Electrically Efficient, Finely Tunable, Low Power Plasma Generator," *Journal of Physics D:Applied Physics*, Vol. 13, pp. 2309-2320, 1980.

22. Behbahani, H. F.,Warris A. M., and Weinberg F. J.,"The Destruction of Nitric Oxide by Nitrogen Atoms From Plasma Jets:Designing for Thermal Stratification," *Combustion Science and Technology,* Vol. 30, pp. 289-302, 1983.

23. Warris, A. M., and Weinberg F. J.,"Ignition and Flame Stabilization by Plasma Jets In Fast Gas Streams," Twentieth Symposium (International) on Combustion, The Combustion Institute, pp. 1825-1831, 1984.

24. Kimura, I., Aoki, H.,and Kato, M.,"The Use of a Plasma Jet for Flame Stabilization and Promotion of Combustion In Supersonic Air Flows," *Combustion and Flame,* Vol. 42, pp. 297-305, 1981.

25. Byers, D. C., and Wasel, R. A. "The NASA Electric Propulsion Program," AIAA-87-1098, Presented at the 19th AIAA/DGLR/JSASS International Electric Propulsion Conference, 1987.

26. Dennis,P. R., Gates D. W., Smith C. R., and Bond, J. B., "Plasma Jet Technology,"NASA SP-5033, 1965.

27. Clover, G. M., and Weinberg F. J.,"Quenching Magnetically Rotated Augmented Flames and Plasma Jets in Mixtures Containing Methane, Oxygen, and Nitrogen," *Proceedings of the Royal Society of London A,* Vol. 326, pp. 375-391, 1972.

28. Cobine, J. D.,*Gaseous Conductors,* Dover Publications, Inc., New York, 1958.

29. Finklnberg, W.,and Maecker, H., *Electric Arcs And Thermal Plasma,* NASA translation of *Electrische Bogen und Thermishes Plasma,* Handbook of Physics Vol. XXII, Springer-Verlag, Berlin, 1956.

30. Hoyaux, M. F., *Arc Physics,* Springer-Verlag, New York, 1968.

31. Sheer, C., Cooney,J. A., and Rothacker D. L.,"Fluid Transpiration through the Anodic Boundary of an Electric Arc," *AIAA Journal,* Vol. 2, No. 3, pp. 483-489, 1964.

32. Vincenti, W. G., and Kruger C. H., *Introduction to Physical Gas Dynamics,* Robert E. Krieger Publishing Company, Malabar, Florida, 1982.

33. Noeske, H. O. ,Kassner, R. R., "Analytical Investigation of a Bipropellant Arc Jet," *ARS Journal,* Vol. 32, No. 11, pp. 1701-1708, 1962.

34. Eberhart R. C., and Seban R. A.,"The Energy Balance for a High Current Argon Arc," *International Journal of Heat And Mass Transfer,* Vol. 9, pp. 939-949, 1966.

35. Link, W. J., and Incropera, F. P., "Experimental Heat Transfer Distribution in an Arc Constrictor of Variable Cross-Sectional Area," *International Journal of Heat And Mass Transfer,* Vol. 15, pp. 873-875, 1972.

36. Shih, K. T., Pfender E., Ibele, W. E., Eckert, E. R. G., "Experimental Anode Heat Transfer Studies in a Coaxial Arc Configuration," *AIAA Journal,* Vol. 6, pp. 1482-1487, 1968.

37. Curren, F. M.," An Experimental Study of the Energy Loss Mechanisms and Efficiency Considerations in the Low Power dc Arcjet," AIAA-85-2017, Presented at the AIAA/DGLR/JSASS 18th International Electric Propulsion Conference, 1985.

38. Hardy, T. L., and Nakanishi, S., "Cathode Degradtion and Erosion in High Pressure Arc Discharges," NASA Technical Memorandum 83638, 1984.

39. Northam, G. B., McLain, A. G., Pellet, G. L., and Diskin, G. S., "Effect of Silane Concentration on the Supersonic Combstion of a Silane/Methane Mixture," AIAA-86-1396, Presented at the AIAA/ASME/SAE/ASEE 22nd Joint propulsion Conference, 1986.

40. Wallner, L. E., Czika, J. Jr, "Arc-Jet Thruster for Space Propulsion," NASA TN D-2868, June, 1965.

41. Mager, A.," Approximate Solution of Isentropic Swirling Flow Through a Nozzle," *ARS Journal,* Vol. 31, No. 8, Aug., 1961, pp. 1140-1148.

42. Batson, J. L., Sforzini, R. H., " Swirling Flow Through a Nozzle," *Journal of Spacecraft and Rockets,* Vol. 7, No. 2, Feb. 1970, pp. 159-162.

43. Sarmiento, C. J., and Gruber, R. P., "Low Power Arcjet Thruster Pulse Ignition," AIAA-87-1951

44. Hardy, T. L., "Electrode Erosion in Arc Discharges at Atmosheric Pressure," AIAA-85-2018, Presented at the AIAA/DGLR/JSASS 18th International Electric Propulsion Conference, 1985.

45. Curran, F. M., and Haag, T. W., "Arcjet Component Conditions Through a Multistart Test," AIAA-87-1060

46. Rogers, R. C., "A Study of the Hydrogen Injected Normal to a Supersonic Airstream," NASA TN D-6114, 1971.

Appendix A

The Physics Of An Electric Arc

A.1 Introduction

There are many possible technical applications of electric arc devices. The arcjet is currently being studied as a high specific impulse engine for spacecraft propulsion [25]. High pressure plasma jets have been used to provide high enthalpy, high speed flows for material testing at conditions simulating atmospheric entry of spacecraft. Plasma jets have also been applied in industry in cutting and spray coating of metals [26], and in chemical synthesis [26,27]. This section gives a brief review of some of the physical processes which occur in low current D.C. electric arcs. Further information on the electric arc can be found in the works of Cobine [28], Finklnburg and Maecker [29], and Hoyaux [30].

In an arc, work is done on charged particles (ions and electrons) by an electric field, increasing their kinetic energy. These particles, in turn, collide with less energetic particles, exchanging energy with them, so that an electrically conducting mixture of electrons, ions, molecules, and atoms is created. This mixture is a plasma. The number of positive and negative particles are approximately equal, so that a plasma is electrically neutral overall. Although the exact definition varies with the author, the electric arc is usually defined as a gaseous discharge in which there is a high current ($I > 0.1$ A) and a low voltage ($V < 1000$ V).

At low pressures, the temperature of the electrons is much greater than that of the heavier particles. At pressures on the order of one atmosphere or higher (high pressure plasmas) the plasma approaches a state of local thermodynamic equilibrium (LTE), where the temperatures of the electrons and the heavier particles are approximately the same. The reason for this is that, at higher pressures, the electrons experience more collisions, and thus exchange more of their kinetic energy with the heavier particles.

A.2 Regions of the Arc

The electric arc is maintained between the cathode (the negative electrode) and the anode (the positive electrode). The spatial potential distribution of a typical arc is shown in figure A1. The arc is composed of the column, cathode fall, and the anode fall regions.

The column is the region of the arc, between the two fall regions, in which a thermal plasma exists. Neutral particles (atoms and molecules) diffuse to the inner regions of the column, where ionization produces charged particles (ions and electrons). The charged particles diffuse radially to the cool region, outside the column, and recombine. The

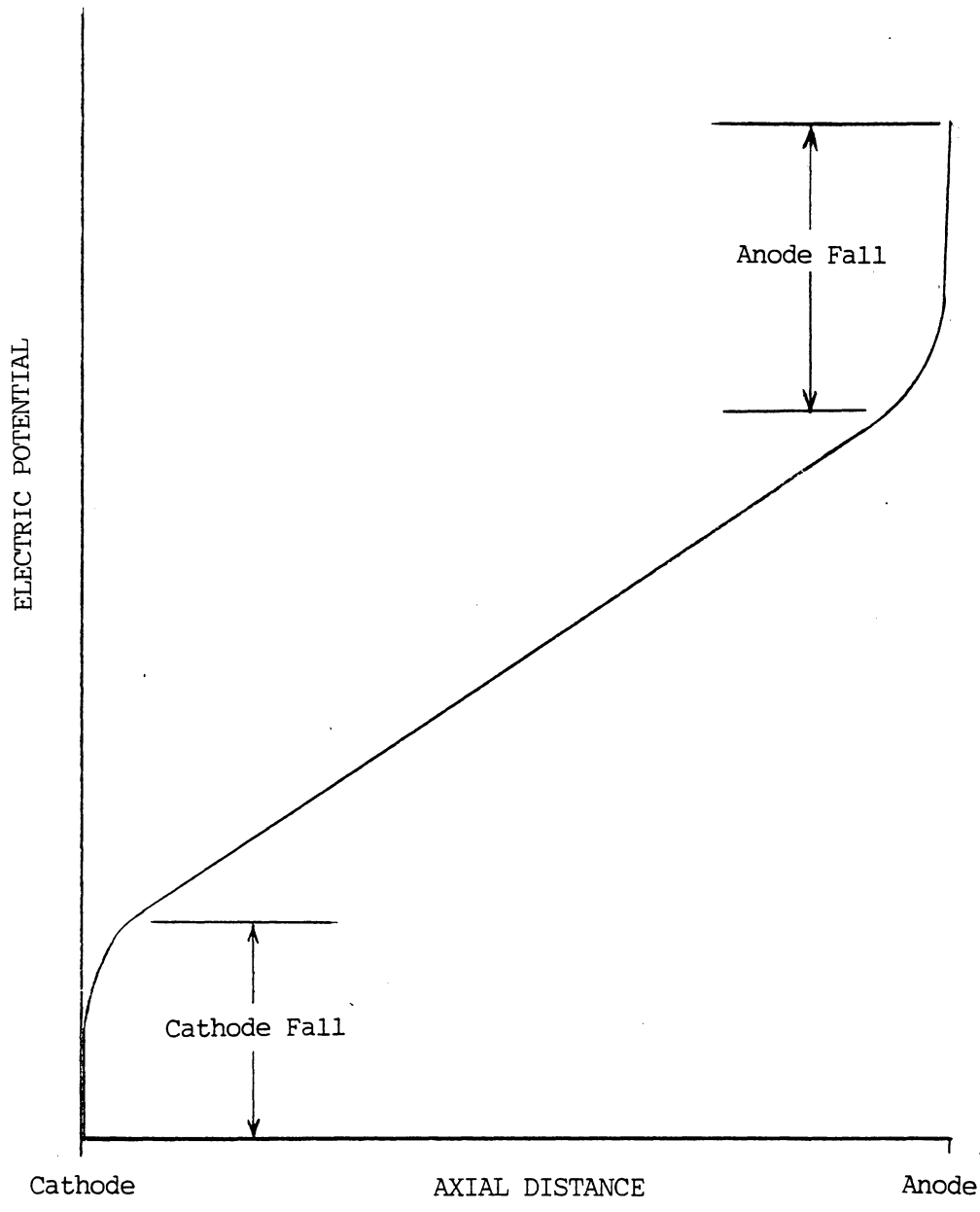

Figure A 1. Electric Potential Distribution for a Typical Arc

column potential gradient is essentially uniform. The voltage drop across the column is simply equal to the product of the electric field and the column length.

The fall regions are characterized by large potential and temperature gradients, and are very thin, having a thickness on the order of a few mean free paths of the electrons [31]. Typical values of the fall voltages are 0-30 V for the anode and less than 20 V for the cathode [29]. In general, there is not an equal number of positive ions and electrons in the fall regions, so, the fall regions are not plasmas.

A.3 Electrical Resistance of the Arc

The total resistance of an arc discharge is equal to the integral of the resistance per unit length, $\rho(x)$, along the length of the arc. If the axial potential distribution (shown in figure A1) is divided by the arc current, the slope of the resulting plot would equal $\rho(x)$, since the current is the same in all portions of the arc. From figure A1 it may be seen, that $\rho(x)$, is higher in the two electrode fall regions than in the column. Also, $\rho(x)$ is uniform in the column due to the constant axial potential gradient there, so that $\rho(x) = \rho_{col}$. This quantity is a function of the electrical conductivity and how it is distributed across the arc, and may be calculated as follows

$$\rho_{col} = \left[\int \sigma \, dA \right]^{-1} .$$

or for a cylindrically symmetric arc

$$\rho_{col} = \left[2\pi \int_0^{r_o} \sigma \, r \, dr \right]^{-1} .$$

The electrical conductivity varies from a maximum at the center of the arc, due to the high temperature there, to almost zero at the cool outer edges of the arc. The cross-sectional area of the arc is the area in which significant electrical current is carried. The outer edge of the arc can be defined as the radial position in which the ratio of the conductivity to that at center of the arc falls below a minimum value.

The overall resistance of an arc then is proportional to its length and inversely proportional to the cross-sectional area and the conductivity in the same way as it is for a solid metallic conductor. However, unlike a solid conductor, the conductivity, cross-sectional area, and length of the arc are complex functions of the arc parameters. The conductivity of the plasma is equal to the product of the charge, number density, and the mobility of the charge carriers. These, in turn, depend on the local temperature and pressure.

In a plasma in local thermodynamic equilibrium (LTE) the degree of ionization, α, is given by the Saha equation, written here for the ionization of a monatomic gas [32]

$$\frac{\alpha^2}{1-\alpha^2} = c\frac{T^{\frac{5}{2}}}{p} \exp\left[\frac{-\varepsilon_i}{kT}\right].$$

In the Saha equation I, k, T, and P are the ionization potential, Boltzmann constant, temperature, and pressure, respectively. From this it may be seen that ionization is favored by high temperatures, low pressures and a low ionization potential. Before a diatomic gas can be ionized it is usually dissociated. The degree of dissociation of a gas at LTE can be calculated from equilibrium considerations. Dissociation is also favored by an increase in the temperature and and a decrease in pressure, so that the number density of the charge carriers is increased by an increase in temperature, or by a decrease in pressure, ionization potential or dissociation energy (if the gas is not monatomic).

The mobility of a charge carrier is defined as the local drift velocity of the charge carrier divided by the electric field strength, in the direction of its motion. The mobility of a charge carrier decreases with an increase in pressure and increases with an increase in temperature [32]. Since the conductivity is proportional to the product of mobility and number density of the charge carriers, it will also increase with temperature and decrease with an increase in pressure. Therefore, the local resistance of a plasma decreases with an increase in temperature and increases with an increase in pressure.

A.4 Overall Electrical Behavior vs Arc Parameters

In an arc with a fixed length and current, the dependent variables which are be adjusted internally are the distribution of the current density, and thus, the conductivity, arc diameter, and the electric field strength. The last two are related by the Steenbeck minimum principle [29], which states that the independent variables of an arc are adjusted so that the rate of entropy production is minimized. The entropy production of an arc per unit length, Θ, is found by considerations of irreversible thermodynamics to be

$$\Theta = \frac{IE}{T_r}$$

where T_r is the temperature of the surrounding gas, E is the electric field strength, and I is the total current. The total entropy production is the integral of this quantity along the length of the arc.

The Steenbeck minimum principle states that the entropy production of an arc must be minimized, so that the electric field strength must be minimized in an arc for a given

current. Therefore, under given external conditions such as the temperature, pressure, and external motion of the gases, the arc length, diameter and the distribution of the conductivity of the plasma across the arc is such that the entropy production is minimized.

An increase in the pressure causes a small increase in the arc voltage. More important than the increased voltage, however, is the change in the cross-sectional area of the arc with pressure. The electrons and ions, present at the edges of the arc, will combine as the pressure is increased, so that the arc contracts to a smaller cross-sectional area. If current remains the same, current density must then increase. This increase in current density is related to the electric field strength and the conductivity by Ohm's law so that either the field strength or the local conductivity must increase. In practice both occur. As noted above, the field strength is increased slightly, but the conductivity (of the smaller arc cross section) increases, in order to minimize the electric field, in accordance with the Steenbeck minimum principle. Since the conductivity of the high pressure column must increase, its temperature must also increase.

In a low current arc, a current increase will cause the electric field to decrease. This may be shown from the Steenbeck minimum principle. In order to decrease the electric field, the resistance of the plasma must decrease. Therefore, the arc must have larger electrical conductivities at each point or have a larger current carrying cross section or both. In practice, both the local conductivity and the area of the arc increase as the current is increased. Since the local electrical conductivity increases, the local temperature must also increase.

Any effect which tends to increase the radial diffusion of the charge carriers to the cool outer regions will cause the column to contract in the same way that a pressure increase does. One way that this can occur is to decrease the temperature of the

surrounding gas, so that the radial heat transfer is increased and the charge carriers in the outer edges of the arc combine. Or, convective heat transfer from the outside of the arc may be increased. The presence of " cold " walls outside of the column will also increase the radial diffusion of the charge carriers.

Appendix B

Data Acquisition Program

```
10 ' Data acquisition for the plasma torch   dt2805 card
20 ' Version Plasma65
40 XGEC=78 :XSB=81 :XSECW=75 :XMCJ =144   ' pctherm entry points
50 XMT=141 :XMV=138 :XEFO=60 :XODV = 66:XSAR=90
60 '
100 DIM VOLTS.NEW(5)
110 DEFINT J
120 '
130 CLS:KEY OFF  '    print the title of the program
140 PRINT :PRINT :PRINT :PRINT :PRINT :PRINT
150 PRINT SPC(15) "PLASMA TORCH DATA ACQUISITION PROGRAM "
160 PRINT :PRINT
170 PRINT "WRITTEN FOR THE HYPERSONIC PROPULSION BRANCH OF THE NASA
LANGLEY RESEARCH CENTER"
180 PRINT SPC(10) "TURBOMACHINERY AND PROPULSION RESEARCH CENTER"
190 PRINT:PRINT  SPC(18) "MECHANICAL ENGINEERING DEPARTMENT ":PRINT
200 PRINT SPC(28)"V. P. I. & S. U." :PRINT
210 PRINT :PRINT :PRINT SPC(21) "PRESS ANY KEY TO CONTINUE "
220 IF INKEY$="" THEN  220
395 '
399 ' INITIAL PARAMETERS
400 DRVON1$="c":DRVON2$="c:" :U1$="##" :U2$=":" :J5SUM=65
410 CLS:PRINT:INPUT "   GIVE THE FILENAME OF THE OUTPUT FILE ";FI1A$
420 FI1$=DRVON2$+FI1A$ :OPEN FI1$ FOR OUTPUT AS #1 :GOSUB 3300
421 PRINT :PRINT :PRINT :PRINT "PRESS ANY KEY TO BEGIN COLLECTING DATA"
425 IF INKEY$="" THEN 425
440 BOARD%=1:CALL XSB(BOARD%)
491 GOSUB 2000
499 '
500 ' ----------------------  START THE DATA ACQUISITION
501 '
501 ' ==== routine to display to the screen before the arc is ignited =====
503 '
```

```
510 FOR CHANNEL%=1 TO 3
520 CALL XMV(CHANNEL%,VOLTS.NEW(CHANNEL%)) :NEXT CHANNEL% '  GET DATA
530 GOSUB 1600  ' convert the data
540 IF AMPS.NEW < 1! THEN GOSUB 3000 :GOTO 510
541 '
550 ' ======= Data acquisition loop ========
551 '
560 GOSUB 5000:TA=T:TA1=T1:TA10=T10:TA100=T100 ' initialize the clock
570 VOLTSUM1=0:VOLTSUM2=0:VOLTSUM3=0
580 FOR J5=1 TO J5SUM
590 FOR CHANNEL%=1 TO 3
550 CALL XMV(CHANNEL%,VOLTS.NEW(CHANNEL%)):NEXT CHANNEL% ' GET DATA
560 VOLTSUM1=VOLTSUM1+VOLTS.NEW(1):VOLTSUM2=VOLTSUM2+VOLTS.NEW(2)
570 VOLTSUM3=VOLTSUM3+VOLTS.NEW(3):NEXT J5
580 VOLTS.NEW(1)=VOLTSUM1/J5SUM:VOLTS.NEW(2)=VOLTSUM2/J5SUM
590 VOLTS.NEW(3)=VOLTSUM3/J5SUM    ' AVERAGE INPUT VALUES
610 GOSUB 1600  ' CONVERT VOLTAGES TO DATA
620 GOSUB 5000   '                READ THE TIME
630 MINS=60*(T-TA)+T1-TA1+1.66667E-02*(T10-TA10)+1.66667E-04*(T100-TA100)
710 PRINT #1, USING "###.###  ###.#   ##.##  ###.#";MINS;VOLTS1.NEW;AMPS.NEW;PRES.NEW
790 GOSUB 3000 '
820 GOTO 570 ' ================================================
1599 '
1600 '================  data conversions as of 1-31-88
1601 '
1610 VOLTS1.NEW=VOLTS.NEW(1)*50.66
1620 AMPS.NEW =VOLTS.NEW(2)*5.02
1630 PRES.NEW=(VOLTS.NEW(3)*40.1) +11.579
1670 RETURN ' ============================================
1999 '
2000 '+++++++++++++++++   PRINT THE DATA SCREEN ++++++++++++++++++++++
2001 '
2010 CLS :PRINT:PRINT SPC(35) "DATA SCREEN ":PRINT :PRINT :PRINT
2020 PRINT SPC(37) "VOLTAGE = " :LOCATE 6,65 :PRINT "volts"
2030 PRINT :PRINT SPC(37) "CURRENT = " :LOCATE 8,65 :PRINT "amps"
2050 PRINT :PRINT SPC(30) "TORCH PRESSURE = " :LOCATE 10,65 : PRINT "psi"
2070 PRINT :PRINT :PRINT :PRINT :PRINT :PRINT :PRINT SPC(39) "TIME = "
2090 RETURN '++++++++++++++++++++++++++++++++++++++++++++++++++++++++
2999 '
3000 ' ===================== write to the data screen ===============
3001 JPRINT=0
3010 LOCATE 6,48:PRINT SPACE$(14):LOCATE 6,48:PRINT USING "###.#"; VOLTS1.NEW
3020 LOCATE 8,48:PRINT SPACE$(14):LOCATE 8,48:PRINT USING "##.##";AMPS.NEW
3040 LOCATE 10,48:PRINT SPACE$(14):LOCATE 10,48:PRINT USING "###.#"; PRES.NEW
3060 LOCATE 20,50:PRINT SPACE$(13):LOCATE 20,50:PRINT USING "###.##"; MINS
3080 RETURN '============================================
3299 '
3300 ' =========  Write a title to the disk ===========
3301 '
3310 PRINT #1,CHR$(13)
3320 PRINT #1, "DATE :  ";DATE$ :PRINT #1,CHR$(13)
3330 PRINT #1,"       TIME          V          I       PRESSURE  "
3340 PRINT #1,"     (minutes)    VOLTS      AMPS        PSI     "
3350 PRINT #1,CHR$(13)
3360 RETURN ' ============================================================
4999 '
5000 ' ============== GET THE TIME ====================
5010 '
5020 X1=INP(&H2C3)
5030 T1=((X1-(X1 AND 15))/16)*10 +(X1 AND 15) '  T1=MIN
5040 X=INP(&H2C4)
5050 T=((X-(X AND 15))/16)*10 +(X AND 15) '     T=HOURS
5060 X100 = INP(&H2C1)
5070 T100 = ((X100-(X100 AND 15))/16)*10 +(X100 AND 15) '  T100=SEC/100
5080 X10 =INP(&H2C2)
5090 T10 = ((X10-(X10 AND 15))/16) *10 +(X10 AND 15) '     T10 =SEC
5100 RETURN  '============================================
```

The vita has been removed from the scanned document